SOFTWARE DEFINED RADIO ATTENUATION CONTROL IN 5G COMMUNICATION SYSTEM

by

SACHIN KUMAR AGRAWAL

(2K13/PHDCO/02)

Submitted

in fulfillment of the requirements of the degree of

Doctor of Philosophy

to the

DELHI TECHNOLOGICAL UNIVERSITY

FORMERLY DELHI COLLEGE OF ENGINEERING

NEW DELHI, INDIA

2019

Certificate

This is to certify that the thesis entitled, **"Software Defined Radio Attenuation Control in 5G Communication System"** being submitted by **Mr. Sachin Kumar Agrawal** (2K13/PHDCO/02) to Delhi Technological University, New Delhi for the award of the degree of **Doctor of Philosophy** is the record of the bona-fide research work carried out by him under my supervision. In my opinion, the thesis has reached the standards fulfilling the requirements of the regulations relating to the degree. The results contained in this thesis have not been submitted either in part or in full to any other university or institute for the award of any degree or diploma.

(Dr. Kapil Sharma)

Professor, Head of IT Department,

Department of Information Technology (IT),

Delhi Technological University (DTU),

New Delhi, India

Acknowledgements

I am blessed with the kind grace of GOD, Who guided me in every step of my life. I would like to express my profound gratitude to my advisor Dr. Kapil Sharma for his invaluable guidance, continuous encouragement and support in every stage of this research work. His technical acumen, precise suggestions, kind nature and detailed timely discussions are wholeheartedly appreciated. Also, my sincere thanks goes to Samsung Research Institute Noida (SRIN) and Delhi Technological University for considering my candidature for this course. My sincere thanks also goes to the respected members of my Computers and Information Technology Department. Special thanks to Dr. Rajni Jindal and Dr. Ruchika Malhotra for their insightful comments and valuable suggestions. Special thanks to my seniors and colleagues of Samsung Research. My sincere thanks to professors, faculty, researchers, Gopal Ji and non-teaching staff of Computers and Information Technology Department.

Most importantly, my heartfelt gratitude is for my parents who are the motivations behind me, without their blessings this work could have not been accomplished. I am deeply grateful to my family for their moral and emotional support in my life. My special gratitude is due to my loving wife Kavita, for her consistent support. I also thank my brothers Vipin and Nitin for their always motivation. I am very much thankful to my kids Anmol and Ridhi, who had to miss lots of occasions of being with me, during the course of this work.

Sachin Kumar Agrawal

Abstract

Millimeter wave (mmWave) frequencies are under research for providing high speed data spectrum for upcoming 5th Generation (5G) communication system. The mmWave frequencies suffer with high propagation attenuation due to various channel obstructions. There is a demand and need to have an effective method for efficient mmWave propagation. The focus of this thesis is to identify the various channel obstructions along with their effect on mmWave propagation in terms of attenuation and channel capacity to have desired controlled user data rate.

In this research, we propose an innovative method for intelligently selecting a grid or group of grids having minimal mmWave propagation attenuation to overcome the effect of obstructions at the transmission end. The proposed 5G ML transmitter system keeps learning mmWave propagation vegetation attenuation values. The ML unit predicts the vegetation attenuation values using regression mode with the algorithms like K-Nearest Neighbors, Decision Tree and Random Forest and also predicts Shannon channel capacity (SCC). Further, we present mmWave propagation losses dataset for four Indian major urban cities like Delhi, Mumbai, Kolkata and Chennai locations in the presence of atmospheric impairments. The simulations have also been performed for the mmWave frequencies 28 GHz, 37 GHz and 39 GHz. The thesis research and results can be used for transmission power loss budget analysis, transmission power control, beamforming, SCC analysis and etc. It significantly improves the 5G system performance by saving the transmitter power radiation and provides multigigabit data rates.

Contents

List of Figures

Abbreviations

5G	5th Generation
AWGN	Additive White Gaussian Noise
BER	Bit Error Rate
CSI	Channel State Information
INR	Interference to Noise Ratio
LoS	Line of Sight
mmWave	Millimeter Wave
MS	Mobile Station
SER	Symbol Error Rate
SCC	Shannon Channel Capacity
SDR	Software Defined Radio
SINR	Signal to Interference and Noise Ratio
SNR	Signal to Noise Ratio

Chapter 1

Introduction

1.1 5G mmWave Communications System

5G millimeter wave (mmWave) communications system research has been started. There is a growth in the system development and research to provide market ready to use 5G system by 2020 [1-5]. 5G mmWave communications system has clear vision to have user devices in the environment of Internet of Things (IoT) and Big-Data. 5G mmWave communications system will provide Big-Data based platform for billions of user connected devices autonomously in a seamless manner. These user devices are interconnected among each other along with the consideration of security. It offers low latency high speed data connection with gigabit speed for the billions of users [5-9]. It provides high speed and high bandwidth so that to accommodate Big-Data users. It also suffers with wireless channel attenuation due to signal losses. 5G system services, applications, requirements, challenges and standardizations are discussed in this

research. There are several challenges for 5G system. The research is in progress to identify and overcome these challenges by enabling technical solution for 5G system. There are challenges like radio wave propagation and network related issues [7-14].

5G mmWave communications system is emerging as promising and potential wireless communication system having along with technologies like green communications, Internet of Things, device- to-device communications, Software defined millimeter wave and etc. 5G system along with these technologies will provide high efficiency long term wireless communications system [8-18]. It will fulfill the requirement of high data rates, low latency, low energy consumption, improved connectivity and reliability, High scalability and etc. 5G system still requires improved security mechanism and there is demand and need for efficient and optimum control in 5G communication system. To full-fill the demand and need of the 5G system in a flexible manner; several research have proposed to use flexible system where SDMW based technology can support in desirable and easy way. SDMW provides programmable hardware as per access control and standards. Such type of programmable system flexibly supports our proposed mechanism [15-23].

1.1.1 Beginning of 5G mmWave Communications System

5G mmWave communications system research is in progress with common vision of high data speed, high bandwidth, mobility support, rich user experience by 2020 and many more. This 5G system will accommodate large number of users along with high

data connectivity. The vision and challenges are discussed in this research thesis for 5G mmWave communications system. Various research solutions and technology enablement are in progress worldwide for 5G mmWave communications system. 5G system research is in progress and standardized definition is progress. 5G mmWave communications system work is in progress and tentatively may be named as IMT 2020 [21-28]. 5G mmWave communications system definition at present can be described as :

- 100 billion devices and more
- 100 Gbps

5G mmWave communications system provides enough economic worth and value for the users. As per demand and need, the number of user will increase will a rapid rate along with Big-Data requirement and this will be fulfill by the 5G system [28-34]. The data demand will be in Exabytes among billions of users. 5G system will revolutionize the wireless communication system It will also revolutionize the way of interaction among the devices in Big-Data and Internet of Things (IoT) environment. The demand will increase in a rapid manner and 5G communications system will accommodate such demands of large number of users and high speed seamless connection among user devices. 5G mmWave communications system in Big-Data and Internet of Things (IoT) environment will provide very low latency in an intelligent and efficient manner [25-33].

5G research is in full swing throughout the world and researchers are aiming 5G speed around 1000 times faster than normal 4G wireless system. Researchers are on

way for getting 10 to 100 times faster data speed than 4G wireless system. This 5G system will also consider high number of users also with the facility of always high data link capacity.

1.1.2 5G Services and Applications

5G communications system is under progress for various services and applications among high speed large number of users. The list is below for various services of 5G communications system [6-7] :

- Internet of Things

  Smart Home, Store and Office

  HealthCare

  Connected Car

- Everything on Cloud

- Intuitive Remote Access

Applications of 5G mmWave communications system are like : driving a car with augmented reality (AR) navigation, watching sport events with virtual reality (VR), ubiquitous health care, wearable device, flexible mobile device, UHD video streaming smart map/navigation, real-time interactive game, mobile cloud and many more [29-31]. Sports event can also be provided with the 5G system based video multicasting this can also have the VR experience for the remote users. 5G system along

with high internet or data link capacity will be quite useful in vehicle to vehicle (V2V) system. Ultra Low Latency (ULL) connection in 5G mmWave communications system can provide immediate responses among automated driving vehicles. Ultra Low Latency (ULL) connection in 5G mmWave communications system will provide additional safety in vehicle to vehicle (V2V) system. Ubiquitous health care through 5G mmWave communications system will provide remote surgical solutions. Ultra Low Latency (ULL) connection in 5G mmWave communications system will provide fast and easy access of networked robotics access for doctors in the remote environment [31-39].

Recent consideration of mmWave with 5G wireless communication system is attracting researchers attraction worldwide for deep wireless channel propagation research and investigation [31-36]. 5G system will use mmWave frequency bands of 3 GHz to 300 GHz. 5G mmWave frequency bands provide capacity to have high data rate with high data capacity. High frequencies of mmWave frequency bands are having small wavelength which makes mmWave frequencies bands more prone to attenuation. 5G D2D mmWave communication allows mobile devices to connect directly and also an important connection in Cellular internet of Things (CIoT) environment [3-8]. Wireless channel is really responsible for mmWave transmission power losses due to various obstructions in the channel. The mmWave frequencies suffer with channel attenuation in the wireless medium due to various channel impairments like atmosphere, seasons, vegetation, urban and etc. The mmWave propagates with high losses in the mmWave frequency bands and requires high research attention to make more effective

system [8-12].

As per 5G system for shifting towards high frequency spectrum; it becomes part of research to have certain fixed or proposed frequencies for research and development from high frequency. Recently, Federal Communications Commission (FCC) has announced 5G mmWave high carrier frequencies along with the bands information. FCC mmWave frequencies bands are 28 GHz band, 37 GHz band and 39 GHz band. For the above mentioned mmWave carrier frequencies, 5G system research is in development worldwide [11-15]. In this research paper, we have used FCC recommended frequency for forming and identifying minimal mmWave propagation attenuation intelligent grids as well as for identifying the right zones (set of two or more grids) for the same. The intelligent grids are selected from the virtual face grid which is formed in a virtual manner on the face of the transmitting antenna. The virtual face consists obstacles and non-obstacles area which are identified and mapped the grids. The mmWave spectrum is promising for 5G communication systems with high bandwidth for users along with various advance services. Extensive research is in progress for mmWave propagation in the environment of various channel obstructions. The mmWave propagation channel obstructions are like; vegetation, atmosphere, building/ urban and etc. Research for mmWave is in progress for getting characteristics of mmWave propagation [10-15]. It is required to have characteristics of mmWave propagation based on various atmospheric, seasons and obstructions for a particular site conditions. Literature discusses mmWave communication systems with various types of attenuations measurements and models to get the characteristics of mmWave propagation [13-17]. In this research

paper we are discussing intelligent grids for mmWave propagation to provide minimal channel losses during propagation. These smart intelligent such grids will show that mmWave systems can have high quality signal strength by using proposed grids. We also represent that the grids can be used in an effective manner for mmWave path loss estimation while 5G cell planning [13-19]. This research provides mmWave propagation effect due to various obstructions for the experimental simulation site. Our work considers a variety of mmWave propagation channel obstructions like building, vegetation in-leaf, vegetation out-leaf, atmospheric impairments and seasonal atmosphere with 5G transmitter. Various types of channel obstructions are considered to calculate the mmWave channel propagation losses. Delhi Technological University (DTU), previously known as Delhi College of Engineering (DCE), New Delhi, India has been considered as calculation experimental site [20-26]. The idea of using grids-forming for 5G transmitters with millimeter-wave spectrum is shown with the results in later sections of this paper. In this research, we calculate the mmWave propagation losses due to vegetation in 5G wireless communication system, it is considered that both devices transmitter and receiver are situated in the DTU area. As per literature several vegetation propagation attenuation models are proposed. Here, we have used fitted radio international telecommunication union (FITU-R) model to calculate the vegetation propagation attenuation with the reason that this model is applicable to mmWave frequency range and provide with-leaf and with out-leaf attenuation values which can be used with the varied seasons[21-25]. Further, mmWave propagation losses due to buildings (urban area) in 5G system are calculated and details are in description

section(s). As per literature several methods are available to calculate the urban area propagation attenuations. Here, we have used geometrical optics (GO) and a uniform theory of diffraction (UTD) to calculate urban area mmWave propagation attenuation with the reason that this model is applicable to mmWave frequency range and provide reliable prediction for the proposed site [23-25]. Also in this research paper, we have calculated mmWave propagation losses due to atmosphere in 5G wireless communication system. As per literature, we have used ITU recommended models to calculate the atmospheric mmWave propagation attenuation. This model is applicable to mmWave frequency range and provides reliable prediction for the proposed site. Here we have simulated results along with the performance and validations of the results for the frequency 28 GHz [12-15],[21-25].

The mmWave propagation in the presence of vegetation obstruction channel environment is part of the research from the several years in the wireless communication domain. The information of the mmWave propagation attenuation in the vegetation environment becomes important while designing 5G mmWave communication system having SDR based transmitter [31-39]. The SDR transmitter has software controlled transmission to control the transmission parameters in the software command mode without having dedicated hardware control. This software controlled transmission provides flexible and efficient transmission. The vegetation medium is discrete and scattered due to random distribution of vegetation medium like leaves, branches, trunk and etc. This vegetation medium causes mmWave propagation losses and takes place due to mmWave behavior of scattering, diffraction, and absorption in the vegetation

medium. The mmWave vegetation propagation generally adds path loss, multipath dispersion, shadowing and etc [11-15].

As per 5G mmWave vision; it will provide pervasive environment to the users to have effective high data rate link among the uses in the range of giga bits (Gbps). 5G mmWave communication system will be capable for providing quality of service (QoS) for large number of user with high data rates along with exponential grown bandwidth. 5G mmWave requires effective mmWave propagation by having minimal propagation attenuation. Worldwide research development is in progress for effective mmWave propagation in the presence of various obstructions. There are several mmWave propagation attenuation factors like; rain, water vapor, oxygen, atmospheric factors, vegetation, building and others channel impairments [13-17].

5G mmWave vision considers high bandwidth and which can be fulfilled by having mmWaves based spectrum. The mmWave frequencies spectrum allows high bandwidth to fulfill the 2020 user demands and need. Moving towards high frequency spectrum also has concerns with low wavelength signal and causes high mmWave propagation attenuation. To have minimal attenuation for mmWave ; it becomes important to have research and select the optimum frequencies in mmWave so that 5G communication system suffers minimal mmWave propagation losses. Recently, Federal Communications Commission (FCC) has mentioned 5G mmWave signal carrier frequencies along with the details of bands. This announcement has been made for research, development and testing purposes to have effective and quality 5G system in upcoming years. As per FCC; 5G mmWave carrier frequencies bands are mentioned

below [18-21]:

- 28-GHz Band
- 37-GHz Band
- 39-GHz Band

The above mentioned 5G mmWave carrier frequencies are used for simulating vegetation attenuations and discussed in the following sections along with Shannon channel capacity. In this research paper, we are using ITU-R based vegetation attenuation model of mmWave outdoor propagation for the FCC recommended frequencies: 1) 28 GHz, 2) 37 GHz and 3) 39 GHz to calculate the vegetation attenuation. SDR based system gets the vegetation attenuation values from the ML prediction unit for the desired frequencies.

The Worldwide continuous demand of data on wireless communication system having user ubiquitous access requires high speed data rate and high bandwidth to full the requirement seamlessly. Around 3GHz several research has been done to justify and provide the efficient data bandwidth and data rates; however this is not sufficient for upcoming years [4-17]. There is demand and need to fulfill this high speed data rate and high bandwidth along efficient frequency spectrum with intelligence in the system. 5th generation (5G) mmWave communication system is an emerging technology which will provide efficient mmWave spectrum utilization to provide high speed data rate and high bandwidth. mmWave frequencies bands are capable to provide

the high speed data rate and high bandwidth by fulfilling the spectrum shortage. 5G mmWave communication system requires efficient spectrum handling by considering various mmWave propagation channel characteristics for the entire mmWave range. mmWave frequencies range from 30 to 300 GHz and provide a large spectrum. It forms the base for the 5G mmWave communication system. In this research, we propose a feature for an intelligent ML based adaptive transmitter for 5G wireless system [4-14].

1.2 Research Objective

The basic aim of this research is to provide software defined radio attenuation control in 5G communication system along with performance analysis. The summary of the goals of the work is provided below:

- : Innovative method for intelligently selecting a grid or group of grids having minimal mmWave propagation attenuation from a virtual grid face of 5G transmitter. The object is to select at least one obstruction free zone and at least one obstruction free beam window, said at least one obstruction free beam window being selected within said at least one obstruction free zone . This grid selection for mmWave propagation is to overcome the various effects of obstacles and simulation for the frequencies 28 GHz, 37 GHz and 39 GHz.

- : 5G mmWave communication system attenuation control using software defined radio (SDR) for the frequencies 28 GHz, 37 GHz and 39 GHz. The soft-

ware defined method keeps on learning mmWave propagation attenuation values for the mmWave frequencies by using supervised ML for various type of attenuations causes like vegetation and predicting the Shannon channel capacity (SCC) calculation at 5G SDR transmitter for the frequencies 28 GHz, 37 GHz and 39 GHz to maintain the desired transmission data rates. Attenuation and SCC calculation for Delhi Technological University (DTU), New Delhi, India based location.

- : Calculation of mmWave attenuations due to atmospheric/ weather obstruction to provide the transmission signal power control in 5G mmWave communication system using software defined radio (SDR) considering frequencies 28 GHz, 37 GHz and 39 GHz. Further, atmospheric/ weather obstruction attenuation calculation for the Indian metro cities like Delhi, Mumbai, Kolkata and Chennai.

As per the objects the research results are generated and are useful for the researchers as well as for the industries to calculate wireless system link budget analysis in the 5G mmWave communication system. This research work presents atmospheric, vegetation, urban or building and vegetation attenuation calculation in SDR manner and attenuation control in 5G mmWave communication system using SDR. The SDR method considers machine learning and predicts the attenuation as well as SCC as per situation. SCC is calculated for Delhi Technological University (DTU), New Delhi, India based location as well as along with the consideration of various type of attenuations like atmospheric, vegetation and building or urban attenuation.

1.3 Outline of the Thesis

The thesis is organized into six chapters. The summary of the work presented in each chapter is briefly outlined as follows:

- **Chapter 2**: In this chapter, we present a state-of-art review of various methodologies available for handling 5G losses and issues present. Here all the existing methodologies are critically evaluated along the various parameters. This chapter would serve as a backbone for our proposal and the rest of the chapters.

- **Chapter 3**: In this chapter, we propose a method for intelligently selecting a grid or group of grids having minimal mmWave propagation attenuation from a virtual grid face. This grid selection for mmWave propagation is described to overcome the various effects of obstacle blockages by forming virtual grid face around the transmission antenna. The simulation for the same has been performed for the proposed 5G mmWave link. Further, one grid (or group of grids) is selected from the virtual face based on the minimal attenuation value the for mmWave propagation. Minimal attenuation grid can be used in several manner in the 5G wireless communication system like for line of Sight (LoS), transmission power link budget analysis, transmission power control, beamforming, Shannon channel capacity analysis, cell planning and etc. This chapter shows smart intelligent method for minimal attenuation grid-forming for of mmWave based communication link. It significantly improves system performance by saving the transmitter power radiation for mmWave propagation through the se-

lected grid having minimal attenuation.

- **Chapter 4**: We propose intelligent ML based transmitter is a supervised ML device and it has provision of self teaching learning machine based on data. The proposed 5G ML transmitter system keeps learning mmWave propagation atmosphere, vegetation and urban attenuation values for the mmWave frequencies. The ML unit predicts the attenuation values using regression mode with the algorithms like K-Nearest Neighbors, Decision Tree and Random Forest. Results are graphed for the mentioned frequencies and for 5G mmWave communication system under different atmospheric conditions, vegetation and urban channel conditions.

- **Chapter 5**: In this chapter, we present atmospheric attenuation control in 5G mmwave communication system for Delhi (India) and other related cities based location using software defined radio (SDR). The software defined radio atmospheric attenuation is calculated for the frequencies 28 GHz, 37 GHz and 39 GHz. The atmospheric attenuation is calculated for Delhi (India) based location by considering 5G mmWave absorption due to atmospheric water vapour and atmospheric oxygen. In this chapter , we present atmospheric effect on 5G mmWave communication system. Atmospheric effects for Delhi (India) based 5G communication system is calculated as per Delhi atmospheric conditions. Atmospheric impairments are major cause of degrading mmWave signal power while mmWave propagation in wireless channel. Due to Atmospheric impair-

ments attenuation takes place and major impairments are like water vapour, oxygen, rain and fog for Delhi (India). 5G mmWave attenuation calculations are performed for the mmWave band frequencies 28 GHz, 37 GHz and 39 GHz.

- **Chapter 6**: This chapter gives the details of results along with discussion the thesis.

- **Chapter 7**: In this chapter, we summarize the contribution of the thesis, present the conclusions and discuss the future scope of our work.

Further sections gives the publications and references details of the thesis.

Chapter 2

Literature Review

2.1 5G

With the explosive research, progress and development for 5G mmWave communications system by considering Gbps data rate among billions of user devices, it is required to have technically rich 5G mmWave communications system. Such enhanced, intelligent, technical 5G mmWave communications system shall consider the following requirements are discussed in next paragraph.

5G mmWave communications system major requirements are High Data Rate, Cell Edge Data Rate, Low Latency, Simultaneous Seamless Connection, Cell Spectral Efficiency and Utilization Optimally, Optimum Cost and Mobility Support . There is need and requirement for seamless billions of user devices connection along with high data rate and low latency [4-9]. billions of user devices in 5G mmWave communications system shall also consider Cell Edge Data Rate, Cell Spectral Efficiency and

Utilization Optimally, Optimum Cost and Mobility Support [4-7] .

2.1.1 Requirements for 5G

With the explosive research, progress and development for 5G mmWave communications system by considering Gbps data rate among billions of user devices, it is required to have technically rich 5G mmWave communications system. Such enhanced, intelligent, technical 5G mmWave communications system shall consider the requirements [3-7]:

5G mmWave communications system major requirements are High Data Rate, Cell Edge Data Rate, Low Latency, Simultaneous Seamless Connection, Cell Spectral Efficiency and Utilization Optimally, Optimum Cost and Mobility Support . There is need and requirement for seamless billions of user devices connection along with high data rate and low latency [4-9] . billions of user devices in 5G mmWave communications system shall also consider Cell Edge Data Rate, Cell Spectral Efficiency and utilization optimally, Optimum Cost and Mobility Support [4-7].

5G mmWave communications system considers frequencies of the mmWave which ranges from 30 GHz to 300 GHz. Considering mmWaves ranging from 30 GHz to 300 GHz has several advantages and benefits to provide high bandwidth and further benefits are [6-9]:

- Big volume of spectrum at mmWave frequencies in 5G mmWave communications system

- 5G mmWave communications system mmWaves suffer with high value channel attenuation in wireless channel. 5G mmWave communications system mmWaves also have penetration. Due to this mmWaves characteristics the frequencies can be can be recycled at a small distance

5G mmWave communications system research for mmWave frequencies is in progress for an optimum communication system by 2020 [7-9].

2.1.2 Challenges

5G mmWave communications system shows various Characteristics Challenges. Majorly 5G mmWave communications system Characteristics Challenges can be classified as shown below with following details. 5G mmWave communications system Characteristics Challenges are mmWave Transmission Characteristics and mmWave communications Network Characteristics [5-11] [34-56].

5G mmWave communications system network Characteristics challenges are:

- D2D communications
- Heterogeneous Networks
- Small Cell Backhaul

5G mmWave communications system transmission characteristics challenges are:

- Channel Characteristics

- Beamforming Technologies due to Channel Propagation Loss and
- Blocking Effect

mmWave 5G communications system will give rich user experience by 2020 and will accommodate large users along with high data connectivity. The challenges are discussed here and the solution, research and development is in progress for the discussed mmWave 5G communications system challenges. 5G mmwave communications system requires Governments rules and regulations along with standards. At present 5G mmwave communications system is emerging and developing in multiple directions which require unidirectional research development and growth.

2.1.3 Standardizations and Regulations

5G mmWave communications system research is in progress worldwide and various standardization organizations are working with the target of year 2020 for market deployment. Several research organizations are involved in research . Standard Timelines for 5G mmWave communications system is announced by ITU-R and 3GPP standard for 5G mmWave communications system is in progress with the aim of year 2020. ITU-R time line considers Vision, requirement, Proposal, Evaluation and Standard Development by 2020. 3GPP standard for 5G mmWave communications system is also in progress with the releases in various years on or before 2020 [3-9]. 5G mmWave communications system standard will incorporate and investigate new mmWave frequency bands. FCC recently has also reported mmWave frequency bands for further system

growth. As per viewpoint for 5G mmWave communications system , it is planned for commercialization by year 2020 [3-17,19].

2.2 Software Defined mmWave 5G Communication

Software defined mmWave 5G communication system can be designed and developed in a flexible architecture mode. Software defined mmWave provides flexible architecture to have more flexible control and updating options along with real time adaptive features. Software defined mmWave 5G communication system provides following features [3-7]:

- Highly Flexible
- Adaptive System reconfiguration
- Quick and Easy
- Seamless Incorporation
- Efficient Resource Utilization and more

Software defined mmWave 5G communication system along with proposed control mechanism will be very useful for upcoming system . Due to the flexibility of Software defined mmWave 5G communication system proposed solution will give high secure system as per demand and need [3-7].

2.3 5G mmWave Frequency Spectrum

High speed data rate and high bandwidth can be achieved under 5G communication system by having mmWave frequency spectrum. Several mmWave frequencies are proposed globally for 5G mmWave communication system. 5G mmWave frequency spectrum offers high speed data rate and high bandwidth . 5G communication system research is under development with mmWave frequencies. Recently; The United States Federal Communications Commission (FCC) authorizes and proposes broadband device operations in the following mmWave bands [13-16]:

- 27.5-28.35 GHz band (28 GHz band)
- 37-38.6 GHz band (37 GHz band)
- 38.6-40 GHz band (39 GHz band)

FCC proposed mmWave bands are considering high speed, low latency, high capacity and advance user experience .

2.4 Obstacles

D2D 5G wireless communications with mmWave frequencies is one of the main important aspect of the networks. The propagation losses are known in the literature due to several propagation impairments and as well as discussed in the prior art literature. 5G mmWave propagation attenuation due to various obstructions plays major role in

the wireless transmitter performance and mmWave wireless propagation paths. As per literature; it is important to plan the mmWave transmission in the urban area as the transmission losses are high due to propagation attenuation. Some of the prior art discusses using omni-directional transmissions with the mmWave communication and which causes large amount of propagation attenuation and loads transmitter with extra transmission power [23-28]. At transmission end beamforming and beam deviation methods have been proposed to avoid channel blockages or obstacles; however prior art does not specifically discusses forming intelligent grids and selecting optimum grids for mmWave transmission. It is quite important to have directional mmWave transmissions in D2D communication and need to solve problem of transmission in the existence of blockages [28-32]. Prior art discusses that major propagation impairment of channels are weather or atmospheric effects for mmWave frequencies. Building and vegetation also adds high value propagation mmWave attenuation for mmWave frequencies. So, it is very important and necessary to have the information of the various blockage effects at transmitter end so that transmitter can decide transmission accordingly [23-28]. In this research paper; we have proposed efficient method for transmitter to avoid blockage effect by avoiding obstacles. In the literature, wireless channel propagation has been discussed with various types of blockage conditions. The blockage conditions discussed and considered are atmosphere, seasons, building, tree, vegetation and etc. The atmospheric impairments are rain, water vapor, oxygen, fog and etc. The attenuation due to building and vegetation plays a high significant role in the mmWave propagation and due to which channel capacity also degrades

[21-34]. Prior art discusses for wireless sensor networks in three-dimensional (3D) environment obstacles avoidance. As per prior art the mobile anchor trajectory path shall avoid collision with obstacles [34]. In this paper, the proposal focuses on intelligently finding and selecting minimal attenuation grid or group of grids from the virtual face at the transmitter end to provide efficient mmWave propagation through wireless channel. In prior art, an obstacle avoidance approach using path planning has been discussed and it uses graph approach along with a depth-first-search based algorithm with greedy strategy [31]-[34]. In prior art, it has been discussed to deal with obstacle obstructions and avoid the losses in channel. However, the prior art literature does not specifically discuss forming virtual face and selecting optimum grids for transmission based on minimal attenuation [29-34]. Such optimum grids provide efficient power transmission and etc.

2.5 Attenuation

Prior art literature discusses SDR based transmission control to tune the transmission parameters as per demand and need. ML based prediction is not new in classifier mode or regression mode and several algorithms in supervised and un-supervised mode are described in literature to predict the data values as per training and testing data sets. However , prior art literature does not specifically discuss to predict the vegetation attenuation values using supervised learning having input parameters like frequency, depth of vegetation and output parameter learning for overall vegetation attenuation.

This proposed research predicts the vegetation attenuation in supervised learning mode by using proposed three algorithms .These three algorithms provides one of the best simulation close approximation results for the required output [5-11] [33-45].

The SDR transmission unit uses software and digital signal processing (DSP) for the transmission control (or tuning) having various input parameters like frequency, transmitter power, angle and etc. The ML prediction unit is part of the SDR system. SDR based ML system learns vegetation attenuation values for the frequencies using ML. ITU has recommended models for vegetation attenuation which is based on vegetation depth and mmWave propagation frequency. The SDR uses ML prediction unit to predict the vegetation attenuation and uses this value to calculate the SCC. Based on the calculated SCC the SDR transmitter controls the transmission in terms of the desired SCC. The location of DTU, formerly known as DCE is selected for this simulation work. The site DTU has big vegetation area and high vegetation density. In addition, the vegetation density adds significant amount of mmWave outdoor propagation attenuation; so it becomes important to know the attenuation and control it for 5G wireless communication [7-17] [45-56].

This research work provides detailed vegetation attenuation ML details for the proposed frequencies and indicates that SDR can tune the transmitter with the required data rate. We obtain vegetation attenuation details as per ITU-R model and present the attenuation values to the ML unit. Further, in this research we discuss SCC calculation using ML results along with the SDR controlling. SCC values are derived for the vegetation attenuation parameters using ML unit. In addition, SDR based control can be

used to manage SCC in different vegetation medium for the various frequencies. This research paper explore new possibilities of calculating the attenuation values based on ML algorithms like K-Nearest Neighbors , Decision Tree and Random Forest [45-87].

2.6 Atmospheric Gaseous Attenuation

mmWave frequency link suffers with atmospheric attenuation and this mmWave attenuation takes place due to atmospheric gaseous absorption. The impact of atmospheric gases on the propagation of mmWave comes in form of signal attenuation, phase shift and angle of arrival variations. Atmospheric attenuation takes place majorly due to atmospheric water vapor and atmospheric oxygen, scattering and scintillation. For certain mmWave frequencies losses are high because of the resonance gas molecules. Atmospheric water vapour attenuation is high as compare to oxygen particles due to atmospheric absorption and scattering To calculate 5G mmWave communication system; atmospheric attenuation here we are using ITU-R recommended method for calculating atmospheric water vapor attenuation and atmospheric oxygen attenuation . This model comprises various parameters like ; Frequency, Path-elevation angle, Height above mean sea level , Water vapor density and etc. The atmospheric gaseous attenuation is calculated by having equi probable summation of the atmospheric water vapor attenuation and oxygen attenuation [16-21] [43-67] .

2.7 Overview of the Work

This research presents atmospheric attenuation calculation for various atmosphere attenuation causes for 5G mmWave propagation attenuation at the frequencies 28 GHz, 37 GHz and 39 GHz for Delhi and other metro cities (India) . It is shown in the research that the atmospheric attenuation due to water vapor, oxygen, rain and fog varies and depends on the mmWave frequencies. This research also signifies the reason of the selection of the frequencies 28 GHz, 37 GHz and 39 GHz for 5G mmWave Communication System. These frequencies 28 GHz, 37 GHz and 39 GHz for 5G mmWave Communication System shows minimal attenuation.

Software Defined mmWave facilitates transmission power control in a real manner. 5G mmWave communication system transmitter and receivers can be controlled by the software defined mmwave communication system . Software Defined mmWave facilitates methods to control the transceiver as per atmospheric attenuation and demand and need of channel capacity in 5G mmWave communication system . Here intelligent an adaptive transmitter which is having machine learning (ML) based on previous trends of the attenuations decides the optimal channel capacity. Its intelligence is based on the various type of attenuations as per various conditions as described. The decision-directed adaptive receiver has the same structure as the gremlin receiver, but uses its own decisions. The adaptive ML based transmitter is useful to intelligently provide the required channel capacity.

This research presents the vegetation attenuation calculation and Shannon chan-

nel capacity calculation in the presence of the vegetation area for the 5G mmWave communication system. The mmWave vegetation attenuation and Shannon channel capacity is calculated for the frequencies. The objective of this research is to study the effect of the vegetation attenuation on the calculation of Shannon channel capacity by using SDR based 5G mmWave communication system. It is visible through graphs that as depth of the vegetation increases, the SCC decreases.

The vegetation and building attenuation adds significant amount of attenuation for mmWaves during free space propagation in 5G wireless communication system. The vegetation attenuation calculation values information provides facility to control the channel capacity using SDR. The research analysis has been presented in this research along with the demonstration of vegetation attenuation calculation for the mmWave as well as prediction of the values using ML (supervised regression mode with KNN, Decision Tree and Random Forest). This research also suggests and demonstrates that SCC can be controlled using SDR and can tune the transmitter with the desired channel data rate by the virtue of SDR based control and use of the prediction values. Such type of intelligent control benefits the link budget analysis and software automatic control as per need and demand.

In this research, we discuss minimal attenuation grid for 5G mmWave D2D devices in DTU campus area which is having open air, vegetation and building area. 5G mmWave antenna forms grids and calculates the minimal attenuation grids for atleast one of the purposes like; beamforming, minimal loss path, line of Sight (LoS), power planning, link budget planning and etc. The method effectively selects at least one

grid from amongst the grids as an optimum grid based on the minimal attenuation. Here we have simulated results and calculations are performed for the frequencies 28 GHz. Further, Shannon channel capacity has also been calculated for various seasons and respectively for vegetation and building. It is clear from simulation results and validation that the Shannon channel capacity in atmospheric impairments is higher as compare to other mentioned grid values.

This research is useful for transmission link budget for 5G mmWave Communication system for instant installation. Future work involves the identifying the various other dynamic atmospheric attenuation causes for the atmospheric attenuation for 5G mmWave Communication. This research shows the importance and consideration of the atmospheric attenuation due to atmospheric water vapour and atmospheric oxygen during transmission link budget for 5G mmWave Communication. The research suggest that the 5G mmWave Communication devices shall consider additional transmission gain to compensate for the atmospheric attenuation or path loss to provide optimum signal strength at the receiver end. Future work involves the identifying the various other causes for the atmospheric attenuation for 5G mmWave Communication and handling with high flexibility and high efficiency through SDR.

Chapter 3

Intelligent Grid Selection for Obstacle Avoidance

3.1 Motivation

The Recent research is focusing on obstacle free transmission approach to provide high directivity power signal transmission. With respect to the related prior art literature [31]-[34], in this paper we found several issues in mmWave transmission. 5G transmission can be done efficiently which are covered in our proposal and we propose the following novel elements:

- We propose, creating and selecting a virtual face for a transmitting antenna
- We Create grids in square metrix form on the selected face and map with the obstructions/ blockages on that particular face

- We calculate attenuation for each grid based on type of obstructions/ blockage
- We select one grid or group of grids from amongst the grids as a minimal attenuation grid by comparing with the rest of other grids attenuation values
- We propose efficient millimeter wave transmission passing through selected grid based on the intelligently selected grid by comparing, calculating , validating the performance with Shannon channel capacity

We have tried best to address blockage avoidance issue in mmWave propagation and as per proposed approach such issue can be resolved. By using the proposed approach the efficient mmWave transmission can take place. This research deals with the obstacle avoidance problem and provides clear approach to have low loss transmission. Further, we have tried to show through simulations that the proposed obstacle avoidance approach has high quality mmWave transmission performance with respect to without obstacle avoidance approach.

3.2 Intelligent Attenuation Grid Formation and Selection

As per Figure 3.1; flow diagram has been shown for a virtual face which is created around a static D2D transmitting antenna. The grids are created on the selected virtual face. The grids divide a face of the virtual shape into an n by n matrix. At least one grid from amongst the grids is selected as an optimum grid based on the minimal mmWave

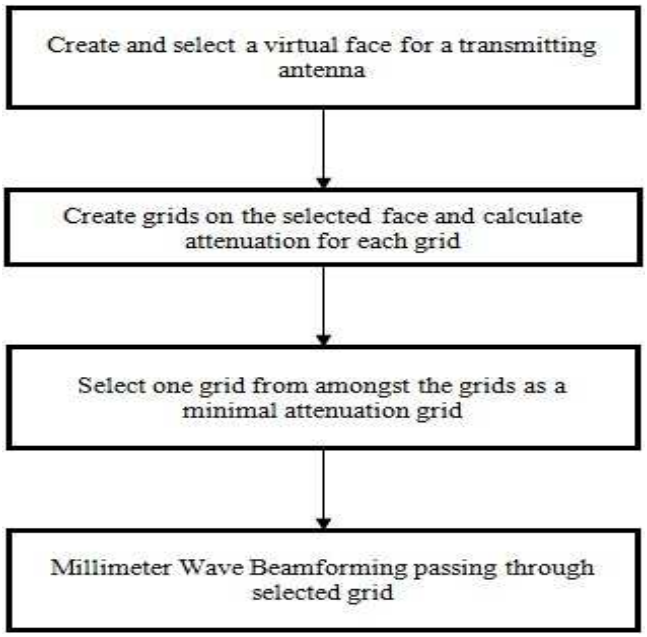

Figure 3.1: 5G mmWave grid selection for 5G transmitting antenna.

attenuation value. The 5G controller includes a grid creator and selector. It creates the grids on at least one selected face and selects at least one grid based on the minimal mmWave attenuation value. Further, beam is formed based on least attenuation grid which is one optimum grid as selected. Beam forming is used to direct and steer an antennas directivity beam in a particular direction. Shannon channel capacity can be calculated in the obstacle free grids and obstacle based grids.

At least one optimum grid allows power transmission in a direction of a particular location with minimal attenuation or losses, thereby allows power control over shaping and steering of antenna beam directivity pattern. Thus, formation of the at least one beam based on at least one optimum grid generates a high directional and efficient beam with minimal losses and overheads. System includes a beam-forming unit and

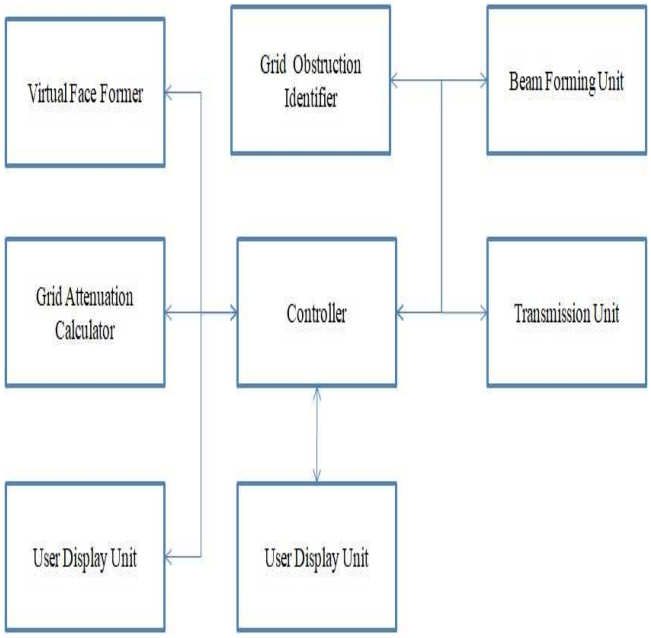

Figure 3.2: 5G mmWave intelligent grid selection and obstacle avoidance system.

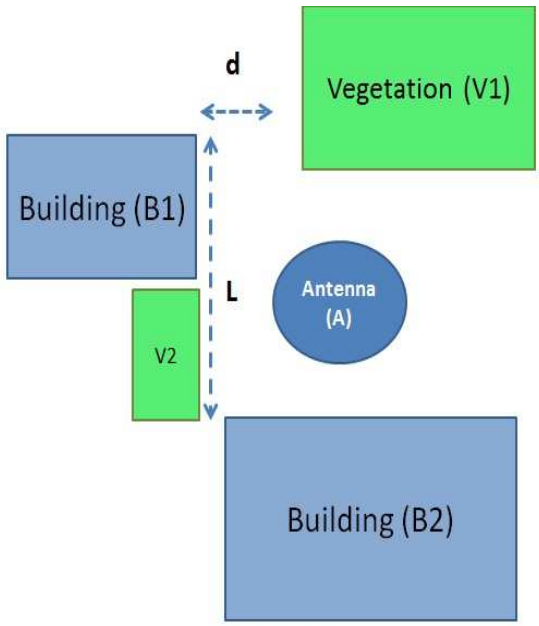

Figure 3.3: 5G mmWave site of DTU; having vegetation, atmosphere and building area.

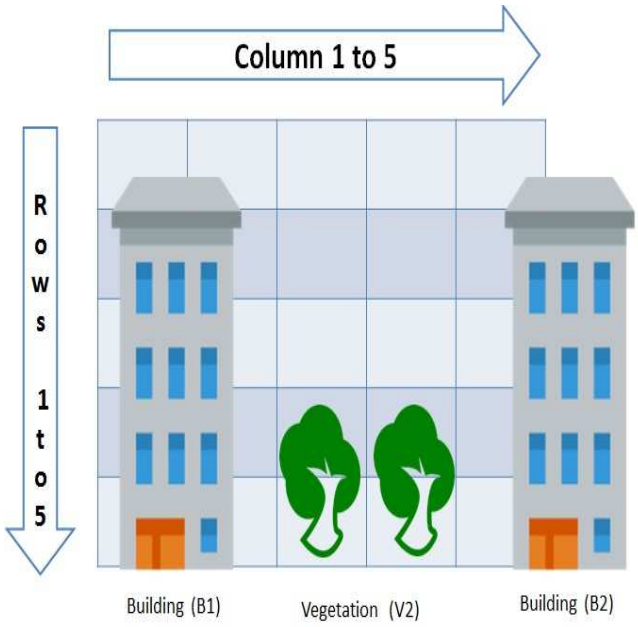

Figure 3.4: 5G mmWave grid for DTU (having vegetation, atmosphere and building area).

forms beam in accordance with the input one optimum grid which is provided by the system. As per this approach system controls and performs a function of transmitting a signal to the receiving antenna through the minimum attenuation grid and transmitting antenna transmits the signal in the direction of the receiving antenna.

As per figure 3.1, device-to-device grid selection for 5G mmWave communication system is shown for one of the transmitting device. As per our work; it is considered that the transmitting, receiving device and obstacles are stationary. 5G grid attenuation controller includes a location detection modular to detect the antenna location and it dynamically detects the current location of the transmitting antenna. The transmitting antenna is part of D2D communication system [4]-[5], [33]. The system has storage

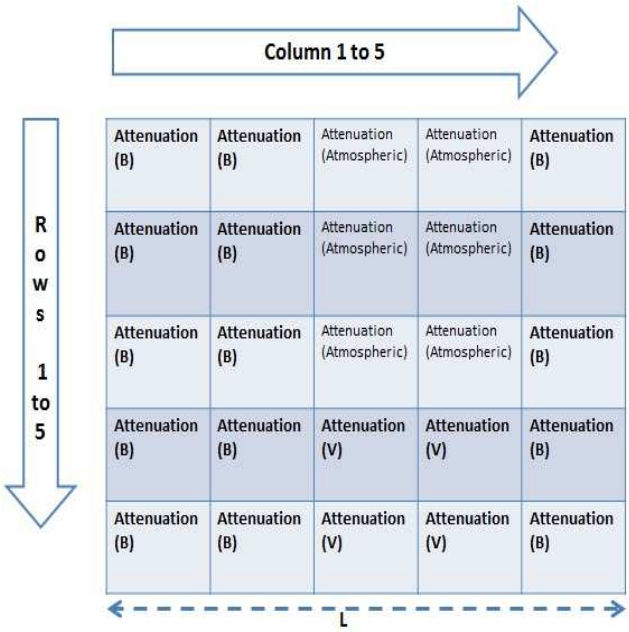

Figure 3.5: 5G mmWave grid with type of attenuations for DTU; having atmospheric, vegetation and building area .

unit to store the data pertaining to obstructions as obstruction data.

Figure 3.2 5G mmWave intelligent grid selection and obstacle avoidance system. The obstruction data can be determined, evaluated or processed and such processing can take place for various terminals/devices/systems used by the various users or antennas. Further obstruction data can be obtained from system. The system can predict /forecast obstruction details such as future building projects and weather conditions. System creates the virtual face based on the received data. The virtual shape or layer is selected and created such that the transmitting antenna is at centre of the virtual face. Further, controller creates the one or more grids on the selected face in nxn metrix form. Accordingly, based on the values of obstructions and the received stored

data, the controller divides the selected face of the virtual mode into an n by n matrix that forms the grids. The controller obtains the attenuation values of the obstructions which are received data from the storage and run time calculations as per the mapped grids with obstructions or obstacles. The controller calculates the grid attenuation and forms the low or high zone attenuation grids and selects the minimal attenuation zone for the beamforming or channel capacity or link power budget or line of sight path for mmWave transmission.

3.3 DTU Campus mmWave Attenuation

In this proposed research simulation, we have considered DTU campus which is formerly known as DCE, located in New Delhi, India. Figure 3.3, illustrates 5G mmWave site for DTU; having vegetation and building area [20]. DTU campus has sports ground, various outdoor game grounds, indoor game complex, library, academic block, administrative and hostel blocks in the campus. DTU also has high vegetation area. DTU site is rich with all of the mixture of buildings, equal air distribution and vegetation. Based on the variety of obstructions and site richness; we are using this area for our simulations. Here we have identified a position of the 5G stationary transmitter which is near the following hostel blocks and sports ground:

- Sir C. V. Raman Hostel
- Sir J.C. Bose Hostel

At this 5G transmitter location, we are calculating attenuations due to obstacles and considering calculation experimental site for grid selection based on vegetation, seasonal atmosphere and building attenuation calculations. This site has buildings, open air and average size Indian vegetation area. The calculations are performed for the university campus by considering equi-probable summation of the attenuation and also we have considered full vegetation for the summer and rainy season [22]-[24]. In winter season we have considered no vegetation or can say out of leaf vegetation attenuation; such type of attenuation is due to branches or trunk of the vegetation. In this calculation experiment we have taken average vegetation density as 10 meter vegetation depth for mmWave propagation along with the consideration equal spaced, equal densed vegetation. DTU site also consists of small vegetation, buildings, concrete roads, soil, sand and grass. This calculation also takes into account no-air to have calculation and results meaningful so that it can be used by the power planning engineer in 5G communication system [16].

As shown in figure 3.4 this site DTU consists vegetation and building area along with open area in the boys hostel area to have D2D 5G transmitter. This figure 3.4 shows side view of the site (based on virtual face) where; we are calculating grid based attenuation and optimum grid selection for transmission. This side view is shown along with 5x5 metrix having grids which are equally spaced. The grids are mapped with the type of obstructions/ blockage (vegetation, building and atmosphere).

Referring to figure 3.5, the grids are created on the selected virtual face and it is considered that row and column shall be equal (here 5x5) for less complex calculations.

5G grid creator and selector module divides the selected virtual face of the virtual dimensional shape into m by m matrix. This matrix forms grids inside virtual face. In this virtual face; user can also enter number of rows or column for the virtual face.

Further system identifies the type of the obstructions for each grid based on the system blockage mapping or obstruction identifications. Each grid is calculated with the attenuation values as per identified type of obstructions. As per proposal; attenuation values are identified based on type of obstructions. Further, calculations are performed by considering the type of obstructions and minimal attenuation value grid is identified by comparing the rest of the grids for efficient transmission. For the identified vegetation blockage, we have used the simulation model through software coding. As per Fitted- International Telecommunication Union (FITU-R) model the vegetation attenuation Av is given by equation (3.1) [21]-[25] :

3.3.1 Radius of Coverage and Visibility

as per literature, we are able to rewrite the radius of the transmitter coverage. The radius of coverage r in km [**?**] for transmitter is expressed as

$$r = R\cos^{-1}\left(\frac{R}{R+h}\cos\alpha\right) - R\alpha \tag{3.1}$$

where h is the height of the transmitter in km, R is the earth radius ($R = 8300\,km$) in km, and α is the elevation angle in $deg.$. The coverage radius is as a function of elevation angle and the altitude of the transmitter. As elevation angle increases the radius of coverage decreases and it increases with height of transmitter.

The visibility [**?**] is defined as the ratio of propagation path in LOS (Line of Sight) situation to the total LOS and NLOS (Non Line of Sight) situation. The visibility is expressed as

$$p_v(\alpha, \theta) = (\sin \alpha)^{0.01} \qquad \text{for } \theta = 0^o \tag{3.2a}$$

$$p_v(\alpha, \theta) = (\sin \alpha)^{\sin \theta} \qquad \text{for } \theta = 30^o, 60^o, 90^o \tag{3.2b}$$

where (α) is the elevation angle in $deg.$ and (θ) is the azimuth angle in $deg.$, $\theta = 0^o$ is in the positive y-axis direction and $\theta = 90^o$ is in the negative x-axis direction explained. It is clear that visibility increases with elevation angle.

3.3.2 Ray Tracing Model

We have developed the mmWave propagation model using geometrical optics (GO) and uniform theory of diffraction (UTD) [**?**] for urban site with the blocks of buildings. The urban model to be presented has been selected to represent the area at DTU, New-Delhi. This model includes LOS component and NLOS component of the signal with reflection and diffraction mechanism effects from buildings and streets. The model employs a virtual transmitter located around the area under simulation in order to overcome the difficulty of applying the ray launching methods for the large separation such as from the transmitter to the mobile station (MS).

The transmitter is positioned at $\theta = 90^o$ and α varies form 20^o to 80^o. The building model are taken with same height $h_b = 15\,m$, length $l_b = 9\,m$ and width $w_b = 9\,m$ are

$Type\,of$ $object$	$Relative\,dielectric$ $constant\ \epsilon_r$	$Conductivity$ $\sigma\,(\Omega^{-1}m^{-1})$
$Building$	3	0.005
$Street$	15	7

Table 3.1: Parameters used in the ray tracing simulation

taken same for complexity reduction. The width of the street w_s is $14\,m$ and assumed to be equal in this model. The mobile station (MS) has $2\,m$ in height and is located at the center of the street $(d_{ms} = w_s/2)$ between building 1 and building 2 with the ray impinging the MS from an arbitrary direction.

In this simulation we have considered five categories of ray. The ray categories are direct (i.e. LOS), single reflection from building, single reflection from street, diffraction from rooftop of the building, and diffraction from building corner. The rays outside the above categories are assumed to leave the target and terminated from the simulation environment. All surfaces in real propagation environments are finite, also edges and corners have to be considered. It is more important for radio wave propagation. Table 3.1 shows electrical parameters that is used in this ray tracing simulation model. In the simulation, two situations are considered, one is LOS and other is NLOS situation. Total complex vector summation includes power impinging the MS separately from direct LOS ray, multipath scattered power (total power from rays except direct LOS ray).

Geometrical optics (GO) and uniform theory of diffraction (UTD) is used in simulation to calculate the attenuation in radio wave propagation. UTD is an extension method of a GO to include diffraction. The transmitting and receiving antennas both are assumed to be an isotropic antenna with a $0\,dB$ gain. The electric field of the rays arriving at the receiving antenna of MS is calculated using the following formulas for direct ray (E_{LOS}), reflected ray (E_R), and diffracted ray (E_D), respectively.

$$E_{LOS} = E_0 \, \frac{e^{-j\beta d_0}}{d_0} \qquad (direct\, ray) \tag{3.3a}$$

$$E_{Refl} = E_0 \, \bar{R} \, \frac{e^{-j\beta(s_1+s_2)}}{s_1+s_2} \qquad (reflected\, ray) \tag{3.3b}$$

$$E_{Diff} = \frac{E_0}{s_3} \, \bar{D} \sqrt{\frac{s_3}{s_4(s_3+s_4)}} \; e^{-j\beta(s_3+s_4)} \, (diffracted\, ray) \tag{3.3c}$$

where $k = \lambda/2\pi$ is the propagation constant, E_0 is the emitted electric field from transmitter, d_0 is the the direct path length, s_1 is the distance from the transmitter to the reflection point, s_2 is the distance from reflection point to the receiver, S_3 is the path length from the transmitter to the diffraction point, and s_4 is the path length from diffraction point to the receiver. $\bar{R}$ denotes a Fresnel dyadic reflection coefficient and $\bar{D}$ denotes a dyadic finite conductivity edge diffraction coefficient.

The Fresnel dyadic reflection coefficient $\bar{R}$ is given by

$$\bar{R} = R_{\parallel} e^i_{\parallel} . e^r_{\parallel} + R e^i_{\perp} . e^r_{\perp} \tag{3.4a}$$

$$R_{\perp}(y) = \frac{\sin(y) - \sqrt{(\epsilon_c - \cos^2(y))}}{\sin(y) + \sqrt{(\epsilon_c - \cos^2(y))}} \qquad for \perp polarization \tag{3.4b}$$

$$R_{\parallel}(y) = \frac{\epsilon_c \sin(y) - \sqrt{(\epsilon_c - \cos^2(y))}}{\epsilon_c \sin(y) + \sqrt{(\epsilon_c - \cos^2(y))}} \qquad for \parallel polarization \tag{3.4c}$$

where y is the incidence angle, ϵ_c is the relative dielectric constant given by

$$\epsilon_c = \epsilon_r - j60\sigma\lambda \tag{3.5}$$

ϵ_r is the permittivity, and σ is the special conductivity of the reflecting surface.

The Diffraction dyadic coefficient $\bar{D}$ for smooth finite conductive surface wedges are given by

$$\bar{D}(\emptyset,\, \emptyset',\, \beta_o) = -\beta'_o.\beta_o D_s(\emptyset,\, \emptyset';\, \beta_o) - \emptyset'.\emptyset D_h(\emptyset,\, \emptyset';\, \beta_o) \tag{3.6}$$

where $D_{s,h}$ is given by

$$D_{s,\,h}(\emptyset,\, \emptyset',\, \beta_o) = \frac{-e^{(-j\frac{\pi}{4})}}{A_1}(C_1 \,+\, C_2 \,+\, C_3 \,+\, C_4) \tag{3.7a}$$

$$A_1 = 2n\sqrt{(2\pi k)}\sin\beta_0 \tag{3.7b}$$

$$C_1 = \cot\left(\frac{\pi + (\emptyset - \emptyset')}{2n}\right).F(kLa^{+}(\emptyset - \emptyset')) \tag{3.7c}$$

$$C_2 = \cot\left(\frac{\pi - (\emptyset - \emptyset')}{2n}\right).F(kLa^{-}(\emptyset - \emptyset')) \tag{3.7d}$$

$$C_3 = R_n^{\perp,\parallel} \cot\left(\frac{\pi+(\emptyset+\emptyset')}{2n}\right).F(kLa^+(\emptyset+\emptyset')) \tag{3.7e}$$

$$C_4 = R_0^{\perp,\parallel} \cot\left(\frac{\pi-(\emptyset+\emptyset')}{2n}\right).F(kLa^-(\emptyset+\emptyset')) \tag{3.7f}$$

where

$$F(x) = 2j\surd(x)exp(jx)\int_{\surd(x)}^{\infty} exp(-j\tau^2)\,d\tau \tag{3.8}$$

is a Fresnel integral

$$L = \frac{s_3 s_4}{s_3 + s_4} \tag{3.9}$$

and

$$a^{\pm}(\beta) = 2\cos^2\left(\frac{2\pi nN^{\pm}-(\beta)}{2}\right) \tag{3.10a}$$

$$\beta = \emptyset \pm \emptyset' \tag{3.10b}$$

and $N\pm$ are the integers that most nearly satisfy the equations

$$2\pi nN^+ - (\beta) = \pi \tag{3.11a}$$

$$2\pi nN^- - (\beta) = -\pi \tag{3.11b}$$

$R_n^{\perp,\parallel}$ is the reflection coefficient for the parallel and perpendicular polarization for zero phase, incidence angle $\emptyset'$. $R_0^{\perp,\parallel}$ is the reflection coefficient for the parallel and perpendicular polarization for n face, reflection angle $n\pi - \emptyset$.

3.3.3 Urban Propagation Path Loss

The vector addition E_{Total} [**?**] of received electric field components at MS in urban are is expressed as

$$E_{Total} = \sum_{i=1}^{5} \left[\sum_{j=1}^{n_i} E_{ij} \right] \tag{3.12}$$

where E_{ij} is the received electric field of the j^{th} ray for i^{th} category of the rays, and n_i is the total number of rays of the i^{th} category.

The total propagation path loss (L_{Urban}) in dB is given as

$$L_{Urban} = 20log\left(\frac{\lambda}{4\Pi}\frac{|E_{Total}|}{|E_0|}\right) \tag{3.13}$$

It is shown that urban site propagation path loss model is the function of elevation angle, azimuth angle, and frequency. It is clear that the path loss decreases as elevation angle increases for a constant frequency and path loss increases as frequency increases for constant elevation angle. For the frequencies $28\,GHz$, $37\,GHz$ and $39\,GHz$ urban site attenuation values are explained for some of the values of elevation angle (for elevation angle $\alpha = 10^o,\ 20^o,\ 30^o,\ 40^o,\ 50^o,\ 60^o,\ 70^o,\ and\ 80^o$).

For the identified building blockage, simulation is performed through software defined coding. D2D 5G total urban mmWave propagation path loss (AUrban) in dB is given below for the buildings in DTU area as per equation (3.13, 3.14) [20-25]: Here, Î» is the wavelength of the transmitted mmWave signal, E0 is the emitted electric field from the 5G D2D transmitter. ETotal is the vector addition of the received electric field components at D2D unit in DTU building area as per equation (3.13, 3.14). Further, Lambda is mmWave wavelength.

3.4 Effect of Weather Impairments

Propagation factors considered for inclusion in the overall prediction procedure are gaseous absorption, cloud attenuation, fog attenuation, rain attenuation, and dust attenuation. Low-angle (around 5^o) fading is a refractive phenomena encountered on very low elevation angle paths when the propagation path passes at grazing incidence across a boundary between two air masses of different refractive index, thereby causing focusing and defocusing of the energy as the air/air boundary moves with respect to the path. Here the minimum elevation angle is 15^o. Calculation procedures used for the selected components are presented below.

3.4.1 Attenuation Due to Atmospheric Gases

When mmWave pass through the atmosphere, they under go interactions with gas molecules that are present in the atmosphere. The atmospheric gaseous constituents in percentage is : N_2 78.08%, O_2 20.95%, Ar 0.93%, CO_2 0.03450% (varies with location), Ne 0.00180%, He 0.00052%, CH_4 0.00014%, Kr 0.00010%, H_2 0.00005%, traces of: SO_2, O_3, NO and NO_2.

Each of these gas molecules interacts with the mmWave, the interactions may or may not cause transmission loss. Transmission losses are especially high near the resonances of the molecules. These losses are greater at certain frequencies, coinciding with the mechanical resonant frequencies of the gas molecules. The important resonances for gaseous absorption up to 300 GHz are those from atmospheric water vapour

and oxygen. The quantities and effects of resonant gases are negligible compared to water vapor at typical millimeter frequencies.

The specific attenuation [**?**] of water vapor γ_w in dB/km is given by

$$\begin{aligned}\gamma_w(f) &= \left(0.05 + 0.021\rho + \frac{3.6}{(f-22.2)^2+8.5}\right. \\ &+ \left.\frac{10.6}{(f-183.3)^2+9} + \frac{8.9}{(f-325.4)^2+26.3}\right) f^2 \rho\, 10^{-4} \end{aligned} \tag{3.14}$$

where ρ is the water vapour concentration in g/m^3 and f is the frequency in GHz. For Delhi ρ varies from $6 - 10\, g/m^3$. The total water vapour attenuation is given by

$$A_w = \frac{h_w \gamma_w}{\sin(\theta)} \qquad \theta > 10^o \tag{3.15a}$$

$$A_w = \frac{\gamma_w \sqrt{R_e h_w}}{\cos(\theta)} F(tan(\theta)\sqrt{R_e/h_w}) \qquad \theta \leq 10^o \tag{3.15b}$$

where R_e is the effective earth radius including refraction $(8500km)$, θ is the elevation angle and $F(x)$ is given by

$$F(x) = \frac{1}{0.661x + 0.339\sqrt{x^2 + 5.51}} \tag{3.16}$$

h_w is the equivalent height of water vapor in km given by

$$h_w = h_{wo}\left(1 + \frac{3}{(f-22.2)^2+5} + \frac{5}{(f-183.3)^2+6} + \frac{2.5}{(f-325.4)^2+4}\right) \tag{3.17}$$

$h_{wo} = 1.6\, km$ in clear weather outside the absorption regions. It is clear that the water vapour has resonances at 22GHz. The attenuation changes with the amount of

water vapour in the atmosphere. At this frequency, absorption results in high attenuation of the radio signal.

The specific attenuation γ_o due to oxygen is given by

$$\gamma_o(f) = \left(7.19 \times 10^{-3} + \frac{6.09}{f^2 + 0.277} + \frac{4.81}{(f-57)^2 + 1.5}\right) f^2 \times 10^{-3}\,, \quad f < 57GHz \tag{3.18a}$$

$$\gamma_o(f) = \left(3.79 \times 10^{-7} f + \frac{0.265}{(f-63)^2 + 1.59} + \frac{0.028}{(f-118)^2 + 1.47}\right)(f+198)^2 \times 10^{-3}\,. \quad f > 63GHz \tag{3.18b}$$

where f is the frequency in GHz. The total attenuation in dB is given by

$$A_o = \frac{h_o \gamma_o}{\sin(\theta)}, \qquad \theta > 10^o \tag{3.19a}$$

$$A_o = \frac{\gamma_o \sqrt{R_e h_o}}{\cos(\theta)} F(tan(\theta)\sqrt{R_e/h_o})\,. \qquad \theta \leq 10^o \tag{3.19b}$$

where h_o is the equivalent height of the oxygen layer.

Between $57\,GHz$ and $63\,GHz$ the model does not apply. An average value of $14.9\,dB/km$ is used. Oxygen has strong bands of resonances around $57 - 60\,GHz$. It is clear that O_2 has strong band of attenuation at $57\,GHz$ corresponding to peak. The spectral regions between the absorption peak provides window where propagation can more readily occur. The transmission windows are at about $35\,GHz$, and $94\,GHz$.

The attenuation due to gaseous absorption A_g in dB due to two constituent gases oxygen and water vapor is given by

$$A_g = A_w + A_o \tag{3.20}$$

The total atmospheric attenuation due to water vapor and oxygen can be calculated for a city. The spectral region between the absorption peaks provides window where propagation can more readily occur. The transmission windows are at about $35\,GHz$, and $94\,GHz$.

3.4.2 Attenuation Due to Fog

Fog remains suspended in the atmosphere. Attenuation due to fog is determined by the quantity of water per unit volume, size of the droplets and radio wave frequency. The specific attenuation as per literature, in dB/Km, within a fog as per Rayleigh approximation is given by

$$\gamma_c = K_l M \tag{3.21}$$

where K_l is the specific attenuation coefficient in $(dB/km).(g/m^3)$ and M is liquid water density for fog in g/m^3. Over northern India, fog occur for a considerable period during winter season. Radiative fog forms during the high pressure zone, sky is clear and winds are calm. The advection fog is caused by the induction of moist winds from South West (SW) (Arabian Sea), thus relatively warm and moist air overrides a substantially cooler surface, causing fog formation in the layer of the atmosphere just

above ground. The relation between water content and visibility of fog (in g/m^3) for two types of fog are

$$M = (42.0V)^{-1.54}\,, \quad \text{radiation fog}$$

$$M = (18.35V)^{-1.43}\,, \quad \text{advection fog}$$

where V is the visibility for fog and its relationship with optics attenuation coefficient α_0 is given as

$$V = (3.912 \times 10^{-3})/\alpha_0\,. \tag{3.22}$$

For Delhi, during fog the optical visibility reduces to less than 100 meter for 0.76% of the time in a year (here we have taken $V = 100\,m$) and the specific humidity in the lowest atmosphere varies $6.0 - 8.0\,gm/m^3$. Here the advection type fog is considered for calculations as this fog is more persistent than radiative fog. On the basis of mathematically modeled Rayleigh scattering, the K_l can be calculated up to 1000 GHz and given as

$$K_l = \frac{0.819f}{\epsilon''(1+\eta^2)} \qquad (dB/km).(g/m^3) \tag{3.23}$$

where f is the frequency in GHz and η is given by

$$\eta = \frac{2+\epsilon'}{\epsilon''} \tag{3.24}$$

The complex dielectric permittivity of water is given by

$$\epsilon''(f) = \frac{f(\epsilon_0 - \epsilon_1)}{f_p[1+(f/f_p)^2]} + \frac{f(\epsilon_1 - \epsilon_2)}{f_s[1+(f/f_s)^2]} \tag{3.25}$$

$$\epsilon'(f) = \frac{\epsilon_0 - \epsilon_1}{[1+(f/f_p)^2]} + \frac{\epsilon_1 - \epsilon_2}{[1+(f/f_s)^2]} + \epsilon_2 \tag{3.26}$$

where

$$\begin{aligned}
\epsilon_0 &= 77.6 + 103.3(\theta - 1)\,, \\
\epsilon_1 &= 5.48\,, \\
\epsilon_2 &= 3.51\,, \\
\theta &= \frac{300}{273.15 + t}\,,
\end{aligned} \tag{3.27}$$

here t is the temperature of the fog layer in ^oC. (for Delhi the minimum temperature is 7.3^oC for the month of January). The principal and secondary relaxation frequency in GHz are

$$\begin{aligned}
f_p &= 20.09 - 142(\theta - 1) + 294(\theta - 1)^2 \\
f_s &= 590 - 1500(\theta - 1)
\end{aligned} \tag{3.28}$$

The attenuation due to fog depends on the specific attenuation γ_c and the distance propagated by the radio waves L_s during fog. L_s for varying heights of transmitter and fog along with elevation angle are

$$\begin{aligned}
L_s &= \tfrac{h_T - h_S}{\sin\theta}\,, && \theta \geq 5^o \quad h_T < h_{fog} \\
L_s &= \tfrac{h_{fog} - h_S}{\sin\theta}\,, && \theta \geq 5^o \quad h_T \geq h_{fog} \\
L_s &= \tfrac{2(h_T - h_S)}{\sin\theta + \sqrt{\sin^2\theta + \frac{2(h_T - h_S)}{k_e a}}}\,, && \theta < 5^o \quad h_T < h_{fog} \\
L_s &= \tfrac{2(h_{fog} - h_S)}{\sin\theta + \sqrt{\sin^2\theta + \frac{2(h_{fog} - h_S)}{k_e a}}}\,, && \theta < 5^o \quad h_T \geq h_{fog}
\end{aligned} \tag{3.29}$$

where h_S is the height of earth station above mean sea level in kilometer, h_T is the height of target (transmitter) above sea level in kilometer, h_{fog} is the fog top layer

in kilometer, θ is the elevation angle in degree, k_e is the effective radius coefficient, and a is the radius of earth. The values of the parameters considered for Delhi, India, are: cell radius $r = 50\,km$, $h_S = 0.213\,km$, $h_T = 20\,km$, $h_{fog} = 3\,km$, $\theta = 21.8^o$, $k_e = 4/3$, and $a = 6370\,km$. The average altitude of Delhi is $293m$ above sea level. As $\theta > 5^o$ and $h_T > h_{fog}$ so the second condition of (3.29) is used to calculate L_s.

Further, the attenuation due to fog is given as

$$\begin{aligned} A &= \gamma_c L_s\,, \\ &= K_l M L_s\,. \end{aligned} \tag{3.30}$$

In Delhi December and January is the period for fog. The temperature during these months varies between 4^oC to 22^oC.

As per observations for the attenuation due to fog for different temperatures, we observe that the attenuation is significant for the frequencies above 20 GHz. Further we also observe that as the temperature increases the attenuation due to fog decreases, implying that for high temperatures the effect of water molecules on electromagnetic waves is less.

3.4.3 Attenuation Due to Rain

Attenuation because of raindrops is greater than attenuation because of other forms of precipitation. Rain attenuation is caused by absorption, in which the raindrop acts as a poor dielectric, absorbs power from the radio wave and dissipates the power by scattering or heat loss. Raindrops cause greater attenuation by scattering than by absorption

at frequencies above 100 megahertz. The modified ITU-R slant path rain attenuation estimates the median rain attenuation based on rain rate, path length and polarization. It is a theoretical prediction model based on the geophysical observations of rain structure, rain rate, and the vertical variation of atmospheric temperature. The model is summarized as

Specific attenuation γ_R in dB/km is given by

$$\gamma_R = kR^{\alpha} \tag{3.31}$$

where R is the rain rate in mm/hr, k and α are frequency and polarization dependent coefficients given by

$$k_H = 4.0848 \times 10^{-5} f^{(1.4550+0.395 \ln f)} \qquad 1 \leq f < 15\, GHz \tag{3.32a}$$

$$= 2.8790 \times 10^{-7} f^{(5.7988-0.5431 \ln f)} \qquad 15 \leq f \leq 400\, GHz \tag{3.32b}$$

$$\alpha_H = 0.8424 + \frac{0.3151}{(\ln f - 2.0462)^2 + 0.6394} \qquad 1 \leq f < 15\, GHz \tag{3.33a}$$

$$= 0.6879 + 0.7005 exp(-0.02600 f) \qquad 15 \leq f \leq 400\, GHz \tag{3.33b}$$

$$k_V = 3.7332 \times 10^{-5} f^{(1.4169+0.4067 \ln f)} \qquad 1 \leq f < 15\, GHz \tag{3.34a}$$

$$= 2.9220 \times 10^{-7} f^{(5.7189-0.5297 \ln f)} \qquad 15 \leq f \leq 400\, GHz \tag{3.34b}$$

$$\alpha_V = 0.8158 + \frac{0.2850}{(\ln f - 2.0775)^2 + 0.5694} \qquad 1 \leq f < 15\, GHz \tag{3.35a}$$

$$= 0.6887 + 0.6371 exp(-0.02493 f) \qquad 15 \leq f \leq 400\, GHz \tag{3.35b}$$

The coefficients k and α can be calculated for linear and circular polarization, and for all path geometries by following equations

$$k = [k_H + k_V + (k_H - k_V)\cos^2\theta \cos(2\tau)]/2 \tag{3.36}$$

$$\alpha = [k_H \alpha_H + k_V \alpha_V + (k_H \alpha_H - k_V \alpha_V)\cos^2\theta \cos(2\tau)]/2k \tag{3.37}$$

where θ is the path elevation angle, and τ is the polarization tilt angle relative to the horizontal for circular polarization $\tau = 45^o$.

The rain height h_g in km is given by

$$h_g = h_o + 0.36 \qquad R_{0.01} < 10\, mm/h \tag{3.38a}$$

$$= \quad h_o + 0.36 + \log \frac{R_{0.01}}{10} \qquad R_{0.01} \geq 10\, mm/h \tag{3.38b}$$

where h_o is the isotherm height in km, and $R_{0.01}$ is the rain rate.

The slant path length L_s in km below the rain height is given by

$$L_s \quad = \quad \frac{h_g - h_s}{\sin\theta} \qquad \theta \geq 5^o \tag{3.39a}$$

$$= \quad \frac{2(h_g - h_s)}{\left(\sin^2\theta + \frac{2(h_g - h_s)}{R_e}\right)^{1/2} + \sin\theta} \qquad \theta < 5^o \tag{3.39b}$$

where h_s is the height above the mean sea level, and θ is the elevation angle.

The horizontal projection L_G of slant path in km is given by

$$L_G = L_s \cos\theta \tag{3.40}$$

The path adjustment factor is given by

$$r_{0.01} \quad = \quad \frac{1}{1 + 0.842 L_G^{0.329} \gamma_R^{0.4} - 1.35(1 - e^{-2.97 L_G})}$$

$$for\ f \leq 15 GHz \tag{3.41a}$$

$$= \quad \frac{1}{1 - 0.519 L_G^{0.702} \gamma_R^{-0.626} - 3.18(1 - e^{0.0572 L_G})}$$

$$for\ f > 15 GHz \tag{3.41b}$$

The values of the parameters considered for Delhi, India, are: $h_o = 5\, km$, $R_{0.01} = 120\, mm/hr$, $h_s = 0.213\, km$, $\theta = 15^o$. As $\theta > 5^o$, $f > 15\, GHZ$, and $R_{0.01} > 10\, mm/h$ so the first, second and second condition of (3.29) (3.29) is used to calculate h_g, $r_{0.01}$, and L_s.

The total attenuation due to rain $A_{0.01}$ exceeded for 0.01% of an year in dB is determined as

$$A_{0.01} = \gamma_R L_s r_{0.01} \tag{3.42}$$

A summary of total attenuation rain model for 0.01% of a year is discussed and the attenuation due to rain is frequency dependent. It is described that as frequency increases the attenuation due to rain increases.

For the identified atmosphere blockage, we have used ITU recommended methods for simulation. For atmospheric attenuation, the total value is equiprobable sum of water vapour attenuation and oxygen attenuation. Water vapor attenuation Aw is expressed as mentioned. Water vapor specific attenuation $gammaw$ is frequency dependent and measured in dB/km. Here, hw is the equivalent height of water vapor in km. Re is the effective earth radius, Î¸ is the elevation angle and F(x) is a function as per literature in equations. For atmospheric oxygen attenuation Ao; attenuation in dB is given by the literature [22]. In equations oxygen specific attenuation is $gammao$. Here, ho is the equivalent height of the oxygen layer. Re is the effective earth radius, Î¸ is the elevation angle and F(x) is a function as per literature [22].

3.5 DTU Campus Grids

As per DTU site calculation example; for finding out minimal attenuation path during mmWave propagation and to calculate the mmWave propagation losses due to atmosphere in 5G wireless communication system, it is considered that both devices

transmitter and receiver are stationary in DTU area. Referring to Figure 3.5 grids are created inside a virtual face as side view is also illustrated for obstructions like building, vegetation and atmospheric attenuation. As per calculations; attenuation values are identified as per type of obstructions atmosphere, vegetation and building. Attenuation values for atmosphere, vegetation and building are calculated by considering type of obstructions. Further minimal attenuation value grid is identified for optimum transmission path as considering blockage avoidance based on relative attenuation values comparison among other grid attenuation values.

Further, 5G mmWave grid attenuation causes for 5X5 matrix are shown in figure 3.6-3.8. These figures indicate type of grid attenuations causes for different seasons of India like summer, rain and winter. The figure shows the type of the obstructions for each grid as per 5G transmitter antenna location in DTU site having mixture of atmosphere, vegetation and building. Further, the grids will have two factor attenuation due to the one of obstruction vegetation or building and additional with atmosphere as atmosphere attenuation which will be in all grids. Figures 3.6-3.8 show the grids for 5G mmWave propagation with the type of attenuations for summer, rain and winter seasons as Atmospheric attenuation: Summer (As), Rain (Ar), Winter (Aw); Building Attenuation (Ab); Vegetation Attenuation: In-Leaf (Avi); Vegetation Attenuation: Out-Leaf (Avo). Figures 3.6-3.8 indicates the causes of the blockage along with the notation of the attenuations. Below are the notation used to depict in figures 3.6-3.8:

- Atmospheric attenuation

Summer (As)

Rain (Ar)

Winter (Aw)

- Building Attenuation (Ab)
- Vegetation Attenuation

  In-Leaf (Avi)

  Out-Leaf (Avo)

Obstruction data can be obtained by calculating obstruction details such as building, vegetation and weather condition at later instance of time. Here we have used software simulation coding to calculate the values and run the program along with the following assumptions:

- Heights of buildings = 20 meter
- Vegetation heights = 2/5 * building height = 8 meter
- Depth of vegetation = 10 meters
- Angle building elevation = 45 degree
- Ab = Building Attenuation
- Aas = Summer Atmosphere Attenuation
- Aar = Rainy Atmosphere Attenuation

- Aaw = Winter Atmosphere Attenuation
- As = Aas
- Ar=Aar+rain
- Aw=Ar=Aar+ winter fog
- Avi = in leaf Vegetation Attenuation (summer rain)
- Avo = out leaf Vegetation Attenuation (winter)

We have used FITU-R model to calculate vegetation propagation attenuation for in-leaf and out-of-leaf attenuation with the various seasons. FITU-R model is employed to calculate vegetation propagation attenuation for the frequency 28 GHz and simulated with the same. For calculating urban area attenuation for 5G mmWave communication; we are using geometrical optics (GO) and a uniform theory of diffraction (UTD) to calculate urban area mmWave propagation attenuation. GO and UTD are applicable to mmWave frequency range and provide reliable prediction for the simulation frequency [19]-[25].

As per literature, we have used ITU recommended models to calculate the atmospheric mmWave propagation attenuation [22]. This model is applicable to mmWave frequency range and provides reliable prediction for the proposed site. Here we have simulated results and calculations are performed for the frequencies 28 GHz. Figures 3.9-3.11 show the grids with blockage attenuations values (vegetation in-leaf, vegetation no-leaf, atmospheric and building) with type of attenuations for summer, rain and

Ab+As	Ab+As	As	As	Ab+As
Ab+As	Ab+As	As	As	Ab+As
Ab+As	Ab+As	As	As	Ab+As
Ab+As	Ab+As	As	As	Ab+As
Ab+As	Ab+As	Avi+As	Avi+As	Ab+As
Ab+As	Ab+As	Avi+As	Avi+As	Ab+As

Figure 3.6: 5G mmWave grids with type of attenuations for summer season .

Ab+Ar	Ab+Ar	Ar	Ar	Ab+Ar
Ab+Ar	Ab+Ar	Ar	Ar	Ab+Ar
Ab+Ar	Ab+Ar	Ar	Ar	Ab+Ar
Ab+Ar	Ab+Ar	Ar	Ar	Ab+Ar
Ab+Ar	Ab+Ar	Avi+Ar	Avi+Ar	Ab+Ar
Ab+Ar	Ab+Ar	Avi+Ar	Avi+Ar	Ab+Ar

Figure 3.7: 5G mmWave grids with type of attenuations for rainy season.

winter seasons for the frequency 28 GHz. In these figures, consolidated attenuation values are shown after summing atmospheric attenuation with respect to vegetation attenuation or building attenuation as per seasons summer, rain and winter for the mentioned frequency as shown and discussed here.

Ab+Aw	Ab+Aw	Aw	Aw	Ab+Aw
Ab+Aw	Ab+Aw	Aw	Aw	Ab+Aw
Ab+Aw	Ab+Aw	Aw	Aw	Ab+Aw
Ab+Aw	Ab+Aw	Aw	Aw	Ab+Aw
Ab+Aw	Ab+Aw	Avi+Aw	Avi+Aw	Ab+Aw
Ab+Aw	Ab+Aw	Avi+Aw	Avi+Aw	Ab+Aw

Figure 3.8: 5G mmWave grids with type of attenuations for winter season.

69.25	69.25	0.82	0.82	69.25
69.25	69.25	0.82	0.82	69.25
69.25	69.25	0.82	0.82	69.25
69.25	69.25	0.82	0.82	69.25
69.25	69.25	28.66	28.66	69.25
69.25	69.25	28.66	28.66	69.25

Figure 3.9: 5G mmWave grids with values of attenuations (atmospheric, vegetation in-leaf and building) in summer season for 28 GHz.

70.23	70.23	1.8	1.8	70.23
70.23	70.23	1.8	1.8	70.23
70.23	70.23	1.8	1.8	70.23
70.23	70.23	1.8	1.8	70.23
70.23	70.23	29.64	29.64	70.23
70.23	70.23	29.64	29.64	70.23

Figure 3.10: 5G mmWave grids with values of attenuations (atmospheric, vegetation in-leaf and building) in rain season for 28 GHz .

69.73	69.73	1.3	1.3	69.73
69.73	69.73	1.3	1.3	69.73
69.73	69.73	1.3	1.3	69.73
69.73	69.73	1.3	1.3	69.73
69.73	69.73	5.77	5.77	69.73
69.73	69.73	5.77	5.77	69.73

Figure 3.11: 5G mmWave grids with values of attenuations (atmospheric, vegetation out-leaf and building) in winter season for 28 GHz .

Chapter 4

Channel Capacity in Vegetation Area

4.1 mmWave Vegetation Attenuation

In this chapter we calculate and predict the vegetation attenuation values for mmWave propagation by using ITR-U and ML algorithms like K-Nearest Neighbors, Decision Tree and Random Forest. The ITU-R model is applicable in the frequency range 200MHz to 95GHz with the assumption that maximum depth of vegetation 400m [**?**]. Here we have assumed that the SPs and customer premises equipments (CPEs) are such that the majority of the radio path falls within the vegetation medium. The frequency is taken 2GHz, 28GHz, and 31GHz for calculation. The mmWave vegetation propagation path losses are shown by the below equation (4.1) as per ITU-R model. As per model the attenuation due to vegetation denoted as L is given by

$$L = 0.2f^{0.3}d^{0.6} \qquad dB \tag{4.1}$$

where f is the frequency in MHz and d is the vegetation depth in $metre$.

In equation 4.1 f is in MHz and denotes frequency. Further, d depth of vegetation is in meters between the 5G transmitter and receiver antennas. This ITU-R attenuation equation is valid for mmWave vegetation propagation which is having depth as d $<$ 400 meter. This model stated in equation 4.1 is applicable for the mmWave frequency range and this model is valid for the frequency range 200 MHz to 95 GHz [18-23]. As mentioned in literate the mmWave suffers with attenuation while passing through vegetation. The vegetation adds extra attenuation on mmWave propagating waves. Vegetation is a random channel having discrete scatters due to random structure and distribution of :

- Foliage Leaves
- Foliage Branches and
- Foliage Tree trunks

5G mmWave transmission suffers various phenomena like:

- Multiple vegetation scattering
- Vegetation diffraction and
- Vegetation absorption of radiation

Due to above mentioned various phenomena, mmWave propagation suffers and attenuation takes place. These phenomena can be combined and lead to overall mmWave

propagation attenuation. This combined attenuation due to vegetation has significant value at GHz frequency range and shall be taken care while planning link budget [13-31].

In this section, we are calculating mmWave vegetation propagation losses for 5G communication system. The calculated vegetation propagation path losses are shown in the graphs using curves. The curves are shown with mmWave vegetation depth for the mmWave frequencies. In Figure 4.1, 5G mmWave attenuation is shown due to vegetation as per ITU-R Model in x-y-z mode where x, y and z axis indicate mmWave frequency, depth of vegetation and vegetation attenuation. It is clear from the figure 4.1 curve that the high depth of foliage impacts mmWave propagation and eventfully increases the foliage losses and also vegetation losses increases as vegetation depth increases. The mmWave vegetation propagation losses curves for the frequencies are shown with the vegetation depth axis as per ITU-R model.

Propagation of mmWave through vegetation suffers with the attenuation and this adds extra attenuation on mmWave propagating waves. Random vegetation channel provides discrete scattering of the mmWaves due to random structure and distribution of leaves branches and tree trunks. 5G mmWave propagation suffers various phenomena like; multiple scattering, diffraction and absorption of radiation during vegetation obstructions [17-28].

4.2 mmWave Vegetation Attenuation Prediction

ML algorithms predict the output based on the input data set and in the supervised ML mode and the output is labeled for the training data set. By using the ML algorithms the system is trained and in the testing / prediction mode the output is predicted for the vegetation attenuation values. Here we are analyzing and using supervised learning based algorithms like Decision Tree, Random Forest and K-Nearest Neighbours (KNN). The toolkits numpy, scipy, and scikit-learn are used with simulation in Python. In the supervised mode Decision Tree regression, KNN regression and Random Forest regression have been analyzed and found that Decision Tree regression and Random Forest regression provide close approximate simulation results. In the supervised mode ML algorithms have been used here along with simulation results to predict the vegetation attenuation values with the training / testing dataset [9-19].

The decision tree prediction model works in the regression mode having tree like structure with the nodes. The tree has nodes and branch to predict the values as per the input data set and learning set. KNN can be used in supervised mode for the continuous values prediction in regression mode. Random Forests creates the random tress and can be used in the regression mode to predict the vegetation attenuation values. Random Forests results are good as it deals with the data over fitting problem to provide the quality predictions. In this research we have used supervised learning for Random Forests regression trees having training data and testing data. In our simulation, training data consists the range of vegetation attenuation for the mmWave frequencies for

the various type of the depth of vegetation in wireless channel. We are specifically predicting the vegetation attenuation values and random forest can be trained in the supervised regression learning mode for the same. The vegetation depth D (from d1 , d2 to ....dn) and frequency F (f1, f2 to .... fn) are considered as the input learning parameters having supervised learning for the output vegetation attenuation Av (Av1, Av2, to ..... Avn) [29-35].

Table 4.1 shows vegetation attenuation values for 5G mmWave channel having vegetation as obstructions. Table 4.1 shows the vegetation attenuation for the proposed and simulated frequencies using ITU-R as well as for the ML based algorithms. Vegetation attenuation values for the proposed and simulated frequencies are shown with the vegetation depth. The high value depth d of vegetation generates the more losses due to dense vegetation. Further, vegetation loss also increases along with high frequencies [31-39].

Figure 4.2 to 4.4 show the mmWave vegetation propagation losses (having supervised Decision Tree Regression) based on predictions by using proposed ML algorithms along with the training data set, testing data set and the prediction data set having supervised learning with frequencies, depth of vegetation and supervised vegetation attenuation values data set. As per graphs it is clearly visible that the vegetation path loss prediction follows closely with the training and testing data sets. Graphs related to KNN method are not shown due to not highly close predictions as compare to other two methods. As per ITU-R and ML prediction; this overall vegetation attenuation has significant value at GHz frequency range and shall be taken care while

planning link budget or channel capacity.

Figure 4.5 to 4.7 show the mmWave vegetation propagation losses based on the predictions by using proposed ML algorithm (Random Forest Prediction) along with the training data set, testing data set and the prediction data set having supervised learning with frequencies, depth of vegetation and supervised vegetation attenuation values data set.

Further, we have also calculated the vegetation attenuation prediction accuracy for the mentioned algorithms as per simulations for the used training and testing data set. It is clear from Table 4.2; that the accuracy is approaching 95 percent plus for the training, testing and prediction data sets.

4.3 Channel Capacity

5G mmWave communication system channel capacity can be controlled by using SDR in the vegetation attenuation condition along with the machine learning (ML) based intelligent SDR solution. 5G mmWave SDR based transceiver can adjust the channel capacity automatically and produce the desired SCC under the vegetation attenuation situation. The 5G system can achieve the desirable Shannon channel capacity by using ML prediction to predict the attenuation values and can tune the system with the SCC accordingly. SDR based transceiver has the capability to reconfigure the transmission parameters and SDR based system is flexible by having programmable functionality. So by the virtue of the SDR transceiver during vegetation attenuation system; it can

transmit high capacity data rate by adjusting the signal to noise (SNR) ratio and can provide the high data capacity [22-25].

As shown in the flow chart of figure 4.8, it is clear that in the beginning step SDR sends the desired input parameters to ML prediction unit and ML prediction unit processes for the received input parameters. Further, ML prediction unit predicts the vegetation attenuation values based on the input parameters like frequency, depth of vegetation and etc. In continuation, the SDR calculates the SCC based on the received vegetation attenuation from the ML prediction unit.

4.4 Shannon Channel Capacity (SCC)

For continuous additive white Gaussian noise channel, as per Shannon expression the channel capacity C in b/s is given by

$$C = B\ log_2\left(1 + \frac{S}{N}\right) \tag{4.2}$$

where B is the channel bandwidth in Hz, and S/N is the power ratio of signal-to-noise in the channel. The channel capacity per unit bandwidth can be written as

$$\frac{C}{B} = log_2\left(1 + \frac{S}{N}\right) \tag{4.3}$$

Here the term C/B is refereed as the channel capacity . If, due to the urban site, weather impairments and vegetation propagation fading, the term S/N in 4.3 is random, with arbitrary but known distribution depending on the type and characteristics of the fading processes considered, then the channel capacity is also random. This

random variability of the channel capacity that imposes performance degradation on the system (transmitter) that utilizes the channel .

Here, in this section we have calculated mmWave propagation Shannon channel capacity for 5G wireless communication system having vegetation attenuation. 5G wireless system needs controlled channel capacity. As per Shannons theorem; Shannon channel capacity is the function of bandwidth, received signal power to noise ratio as shown in equation 4.2. As per equation 4.2; C is the theoretical Shannon channel capacity which is maximum channel capacity of 5G mmWave AWGN channel in bits per second. Here B is the 5G mmWave bandwidth in Hertz and signal to noise ratio. Vegetation Shannon channel capacity per unit bandwidth is calculated based on ITU-R vegetation attenuation model for the frequencies 28 GHz, 37 GHz and 39 GHz [22-25].

Shannon channel capacity equation indicates various variables to control the 5G mmWave channel capacity. The mmWave spectrum shall be used efficiently to allocate to the users as we have limited amount mmWave bandwidth for a mmWave 5G channel. 5G Signal-Noise Ratio (SNR) is also one of the factors and which also impacts the Shannon channel capacity [23-25].

Figure 4.9, figure 4.10 and figure 4.11 show the Shannon capacity for the 5G mmWave channel having vegetation obstructions and also for the simulated frequencies. Shannon channel capacity curves for the frequencies are shown with the S/N and the vegetation depth axis. It is clear from the Shannon channel capacity curves that Shannon channel capacity keeps decreasing as vegetation depth increases. Increasing vegetation depth increases vegetation attenuation and which leads for the low signal

strength. High vegetation attenuation shows low Shannon channel capacity as per figures 4.9-4.11.

From the figures 4.9-4.11; it can be observed that there is channel capacity decrement, while the vegetation distance increases. The SCC decreases drastically as a function of vegetation distance. We can increase the 5G channel bandwidth or S/N, or both to improve the Shannon channel capacity for the mmWave propagation during vegetation obstruction. As per the figures, channel capacity varies as per frequency and SNR. It is quite visible from the simulation results that by increasing the signal power by using SDR and the desired SCC can be achieved. 5G communication system along with SDR based control can provide the controllable and achievable data rates even in the vegetation attenuation environment. As shown in the graphs that channel capacity varies as per frequency and SNR. It is quite visible from the simulation results that by increasing the signal power by using SDR the desired SCC can be achieved. 5G communication system along with SDR based control can provide the controllable and achievable data rates even in the vegetation attenuation environment [23-28].

As per figure 4.9, figure 4.10 and figure 4.11; it is visible that Shannon channel capacity depends on signal-to-noise ratio (SNR) and vegetation depth. Vegetation depth adds vegetation attenuation to mmWave propagation as per depth. SDR based 5G mmWave communication system can control channel capacity by having flexible control with S/N. SDR based 5G mmWave communication system can increase or decrease the 5G channel bandwidth or S/N ratio or frequency or in combination to improve the SCC for mmWave propagation during vegetation obstruction. Dur-

ing link budget analysis low vegetation area or high vegetation area or low vegetation link/ path or high vegetation link/ path can also be selected to have optimum mmWave power transmission using SDR. Here as per this research work; it is quite clear that the ML prediction unit predicts the vegetation attenuation values for the required depth of vegetation or frequency. The ML unit predicted vegetation attenuation values are given to SDR to control or tune the transmitter accordingly to meet the system data rate or SCC requirement.

Here in Tables 4.1-4.3 SNR values are taken for demonstration and discussion purpose. Table 4.3, shows the Shannon capacity for 5G mmWave channel having vegetation obstructions. Shannon channel capacity values for the proposed and simulated frequencies are shown with the S/N (SNR) and vegetation depth. It is clear from the Shannon channel capacity values that Shannon channel capacity keeps decreasing as vegetation depth increases. Increasing vegetation depth increases vegetation attenuation and which leads for low signal strength. ML based SDR system can tune to the required and desired channel capacity. ML based system tunes to the desired channel data rate in the efficient manner. High vegetation attenuation shows low Shannon channel capacity as per Table 4.3.

$Freq.\ (f)$ (GHz)	$Depth\ (d)$ (M)	$Av\ \ (ITU-R)$ (dB)	$Av\ \ (KNN)$ (dB)	$Av\ \ (DT)$ (dB)	$Av\ \ (RF)$ (dB)
28	10	17.19	15.13	15.03	14.99
37	10	18.68	16.83	16.78	16.69
39	10	18.98	16.97	16.98	16.97
28	9	16.13	14.55	14.71	14.51
37	9	17.54	15.68	15.62	15.81
39	9	17.82	15.87	15.91	15.93

Table 4.1: 5G mmWave Vegetation Attenuation Values based on ITU-R Model and ML Prediction

$Data$	$K-Nearest\ Neighbors$	$Decision\ Tree$	$Random\ Forest$
$Training$	0.97	0.98	0.99
$Testing$	0.96	0.78	0.76
$Prediction$	0.94	0.85	0.97

Table 4.2: 5G mmWave Vegetation Attenuation Prediction Accuracy

$Depth$ d/SNR	C $(28GHz)$ $50dB$	C $(28GHz)$ $60dB$	C $(37GHz)$ $50dB$	C $(37GHz)$ $60dB$	C $(39GHz)$ $50dB$	C $(39GHz)$ $60dB$
1	5.545	5.825	5.533	5.815	5.531	5.813
2	5.474	5.767	5.456	5.752	5.452	5.749
3	5.415	5.718	5.39	5.698	5.385	5.694
4	5.36	5.675	5.33	5.65	5.324	5.645
5	5.31	5.634	5.273	5.605	5.266	5.599
6	5.261	5.595	5.219	5.562	5.211	5.555
7	5.214	5.558	5.167	5.521	5.157	5.513
8	5.169	5.523	5.115	5.481	5.104	5.472
9	5.124	5.488	5.064	5.442	5.052	5.432
10	5.08	5.453	5.014	5.403	5.001	5.393

Table 4.3: 5G mmWave Channel Capacity in the Vegetation Medium Attenuation for Frequencies

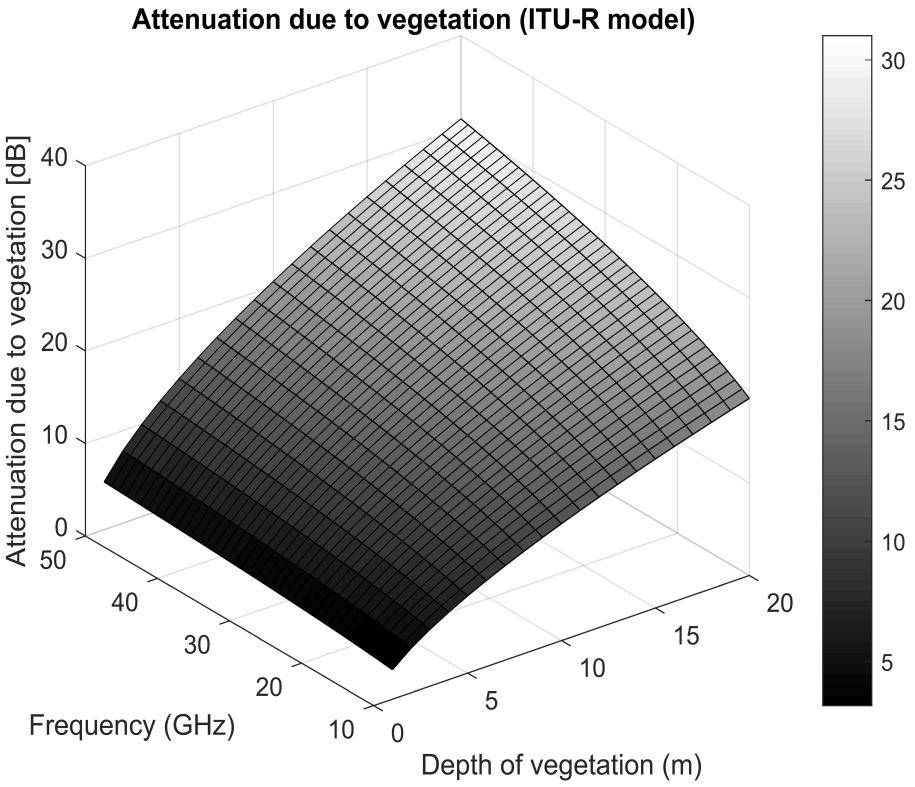

Figure 4.1: 5G mmWave Attenuation due to Vegetation (ITU-R Model).

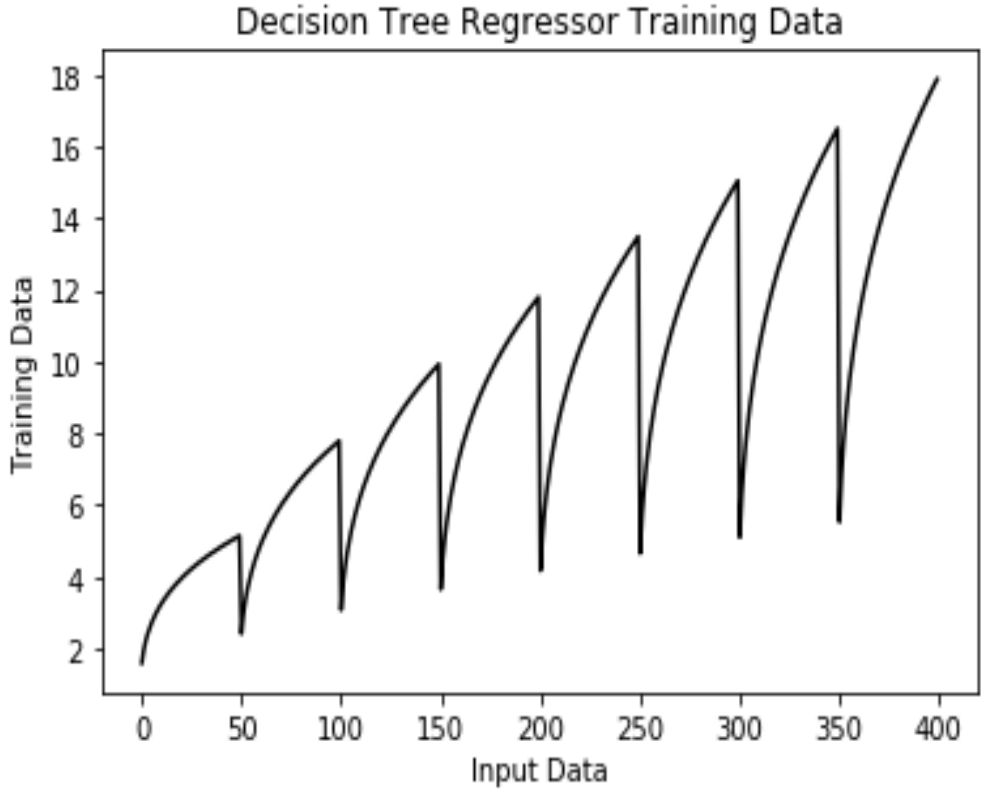

Figure 4.2: Vegetation Attenuation Decision Tree Regressor Training Data Output vs Inputs.

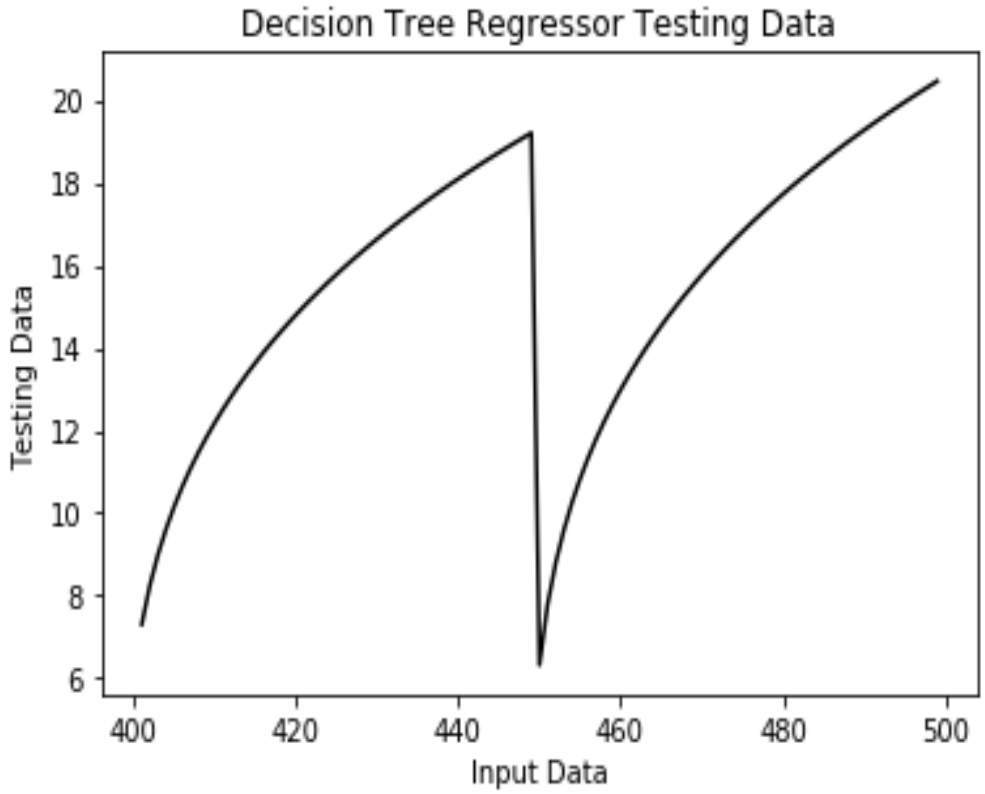

Figure 4.3: Vegetation Attenuation Decision Tree Regressor Testing Data Output vs Inputs.

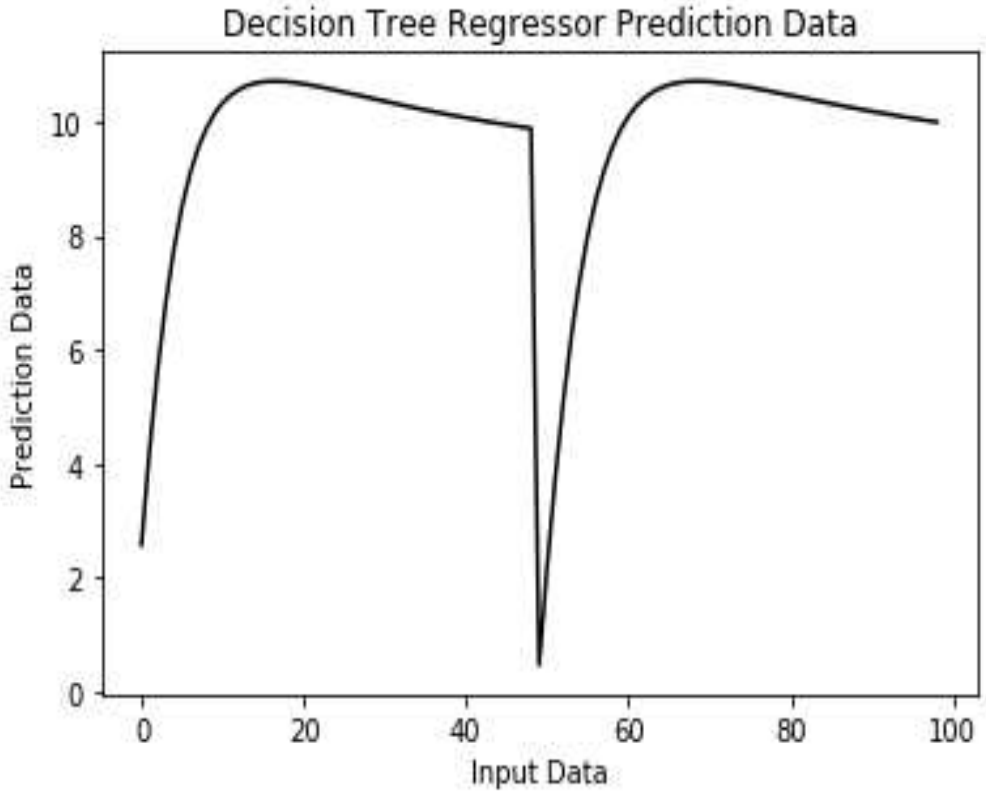

Figure 4.4: Vegetation Attenuation Decision Tree Regressor Prediction Data Output vs Inputs.

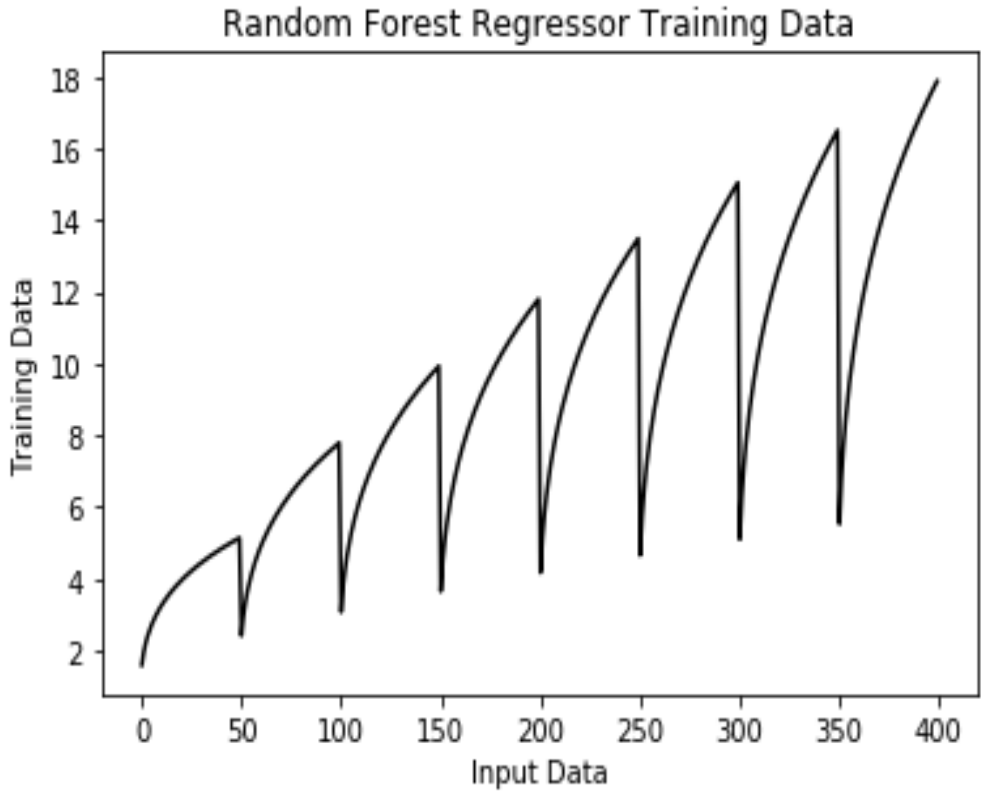

Figure 4.5: Vegetation Attenuation Random Forest Training Data Output vs Inputs.

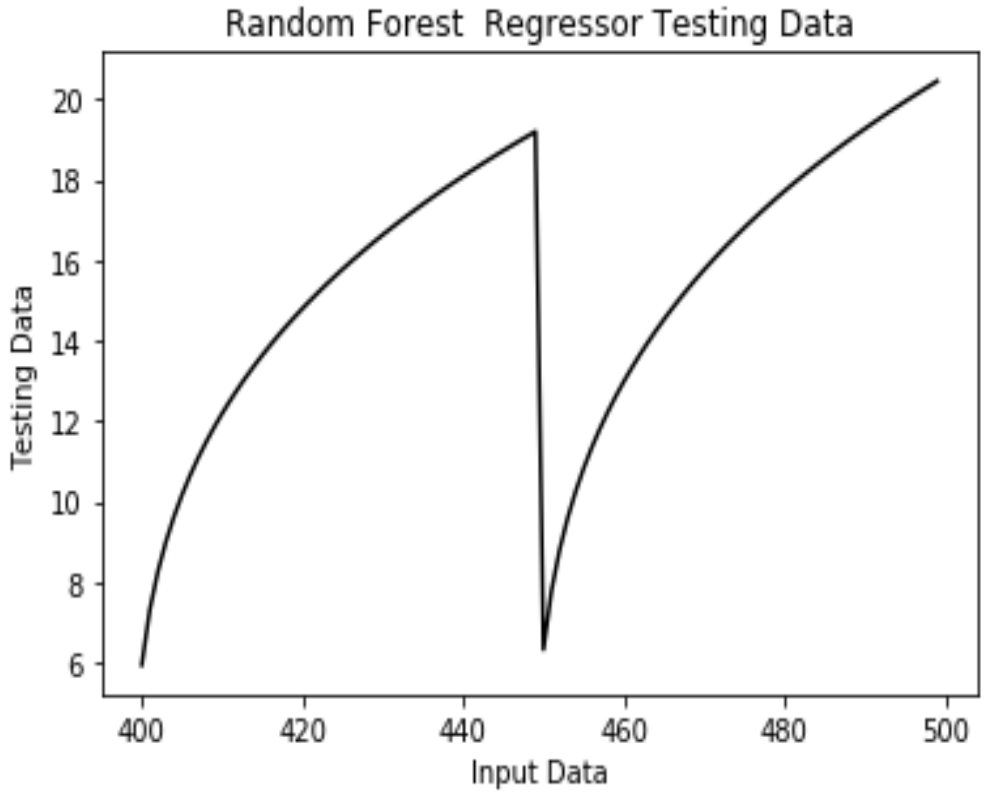

Figure 4.6: Vegetation Attenuation Random Forest Testing Data Output vs Inputs.

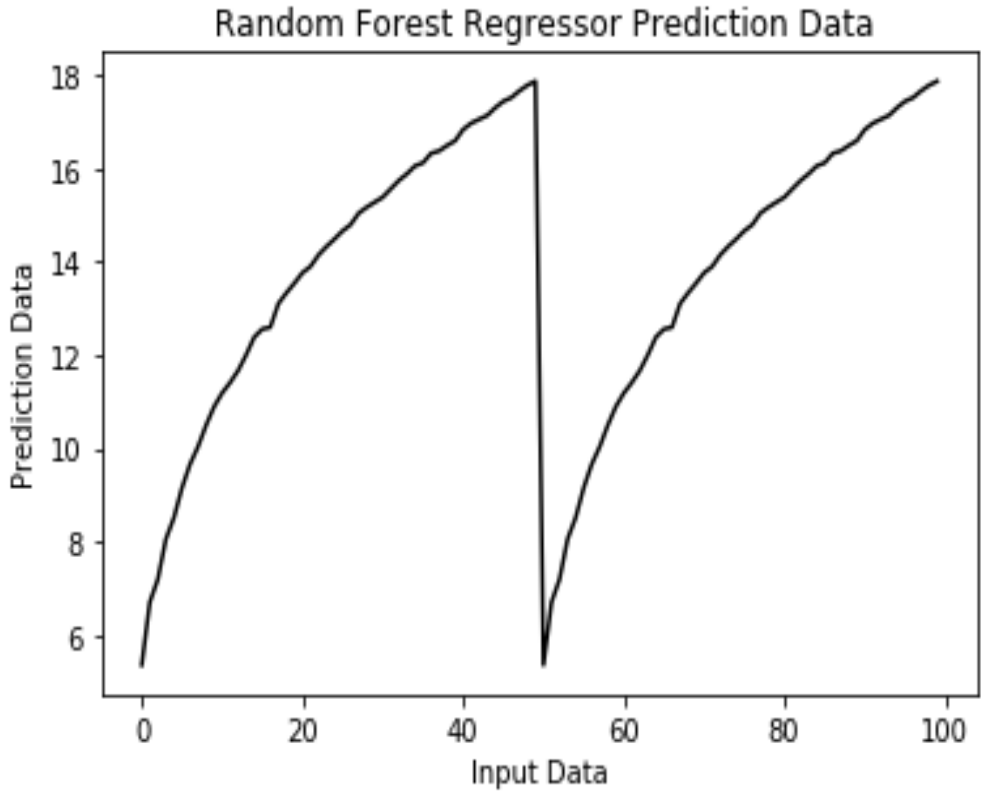

Figure 4.7: Vegetation Attenuation Random Forest Prediction Data Output vs Inputs.

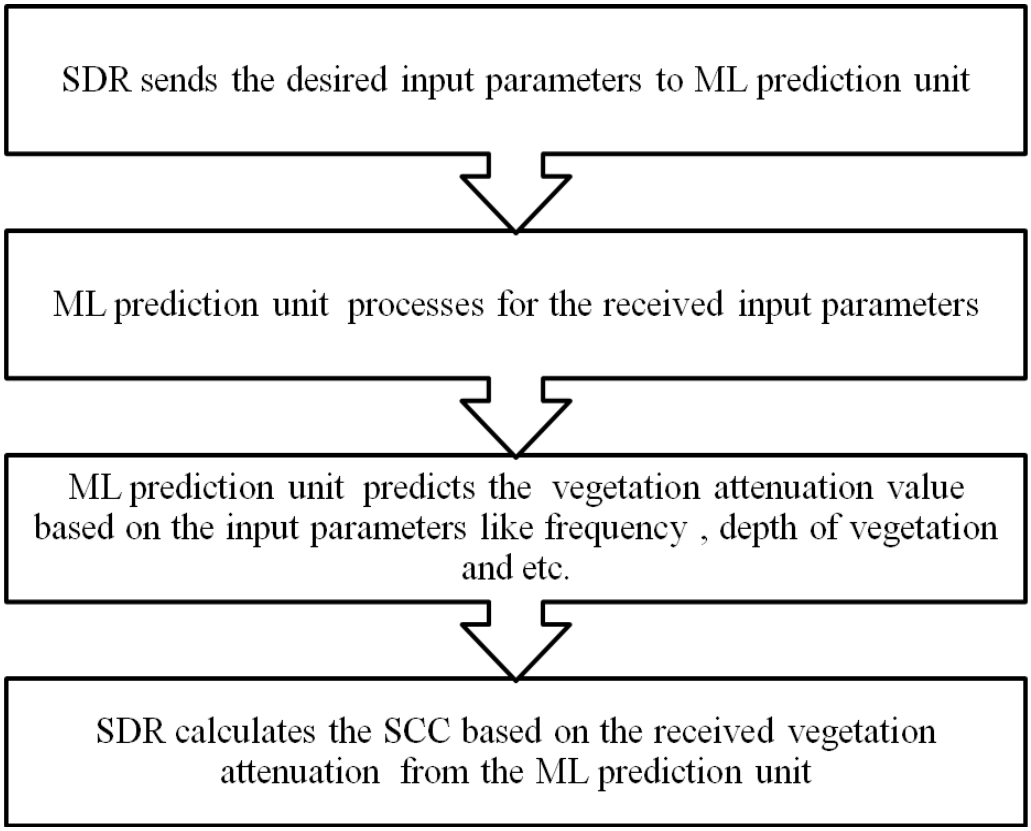

Figure 4.8: SDR with ML Prediction Unit to Control the SCC.

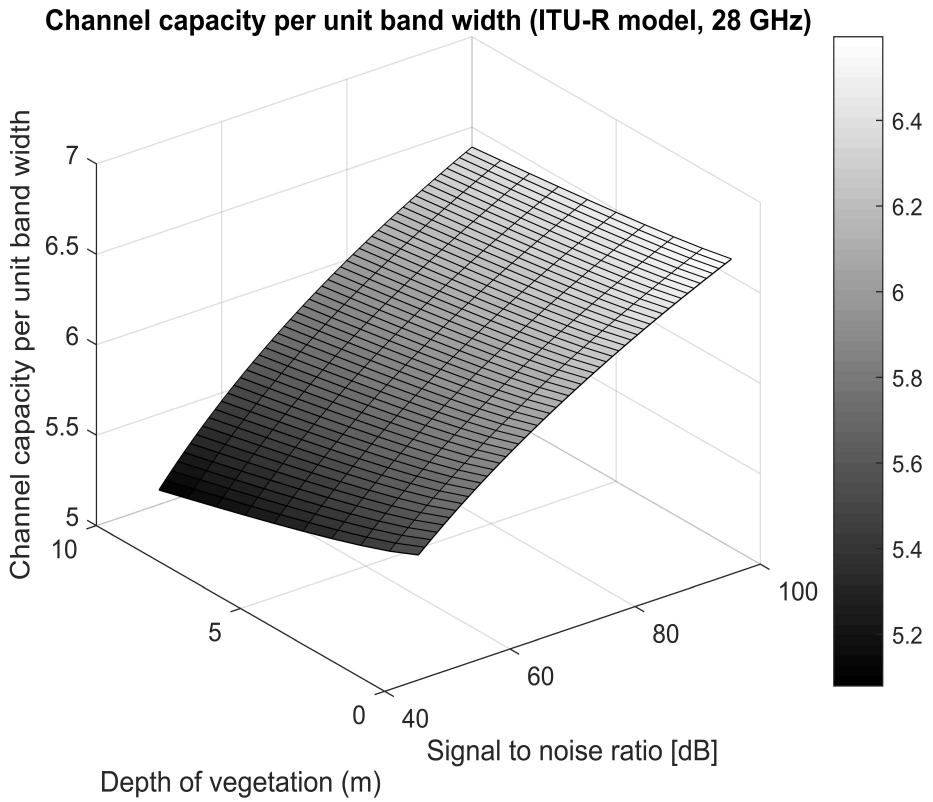

Figure 4.9: 5G mmWave Channel Capacity in the Presence of Vegetation Attenuation (ITU-R Model) for Frequency 28 GHz.

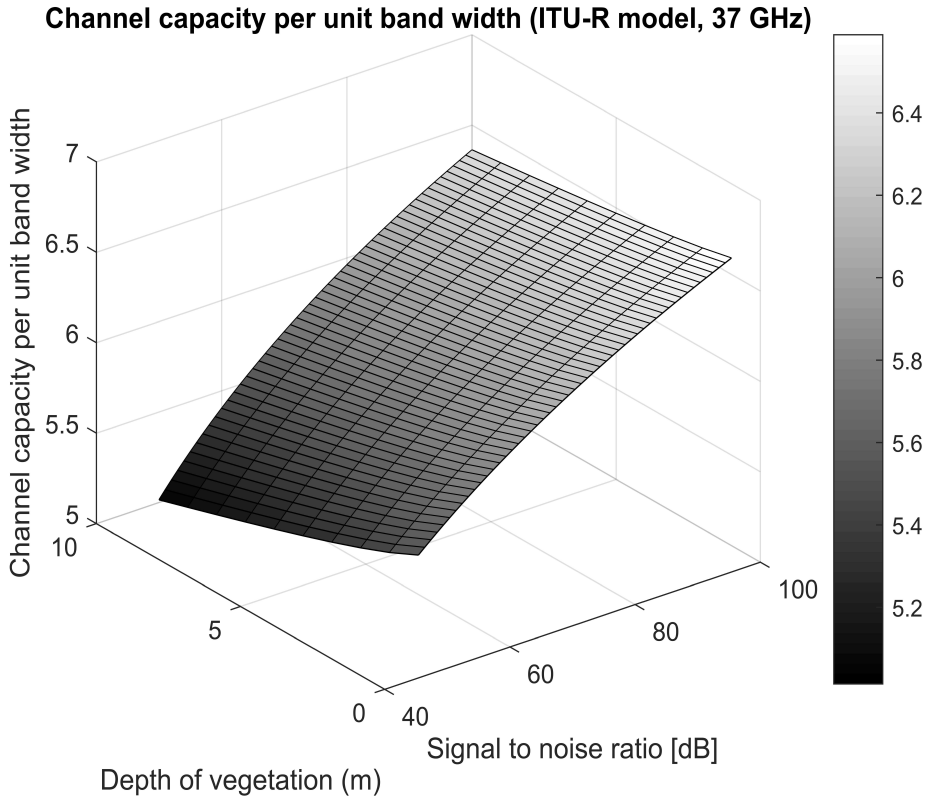

Figure 4.10: 5G mmWave Channel Capacity in the Presence of Vegetation Attenuation (ITU-R Model) for Frequency 37 GHz.

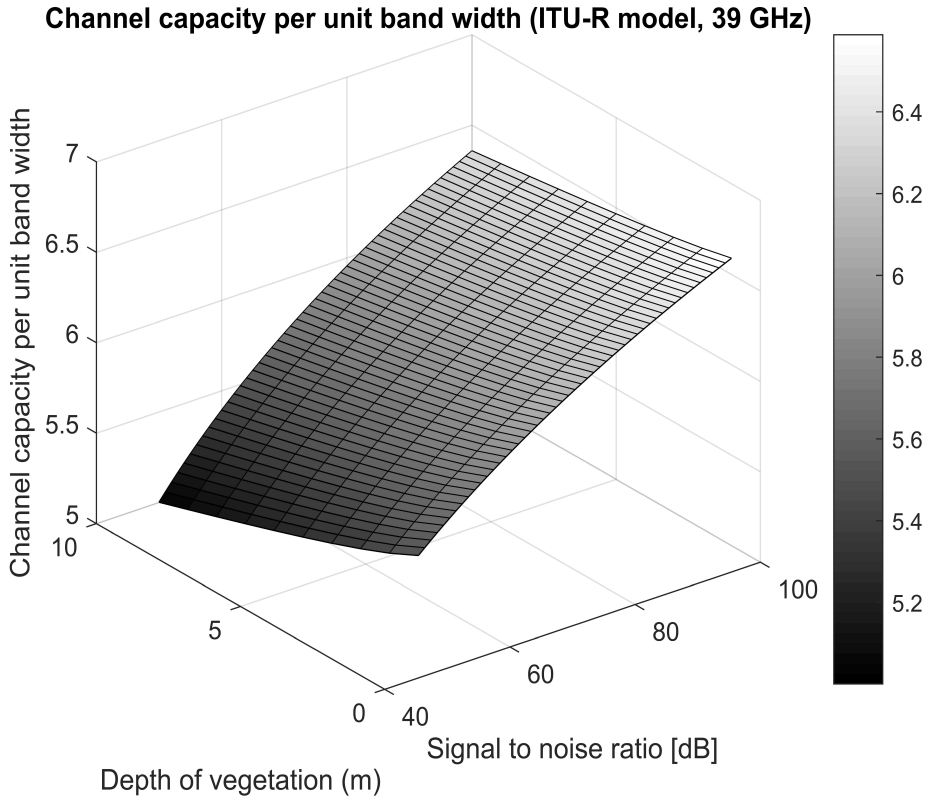

Figure 4.11: 5G mmWave Channel Capacity in the Presence of Vegetation Attenuation (ITU-R Model) for Frequency 39 GHz.

Chapter 5

Propagation Losses for Indian Metro Cities

Four major Indian cities are considered here to generate the mmWave frequencies propagation path losses data set for 5G mmWave communication system under various weather conditions. The various weather conditions are like; summer, rain and winter. The four major Indian cities are Delhi, Mumbai, Kolkata and Chennai. The summer season attenuation calculation considers propagation path losses due to atmospheric gases impairments (water vapour and oxygen) only for all four cities. The rainy season attenuation calculation considers propagation path losses due to atmospheric gases (water vapour and oxygen) and rain for all four cities. The winter season attenuation calculation considers propagation path losses due to atmospheric gases (water vapour and oxygen) and fog for Delhi. Further, the winter season attenuation calculation considers propagation path losses due to atmospheric gases (water vapour and oxygen) for

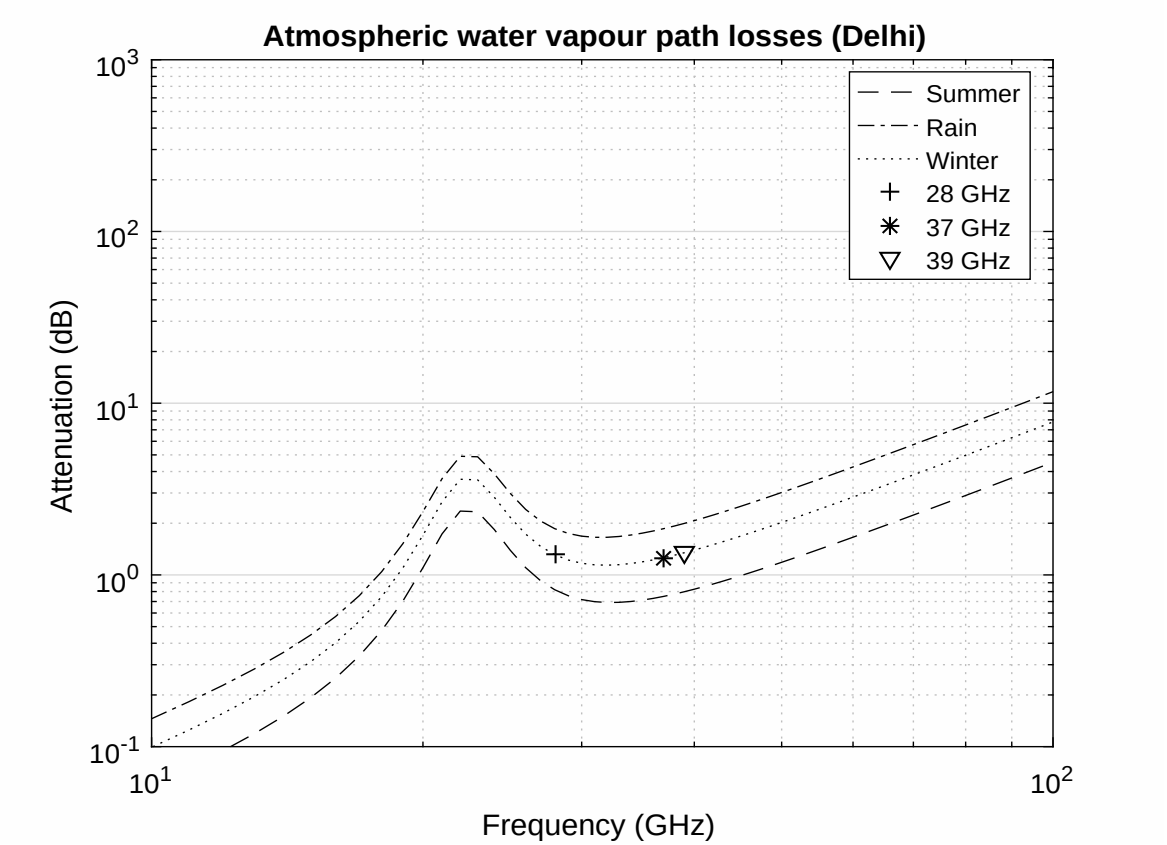

Figure 5.1: Attenuation due to atmospheric water vapor for 5G mmWave Communication System (Delhi).

rest three cities [1-5]. In this article, we have considered that both transceiver units are having direct or line of sight communication link and there is no non line of sight path. This data article calculates mmWave frequencies propagation path losses due to WIs for the certain mmWave frequencies. This article shows data for mmWave propagation under different WIs [5-10].

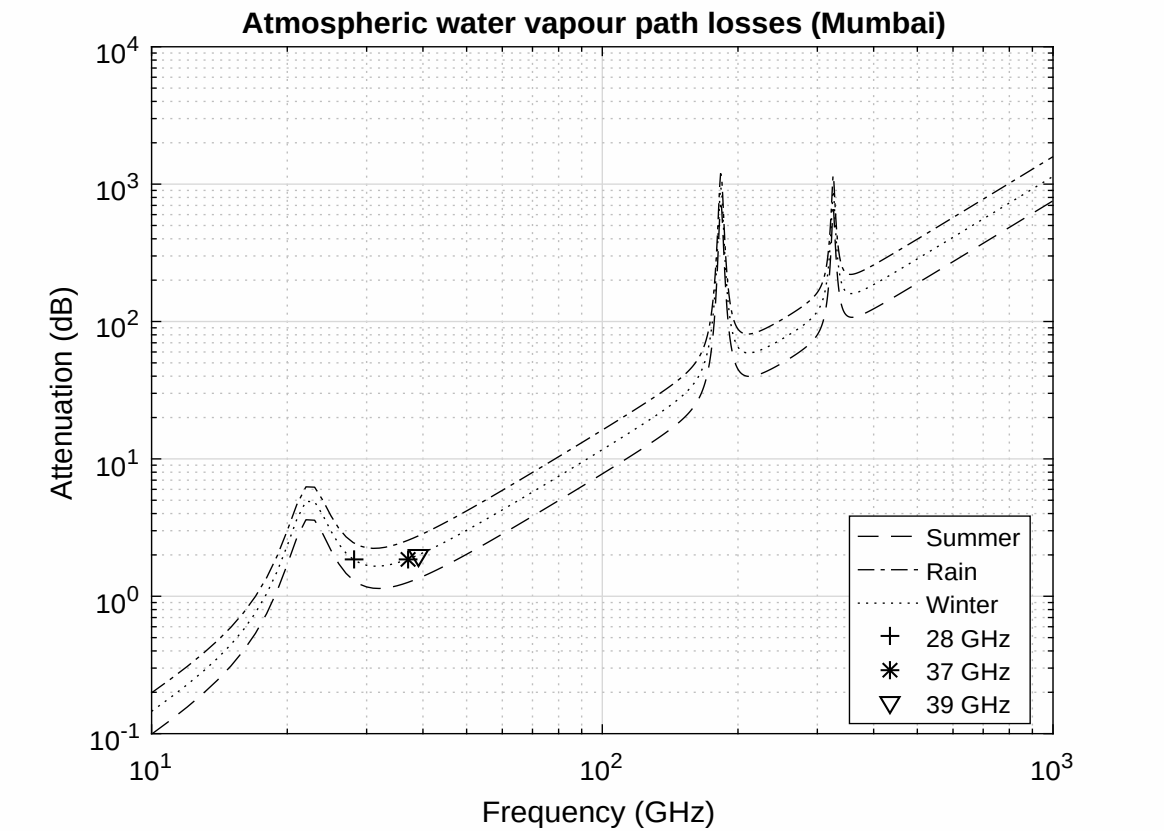

Figure 5.2: Attenuation due to atmospheric water vapor for 5G mmWave Communication System (Mumbai).

5.1 Value of Data

In India, 5G research and deployment are under year 2020 plan and such dataset is not specifically available for Indian Metro cities (like Delhi, Mumbai, Kolkata and Chennai). This proposed data set of the mmWave attenuation values for various Indian metro cities in various seasons will be highly useful for future 5G research and 5G system deployment. This Indian scenario 5G dataset can be used during network planning, determine the additional transmission power margin and operations. It is quite

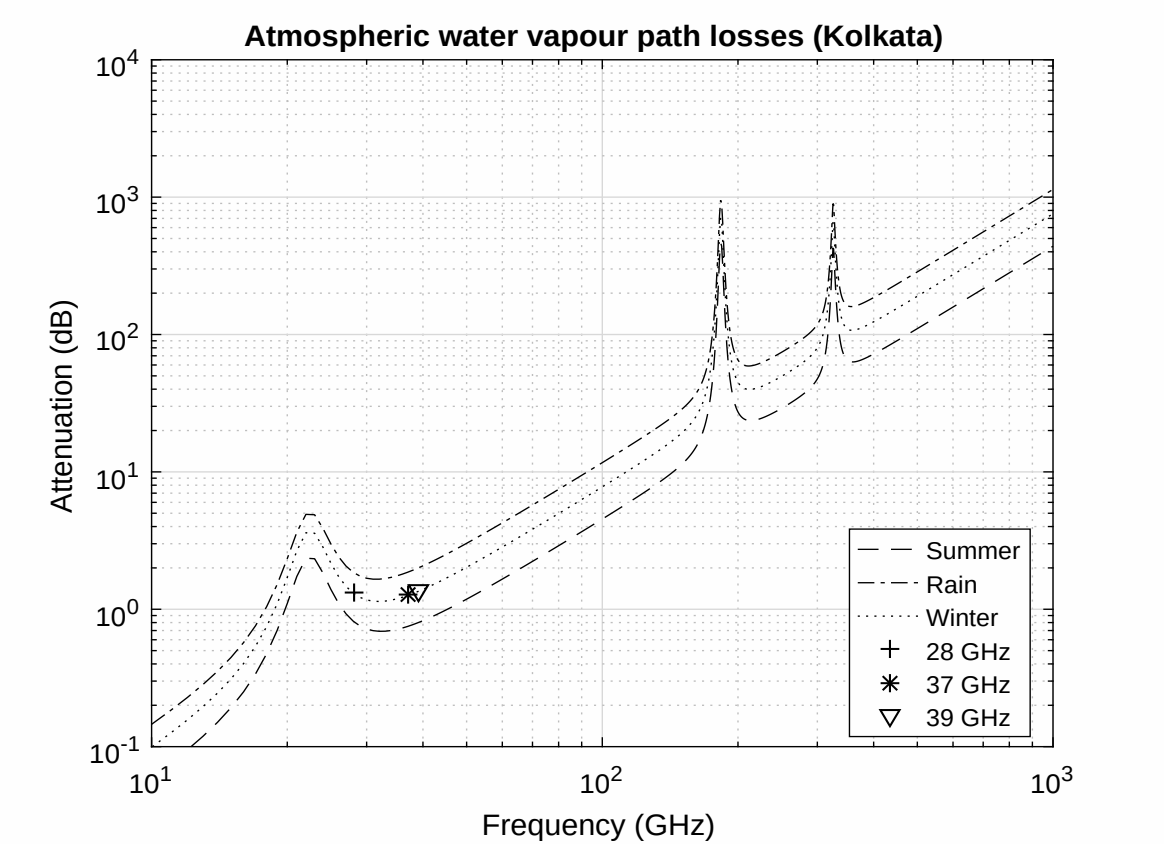

Figure 5.3: Attenuation due to atmospheric water vapor for 5G mmWave Communication System (Kolkata).

important for mmWave power link budget and reliable system operations which is feasible using this data. Based on presented dataset adaptive mmWave power transmission techniques can be used for large fixed link power budget margins for 5G mmWave communication system. Based on the presented dataset the 5G can be used to utilize resources in an efficient manner and controls the power transmission in an optimum manner.

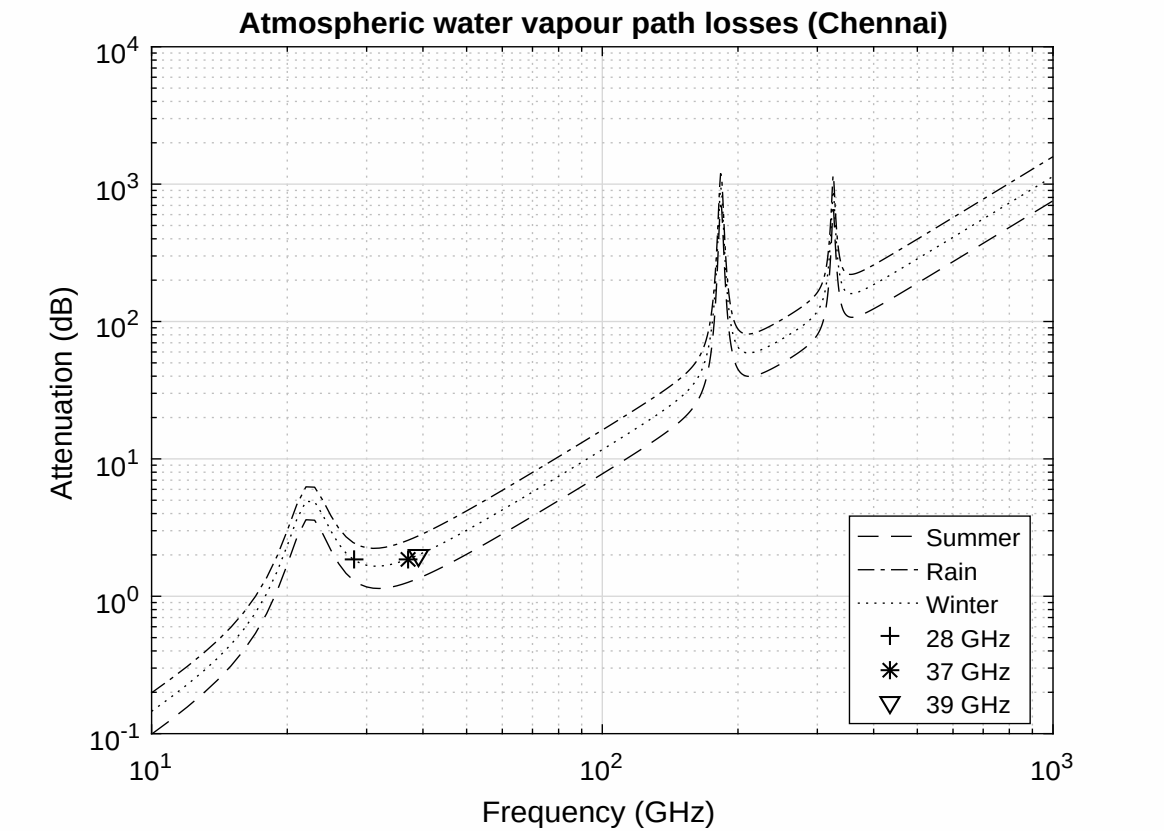

Figure 5.4: Attenuation due to atmospheric water vapor for 5G mmWave Communication System (Chennai).

5.2 Data

Four major Indian cities are considered here to generate the mmWave frequencies propagation path losses data set for 5G mmWave communication system under various weather conditions. The various weather conditions are like; summer, rain and winter. The four major Indian cities are Delhi, Mumbai, Kolkata and Chennai. The summer season attenuation calculation considers propagation path losses due to atmospheric gases impairments (water vapour and oxygen) only for all four cities. The rainy sea-

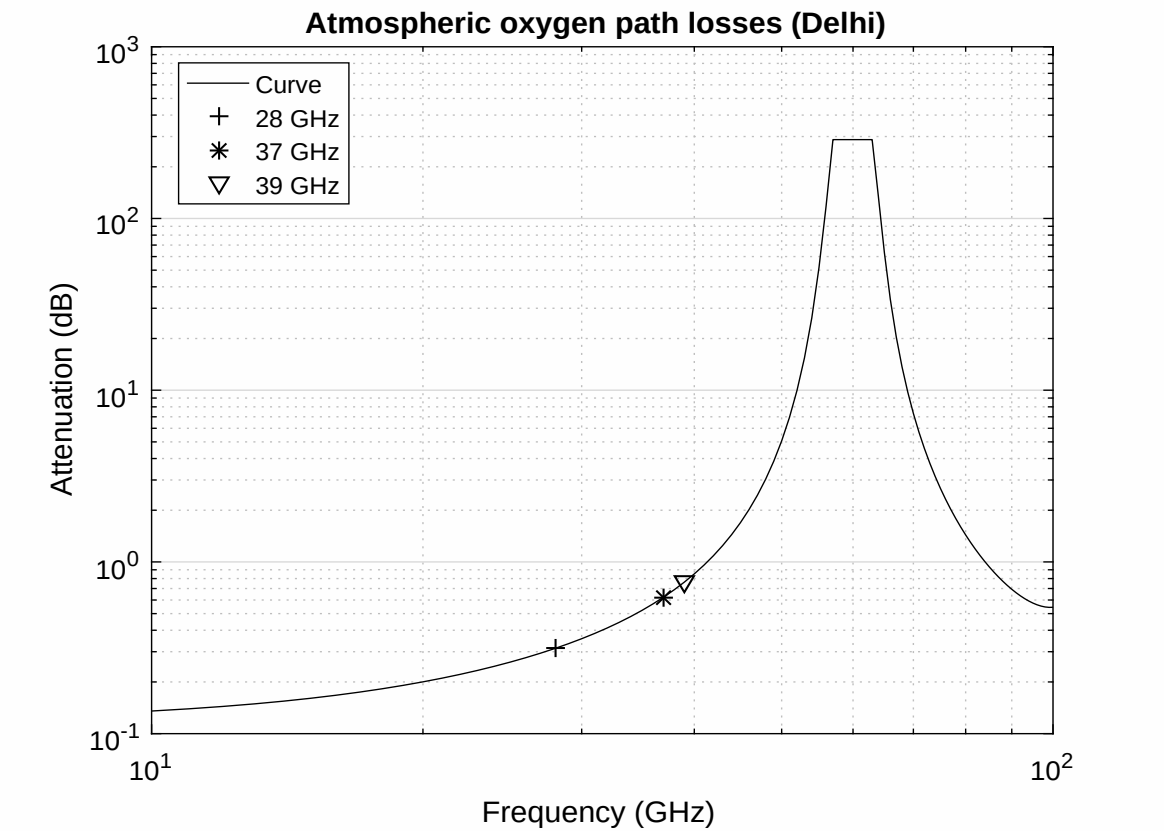

Figure 5.5: Attenuation due to atmospheric oxygen for 5G mmWave Communication System (Delhi).

son attenuation calculation considers propagation path losses due to atmospheric gases (water vapour and oxygen) and rain for all four cities. The winter season attenuation calculation considers propagation path losses due to atmospheric gases (water vapour and oxygen) and fog for Delhi. Further, the winter season attenuation calculation considers propagation path losses due to atmospheric gases (water vapour and oxygen) for rest three cities. In this article, we have considered that both transceiver units are having direct or line of sight communication link and there is no non line of sight path. This data article calculates mmWave frequencies propagation path losses due to WIs

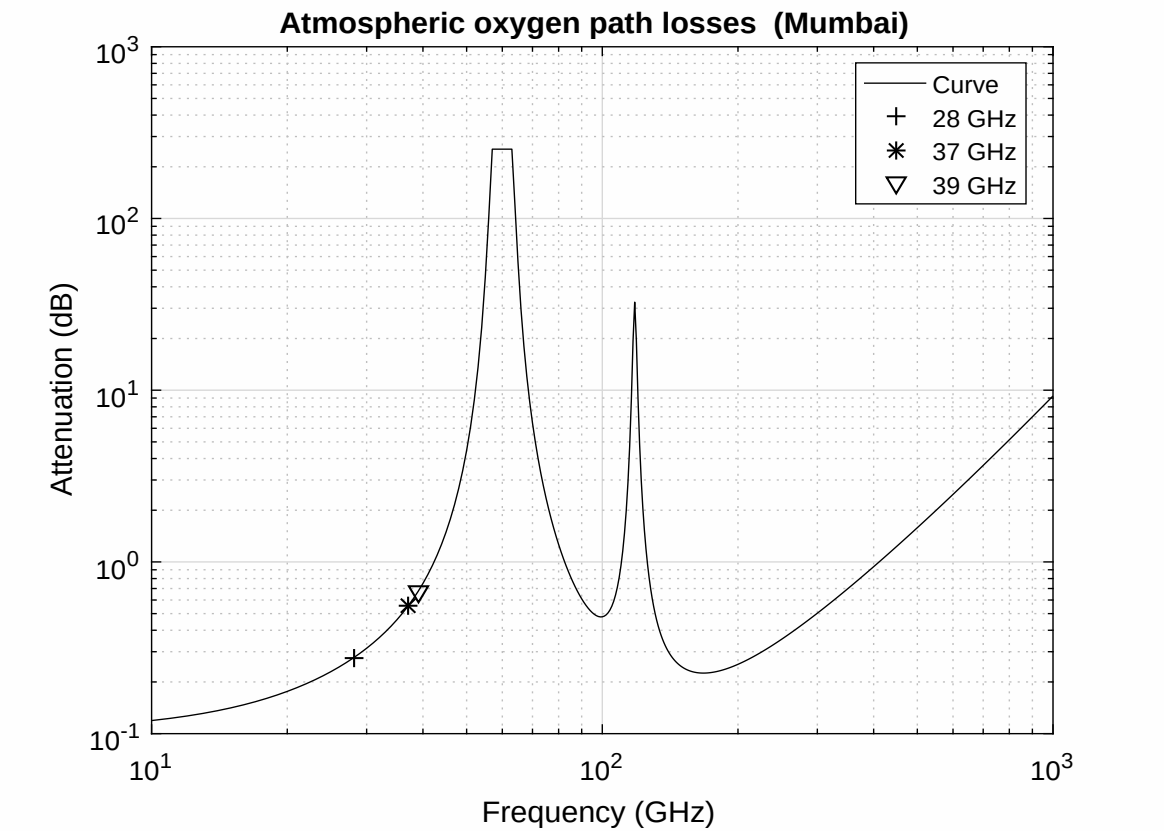

Figure 5.6: Attenuation due to atmospheric oxygen for 5G mmWave Communication System (Mumbai).

for the certain mmWave frequencies. This article shows data for mmWave propagation under different WIs . Figures 5.1-5.13 and Tables 5.1 are presented.

5.3 Experimental Design, Materials and Methods

The calculations/experiments were carried out with MatLab for four Indian Metro cites during summer, rain and winter season. The seasons were considered along with their corresponding type of attenuation causes. As per recent analysis done by The United

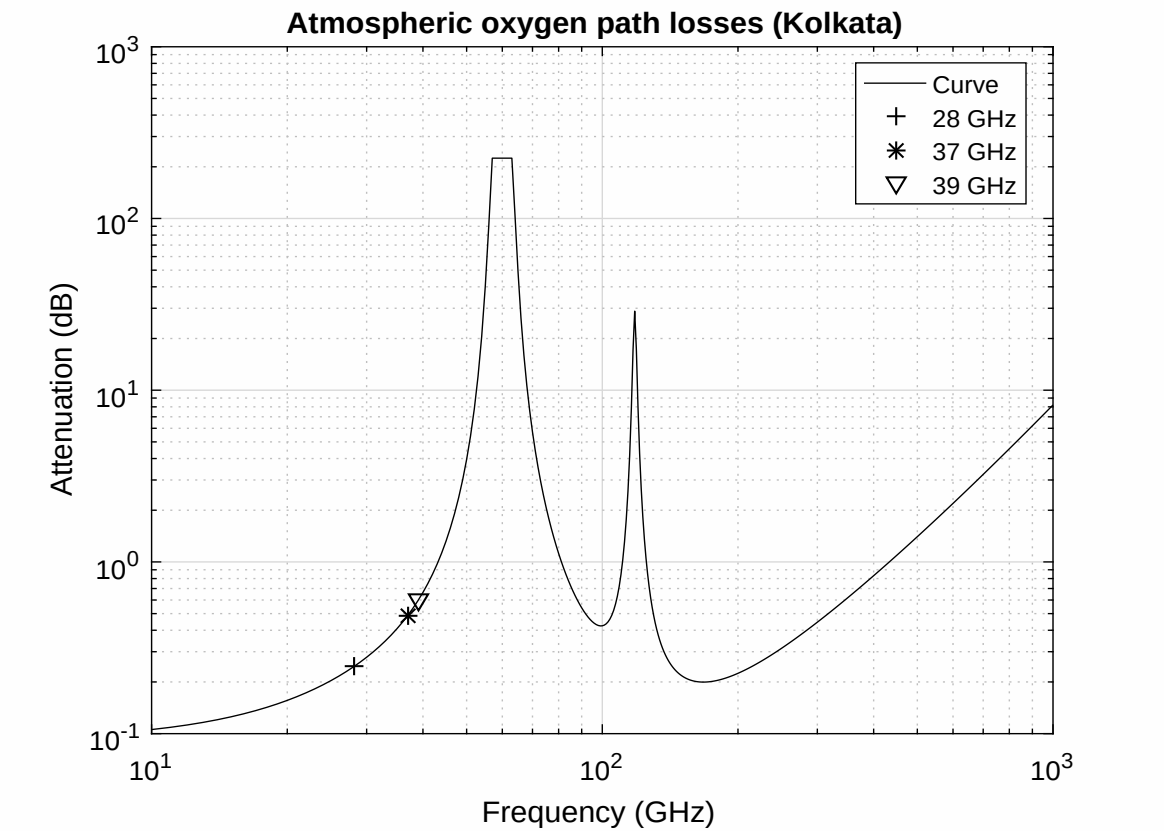

Figure 5.7: Attenuation due to atmospheric oxygen for 5G mmWave Communication System (Kolkata).

States Federal Communications Commission (FCC) for mmWave frequency bands : 28, 37 and 39 GHz, FCC authorizes and proposes broadband device operations in these mmWv bands [3-9]. Atmospheric parameters for the four Indian metro cities were collected as per literature and simulation was performed for the same using software experiment / calculations. The details about equations and related functions are explained the cited reference [5-10]. As per propagation loss equations; the attenuation due to atmospheric gases (combined water vapour and oxygen) has been plotted with mmWave frequencies for the four Indian metro cities i.e. Delhi, Mumbai, Kolkata and

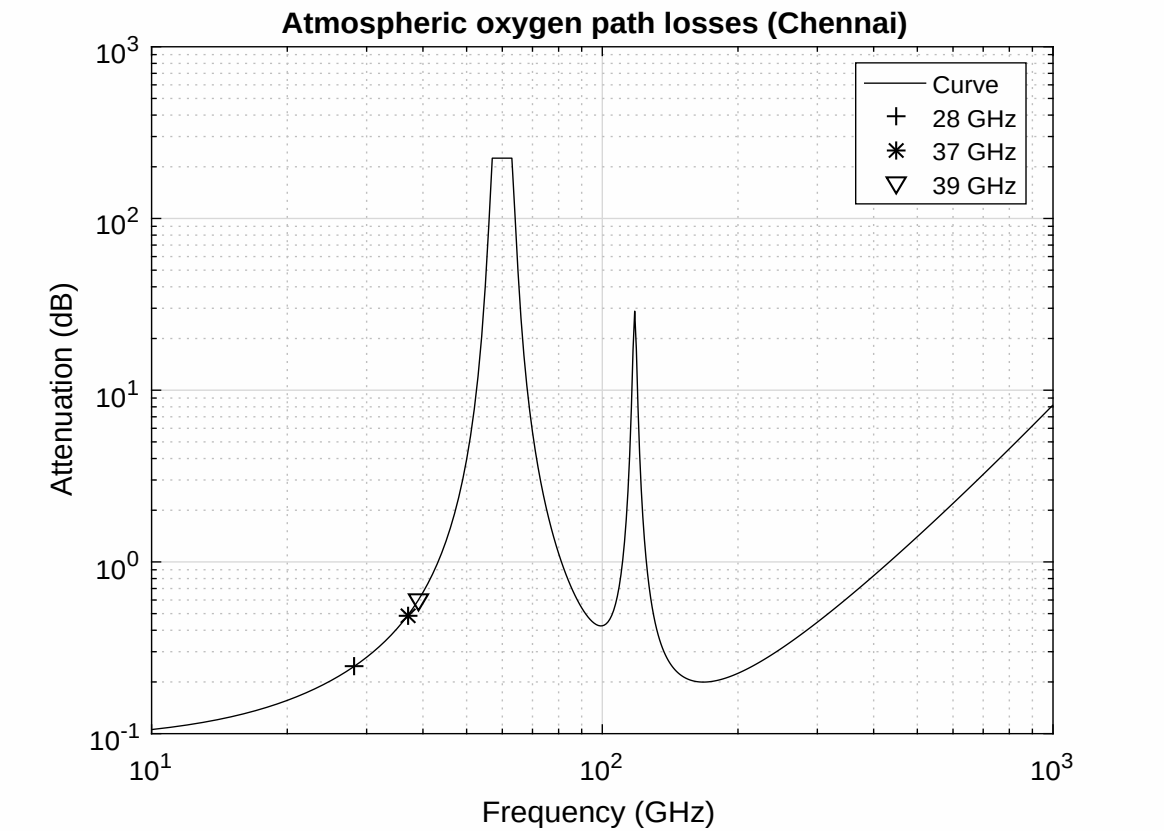

Figure 5.8: Attenuation due to atmospheric oxygen for 5G mmWave Communication System (Chennai).

Chennai.

As per the Figures 5.1, 5.2, 5.3 and 5.4 atmospheric water vapor shows high value resonances at 22 GHz for all four metro cities. The variation of attenuation due to the atmospheric gases along with mmWave frequencies is shown in the graphs. Figures 5.1-5.3 show the attenuation values for the four metro cities for various seasons like summer, rain and winter. Figure 5.4 shows the attenuation values due to rain for 0.01 percent of a year for four Indian metro cities. Figure 5.5 shows the attenuation values due to fog for Delhi. Further, the graphs also plots rain attenuation for the rain

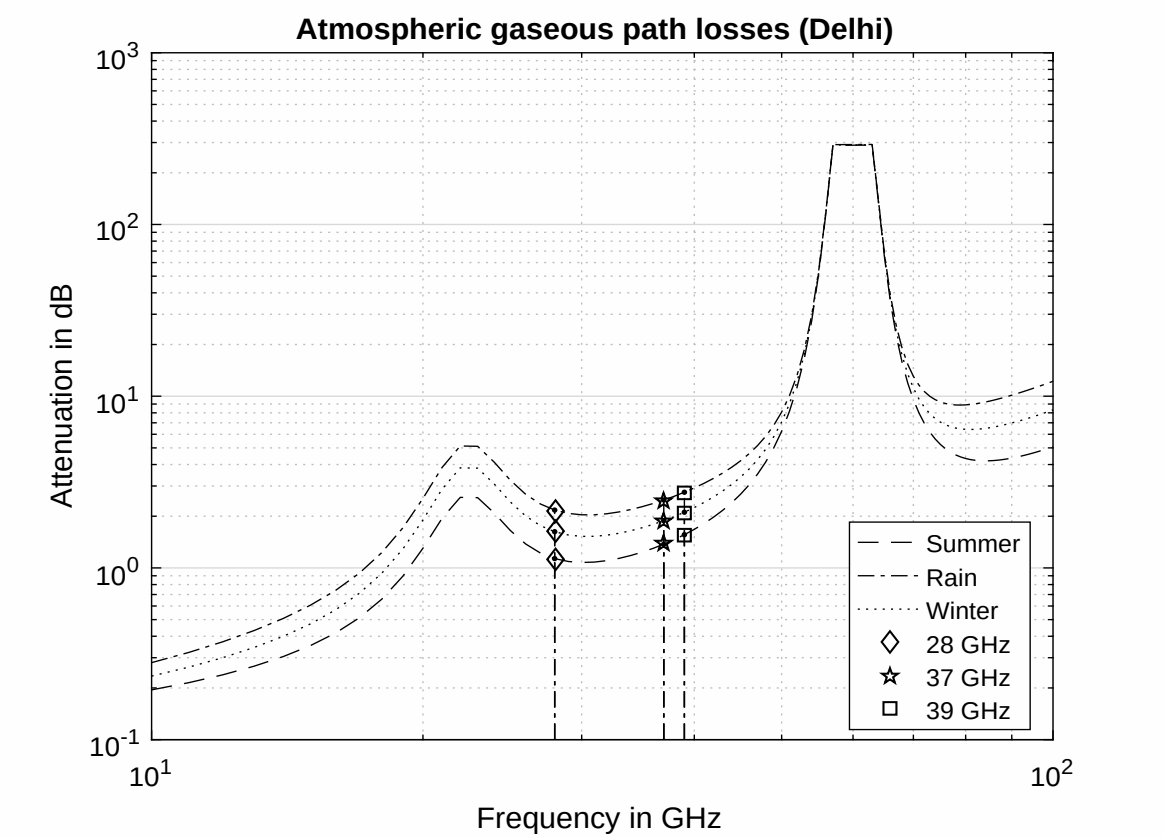

Figure 5.9: Attenuation due to atmospheric gases for 5G mmWave Communication System (Delhi).

season for these four cities. Figures 5.5-5.8 represents the attenuation for four cities respectively. Figure 5.9 shows the fog attenuation for Delhi in winter season. Figures 5.10-5.13 show the plot of the total atmospheric attenuation due to water vapour, oxygen, rain and fog for Delhi, Mumbai, Kolkata and Chennai. The attenuation applicability due to water vapour, oxygen, rain and fog have been considered as per cities respectively Delhi, Mumbai, Kolkata and Chennai.

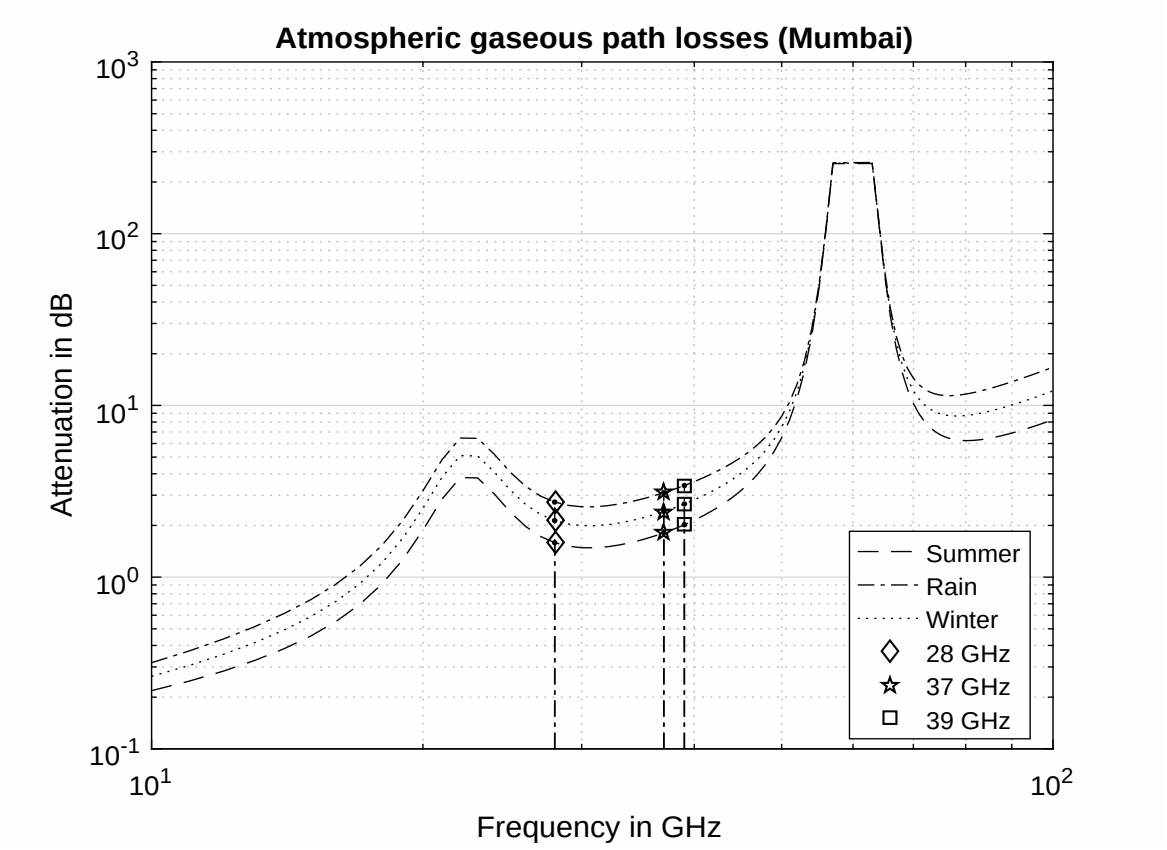

Figure 5.10: Attenuation due to atmospheric gases for 5G mmWave Communication System (Mumbai).

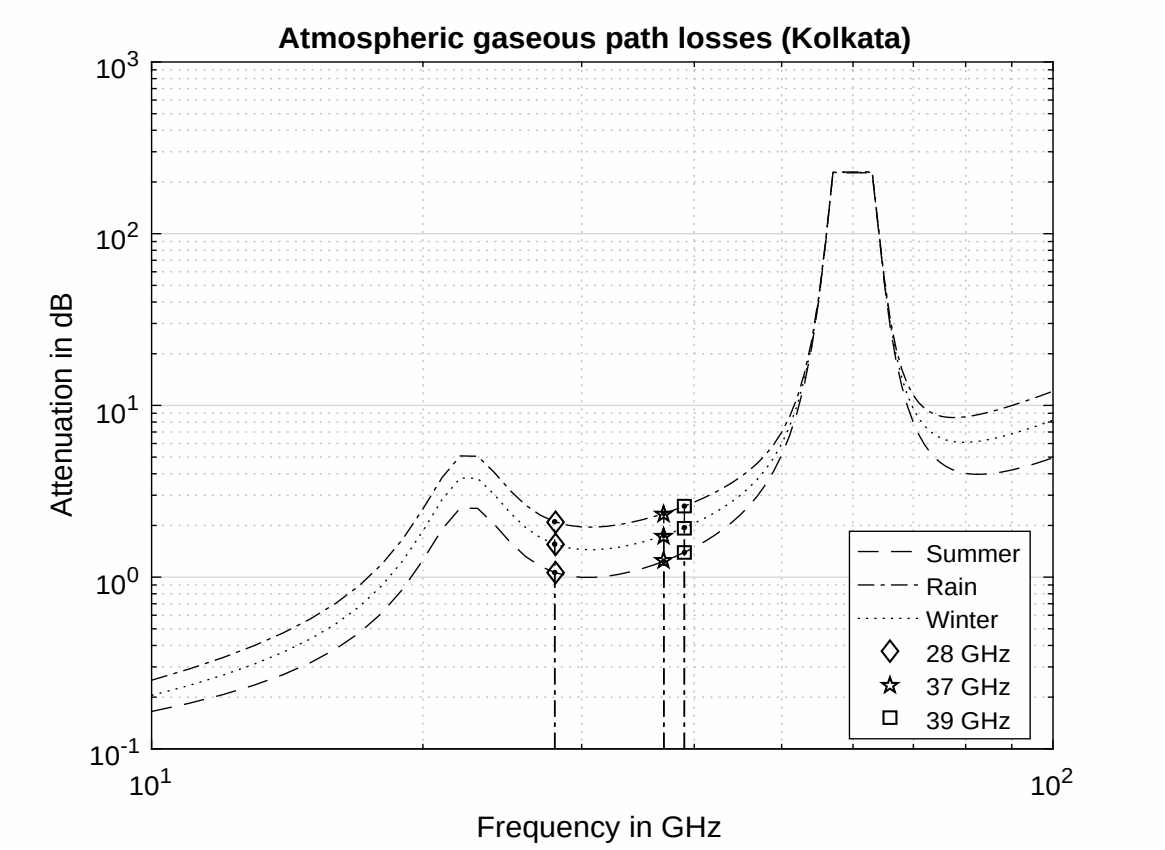

Figure 5.11: Attenuation due to atmospheric gases for 5G mmWave Communication System (Kolkata).

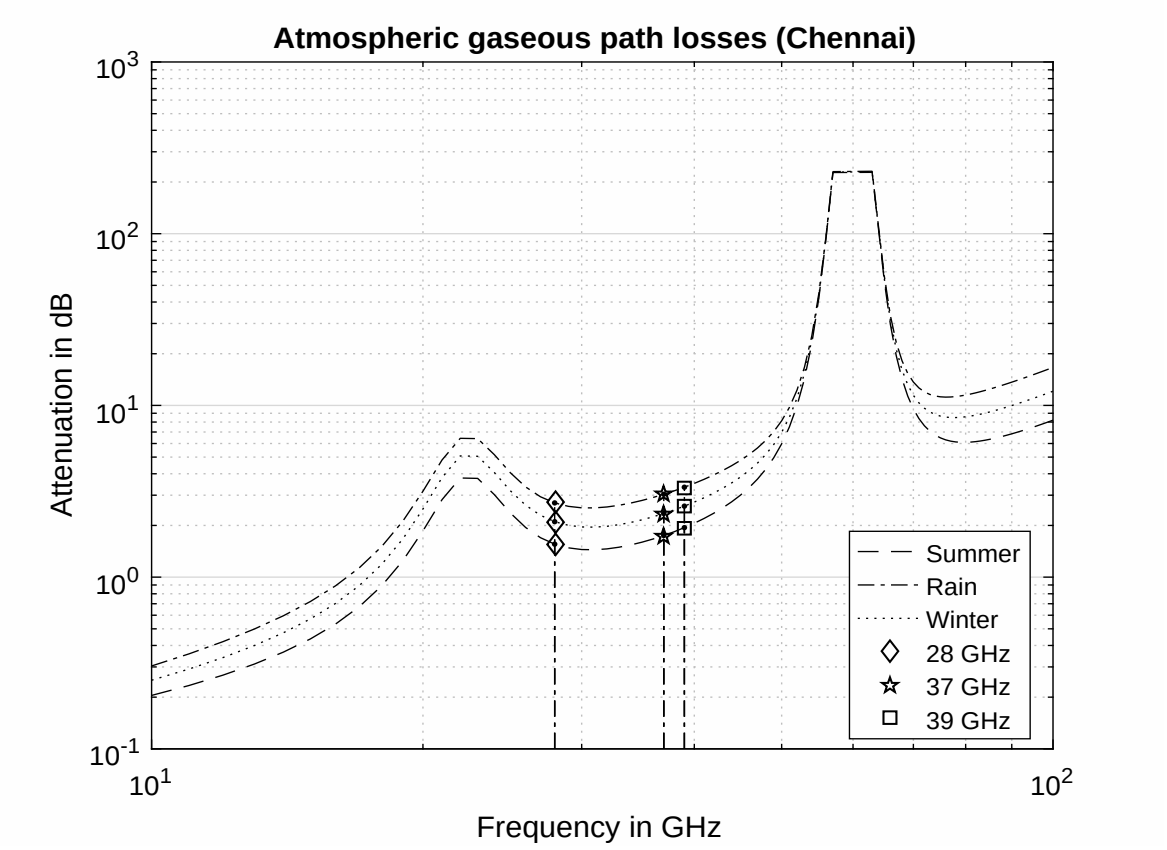

Figure 5.12: Attenuation due to atmospheric gases for 5G mmWave Communication System (Chennai).

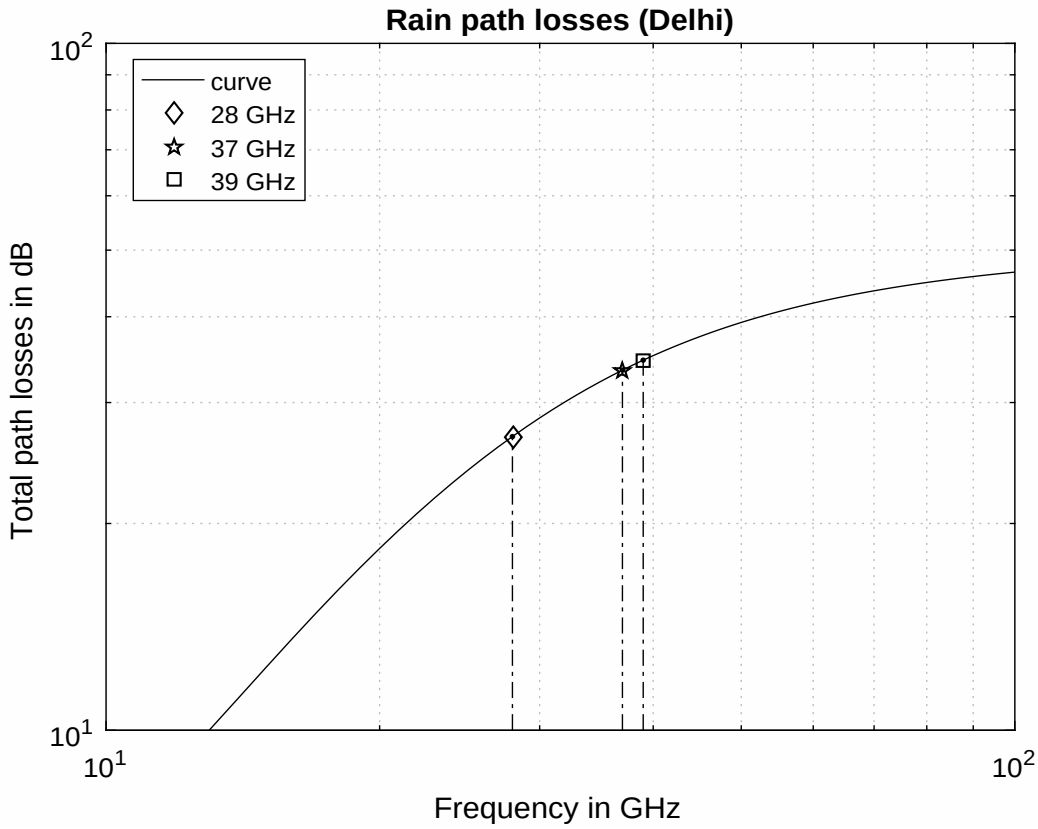

Figure 5.13: Attenuation due to rain for 5G mmWave Communication System (Delhi).

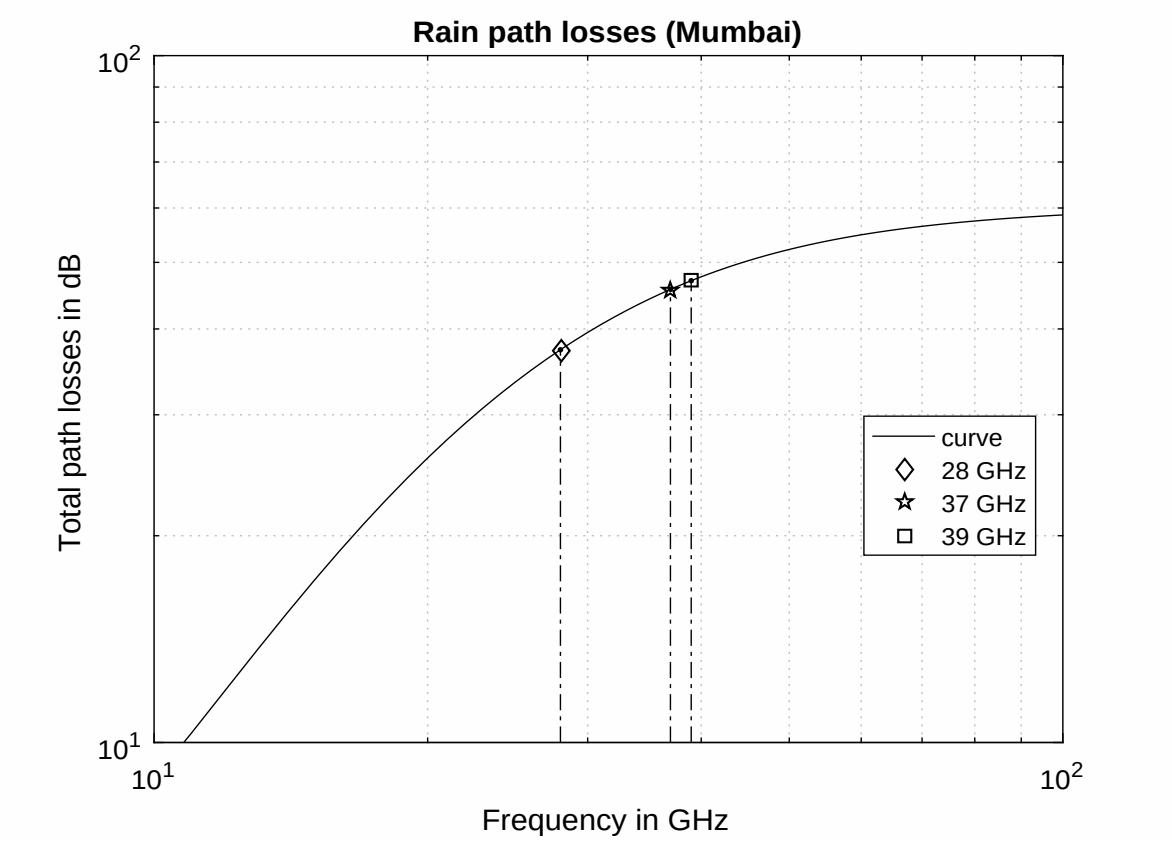

Figure 5.14: Attenuation due to rain for 5G mmWave Communication System (Mumbai).

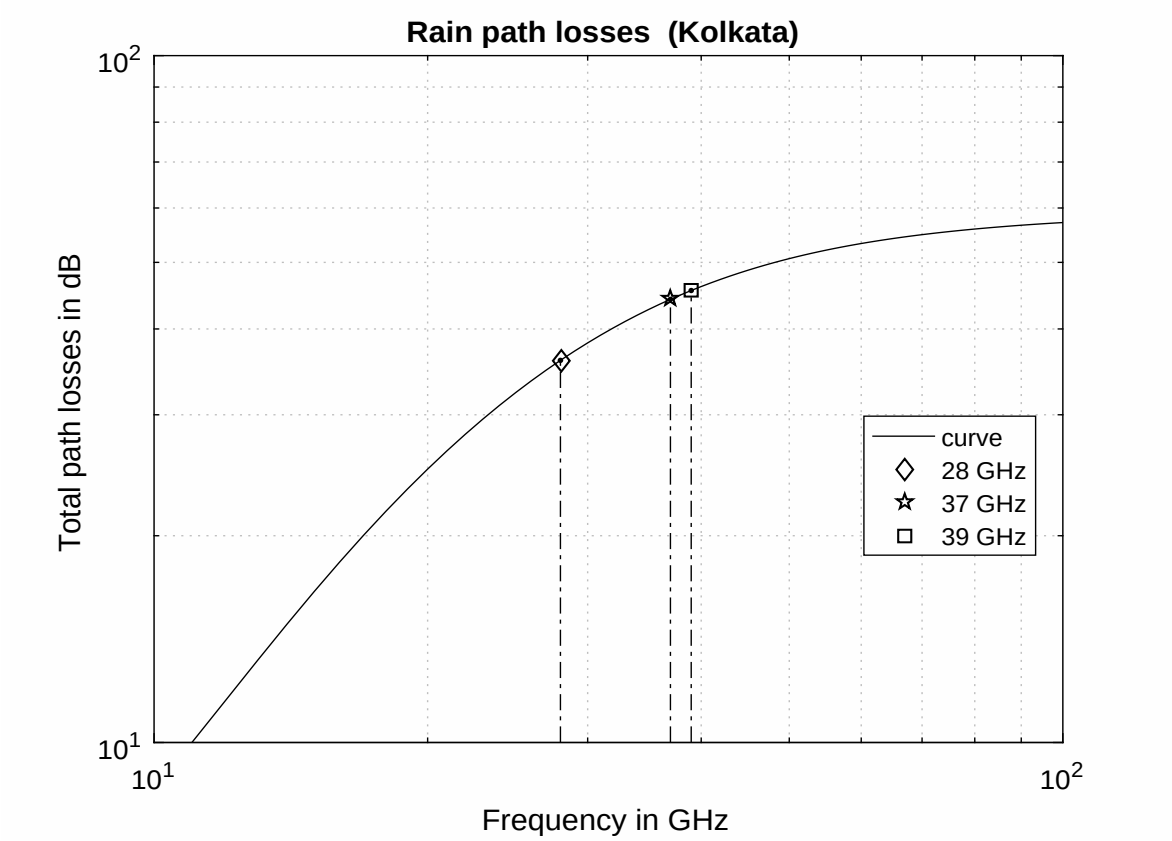

Figure 5.15: Attenuation due to rain for 5G mmWave Communication System (Kolkata).

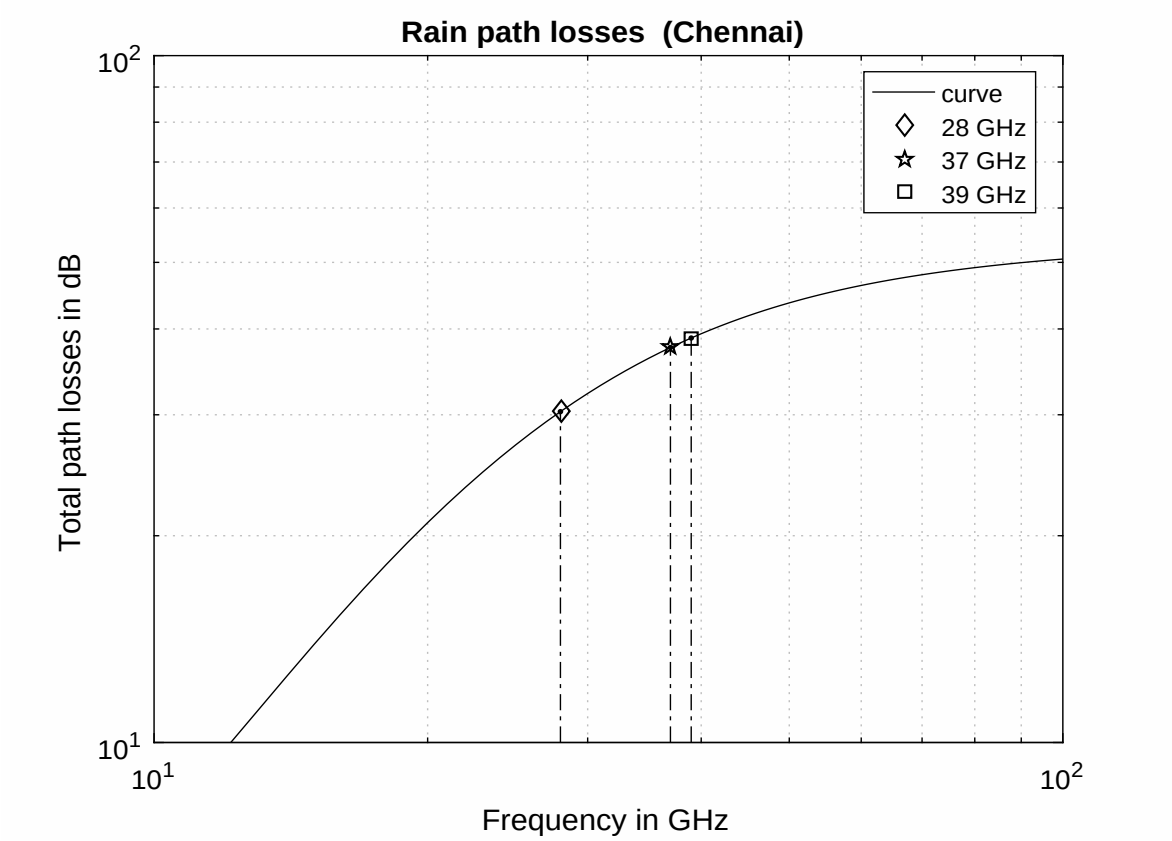

Figure 5.16: Attenuation due to rain for 5G mmWave Communication System (Chennai).

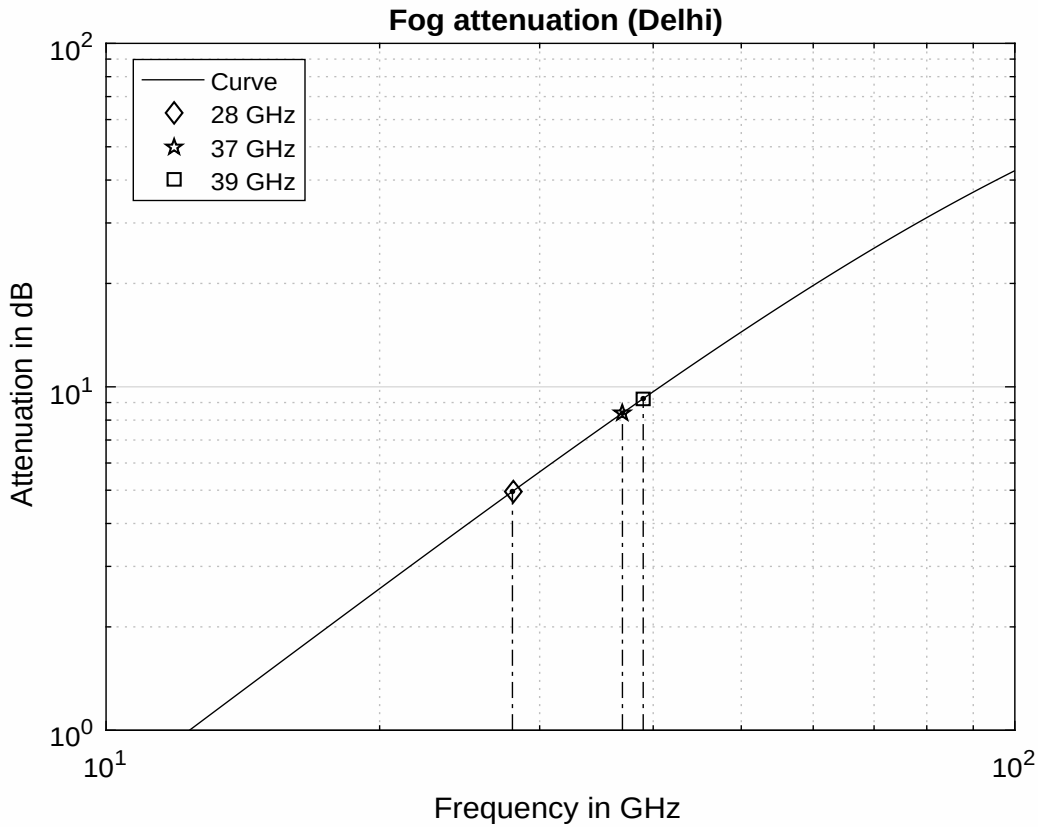

Figure 5.17: Attenuation due to fog for 5G mmWave Communication System (Delhi).

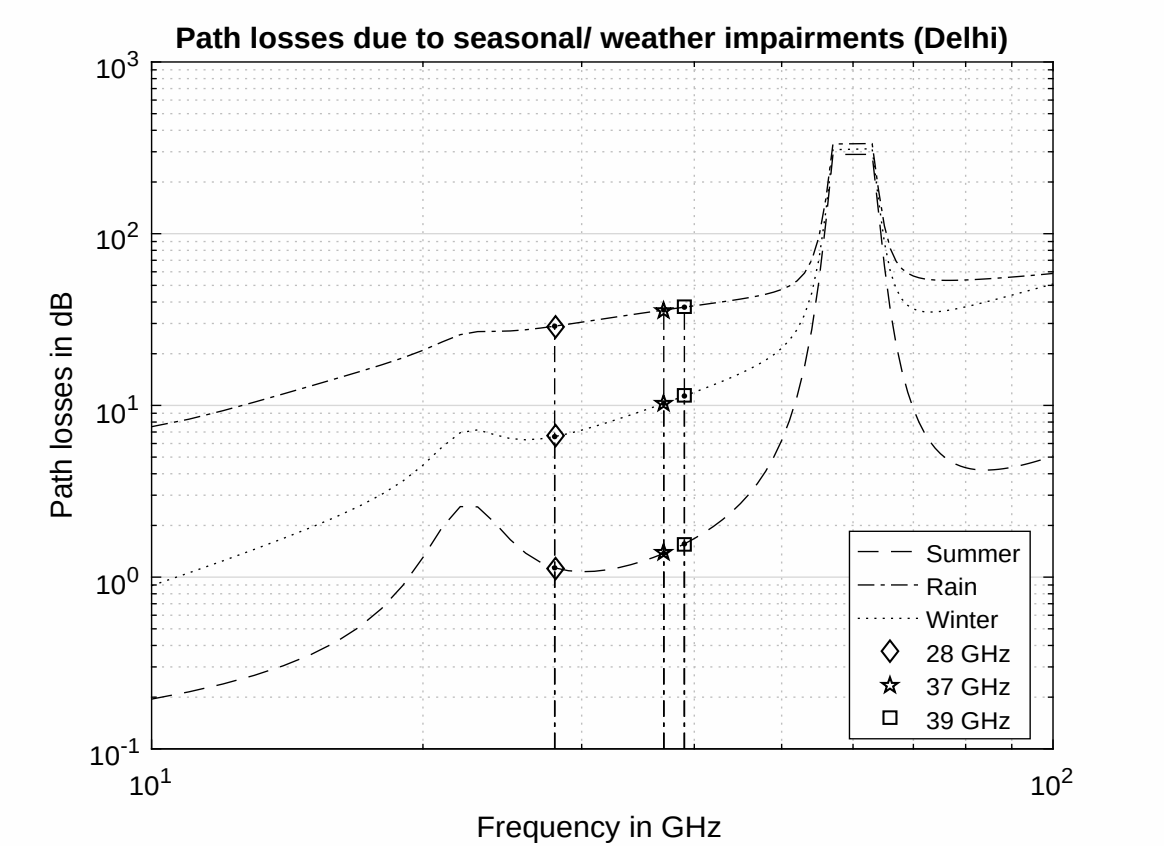

Figure 5.18: Attenuation due to Seasons (Summer, Rain and Winter) for 5G mmWave Communication System (Delhi).

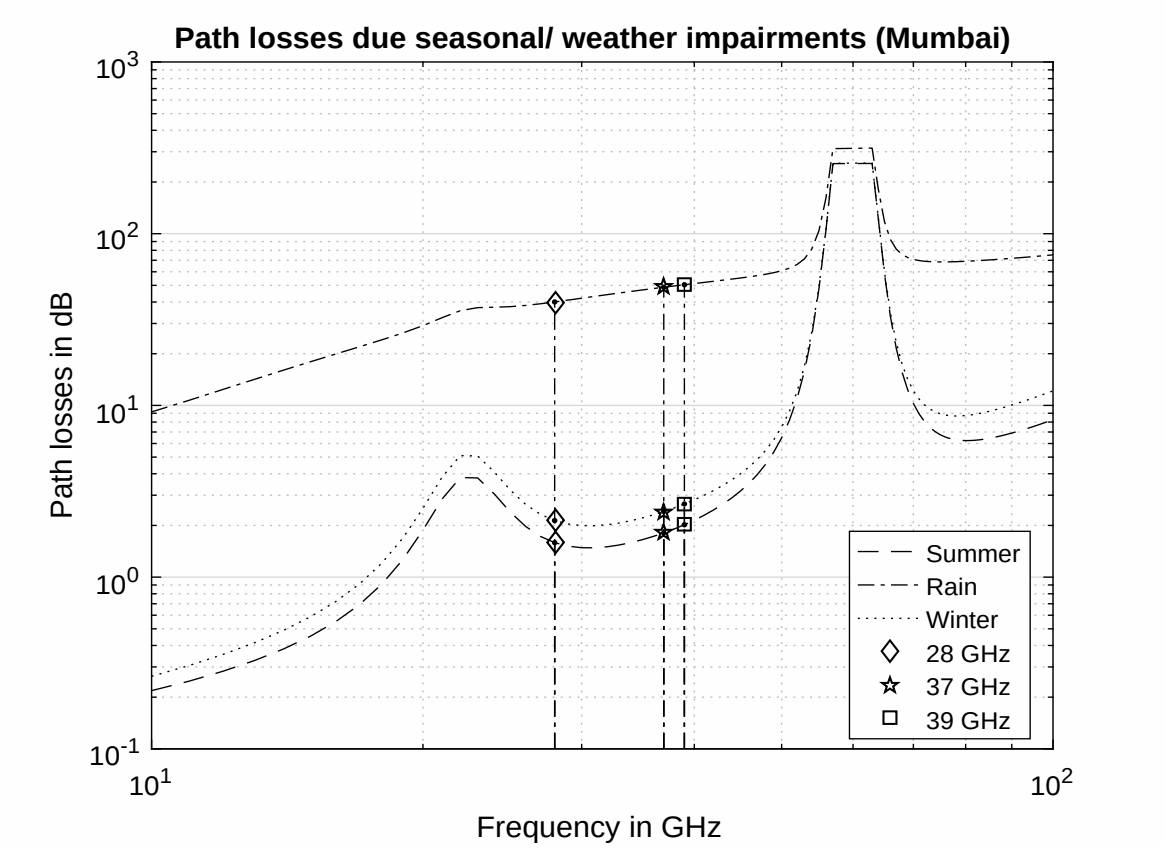

Figure 5.19: Attenuation due to Seasons (Summer, Rain and Winter) for 5G mmWave Communication System (Mumbai).

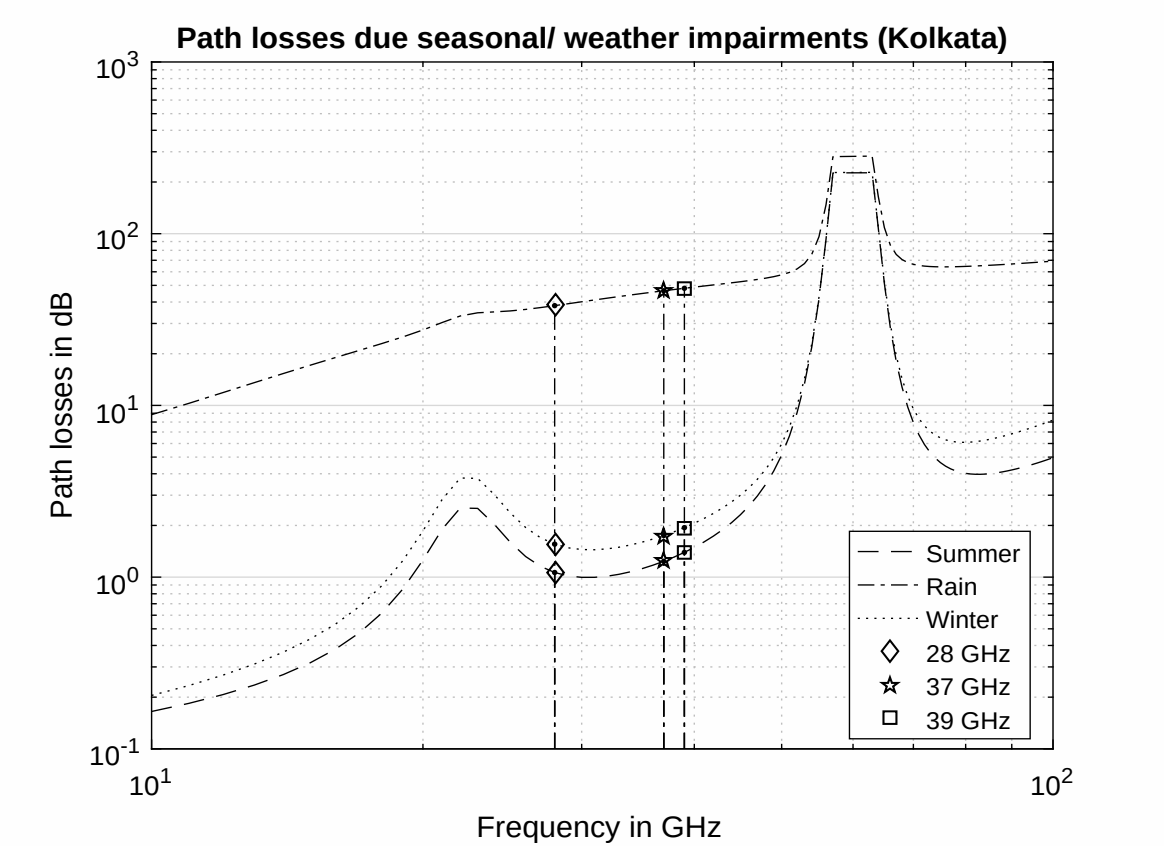

Figure 5.20: Attenuation due to Seasons (Summer, Rain and Winter) for 5G mmWave Communication System (Kolkata).

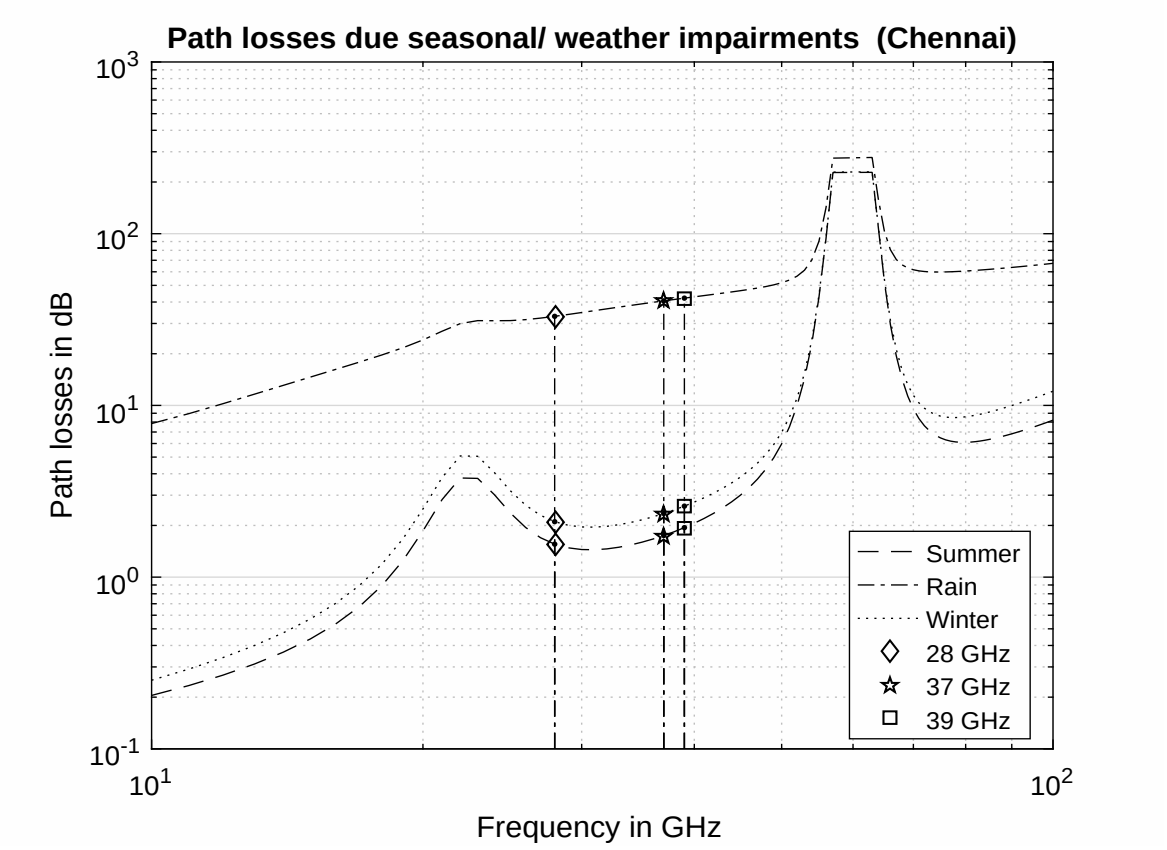

Figure 5.21: Attenuation due to Seasons (Summer, Rain and Winter) for 5G mmWave Communication System (Chennai).

Chapter 6

Result and Discussion

6.1 OFBW Grid Performance Results and Discussion

Based on the previous section findings of the grids having attenuation values due to various blockage or obstructions; in this section we will intelligently select the minimal attenuation grid by avoiding the obstructions or blockage to have efficient power transmission. Here, we classify and identifies zones as attenuation low (Al) or attenuation high (Ah). We have used threshold value (15dB) based deciding factor for attenuation low (Al) and attenuation high (Ah) to fill the grids/ metrix accordingly. As per simulation results and based on threshold value the attenuation values are classified in Ah and Al categories. The classified attenuation values are mapped with the grid values for the performance results evaluation and discussion to identify the optimum zone or set of grids for mmWave transmission. Figures 6.1-6.3 show the grids attenuation values for the frequency 28 GHz for DTU. Figures 6.1-6.3 show mmWave attenuation values

for various grids for 5G mmWave channel having building, atmosphere and vegetation as obstructions. It is clear that low attenuation zone has significant amount of less attenuation as compare to high attenuation zone values. It is shown that the grids with values of attenuations (low/ high) zones for 5G mmWave with type of intensity for the frequencies 28 GHz.

The 5G grid creator creates the grids on the at least one selected face and selects the at least one grid based with the minimal mmWave attenuation value by using low and high attenuation zones as shown in figures. The grids are created for the frequencies 28 GHz for DTU. Further, beam can be formed based on least attenuation value grid by avoiding obstruction or blockage (high attenuation values) which is one optimum grid as selected. By having minimal attenuation grid or grids; the 5G system can avoid high attenuation blockage from the mmWave propagation path. At least one optimum grid allows formation of the beam in a direction of a particular location with minimal attenuation or losses, thereby allowing control over shape and steering of antenna directivity pattern. Thus, formation of the at least one beam based on the at least one optimum grid generates a high directional and efficient beam with minimal losses and overheads. Beam-forming unit forms beam in accordance with the minimal attenuation zone which is provided by the system. As per this approach system controls and performs a function of transmitting a signal to the receiving antenna through at least one formed beam and transmitting antenna transmits the signal in the direction of the receiving antenna by avoiding high attenuation obstacles.

6.1.1 Validation and Discussion

5G provides wireless communication among nearby electronics devices using mmWave frequencies. This research carries importance especially in Cellular-Internet of Things (C-IoT) environment; where transmission power control is really important [1]-[5]. These minimal propagation attenuation grids are selected by avoiding obstacle(s). This grids-forming is done for mmWave 5G communication by considering obstruction attenuation into account and grid(s) selection for propagation path. Based on intelligent grid selection for optimal mmWave transmission; channel capacity has been calculated and validated with the obstacle and no-obstacle situation. The comparative Shannon channel capacity validates the performance of the 5G D2D propagation [3]-[5]. Shannon channel capacity per unit bandwidth (C/B) can be defined by the equation 4.1-4.3 as [23]-[25].

In equation 4.1-4.3, B is the 5G bandwidth in Hz, and S/N is the signal-to-noise ratio (SNR) of received mmWave signal power. The channel capacity per unit bandwidth C/B here is refereed as the 5G channel capacity [21]-[25]. Based on the intelligent selection of minimal attenuation grid; the 5G D2D application on the same for the minimal attenuation grids is shown here with channel capacity simulation result.

Figure 6.4 shows the grid attenuation values in a graph form for atmospheric, vegetation in-leaf and building in summer season for 28 GHz. In summer season only attenuation is due to water vapor and oxygen and in this time or season the water vapour moisture is less as compare to rain or winter. X axis and Y axis in figure 6.4

indicates the number of grids and z axis indicates the attenuation values for the summer season. It is clear from the figure that the low attenuation values show the valley which indicates the low attenuation zone / or grids around grid 3 to 4.

Figure 6.5 indicates 5G mmWave channel capacity in summer season for 28 GHz for urban, vegetation and atmospheric season summer. It is clear from figure 6.5 that the minimal attenuation grids provide the highest channel capacity by avoiding the obstacles in that virtual face. The figure 6.5, validates the simulation that air / summer atmospheric grids show the highest channel capacity by avoiding the obstructions/ blockage.

Figure 6.6 shows the grid attenuation values in a graph form for atmospheric, vegetation in-leaf and building in rain season for 28 GHz. It is clear from the figure that the low attenuation values show the valley which indicates the low attenuation zone around grid 3 to 4. In rain season air attenuation is due to water vapor, oxygen and rain. Figure 6.7 indicates 5G mmWave channel capacity in rain season for 28 GHz for urban, vegetation and atmospheric rain. It is clear from figure 6.7 that the minimal attenuation grids provide the highest channel capacity by avoiding the obstacles in that virtual face. This figure 6.7 validates the simulation that air / rain atmospheric grids show the highest channel capacity by avoiding the obstructions/ blockage. Beam forming is used to direct and steer an antennas directivity beam in a particular direction of minimal attenuation.

Figure 6.8 shows the grid attenuation values in a graph form for atmospheric, vegetation in-leaf and building in winter season for 28 GHz. Figure 6.9 indicates 5G

mmWave channel capacity in winter season for 28 GHz for urban, vegetation and atmospheric rain. It is clear from the figure 6.8, that the low attenuation values show the valley which indicates the low attenuation zone / or grids around grid 3 to 4. In winter season air attenuation is due to water vapor, oxygen and fog takes place. It is clear from figure 6.9 that the minimal attenuation grids provide the highest channel capacity by avoiding the obstacles in that virtual face. This figure 6.9 validates the simulation that air / winter atmospheric grids show the highest channel capacity by avoiding the obstructions/ blockage. In summer season mmWave attenuation is due to water vapor and oxygen. In summer time or season the water vapour moisture is less as compare to rain or winter. In rainy season attenuation is due to water vapor, oxygen and rain drops. In rainy time or season the water vapour moisture is very high as compare to rain or winter. In winter season attenuation is due to water vapor, oxygen and fog. In winter season the water vapour moisture is high as compare to summers. Such additional or extra air moisture also adds attenuation in mmWave propagation which is clear from the simulation results.

Such additional losses or attenuation effects the channel capacity by lowering the values. It is also clear from the Table 6.1 that the summer air shows the highest channel capacity due to minimal atmosphere attenuation and vegetation as well as urban shows the significant high attenuation values. Hence, it becomes important to avoid obstacles in mmWave propagation.

Capacity	*Air*	*Vegetation*	*Building*
Summer	6.64	6.17	4.98
Rain	6.63	6.15	4.94
Winter	6.63	6.57	4.96

Table 6.1: 5G mmWave channel capacity in various seasons for 28 GHz

Ah	Ah	Al	Al	Ah
Ah	Ah	Al	Al	Ah
Ah	Ah	Al	Al	Ah
Ah	Ah	Al	Al	Ah
Ah	Ah	Ah	Ah	Ah
Ah	Ah	Ah	Ah	Ah

Figure 6.1: 5G mmWave grids with zones of Attenuation high (Ah) and attenuation low (Al) in summer season for 28 GHz.

6.2 Attenuation with Channel Capacity Results and Discussion

In this research article , we have identified that vegetation is one of the cause in wireless for adding attenuation for mmWaves frequencies. This research articles uses ML algorithms for prediction of vegetation attenuation calculation as per training data set.

Ah	Ah	Al	Al	Ah
Ah	Ah	Al	Al	Ah
Ah	Ah	Al	Al	Ah
Ah	Ah	Al	Al	Ah
Ah	Ah	Ah	Ah	Ah
Ah	Ah	Ah	Ah	Ah

Figure 6.2: 5G mmWave grids with zones of Attenuation high (Ah) and attenuation low (Al) in rain season for 28 GHz .

Ah	Ah	Al	Al	Ah
Ah	Ah	Al	Al	Ah
Ah	Ah	Al	Al	Ah
Ah	Ah	Al	Al	Ah
Ah	Ah	Ah	Ah	Ah
Ah	Ah	Ah	Ah	Ah

Figure 6.3: 5G mmWave grids with zones of Attenuation high (Ah) and attenuation low (Al) in winter season for 28 GHz.

Based on calculation of vegetation attenuation prediction , the SCC can be calculated to control the data rate accordingly. As a result , in this research article we have predicted vegetation attenuation and calculated SCC for DTU campus for mmWaves . This research paper demonstrates the procedure along with the calculated values for

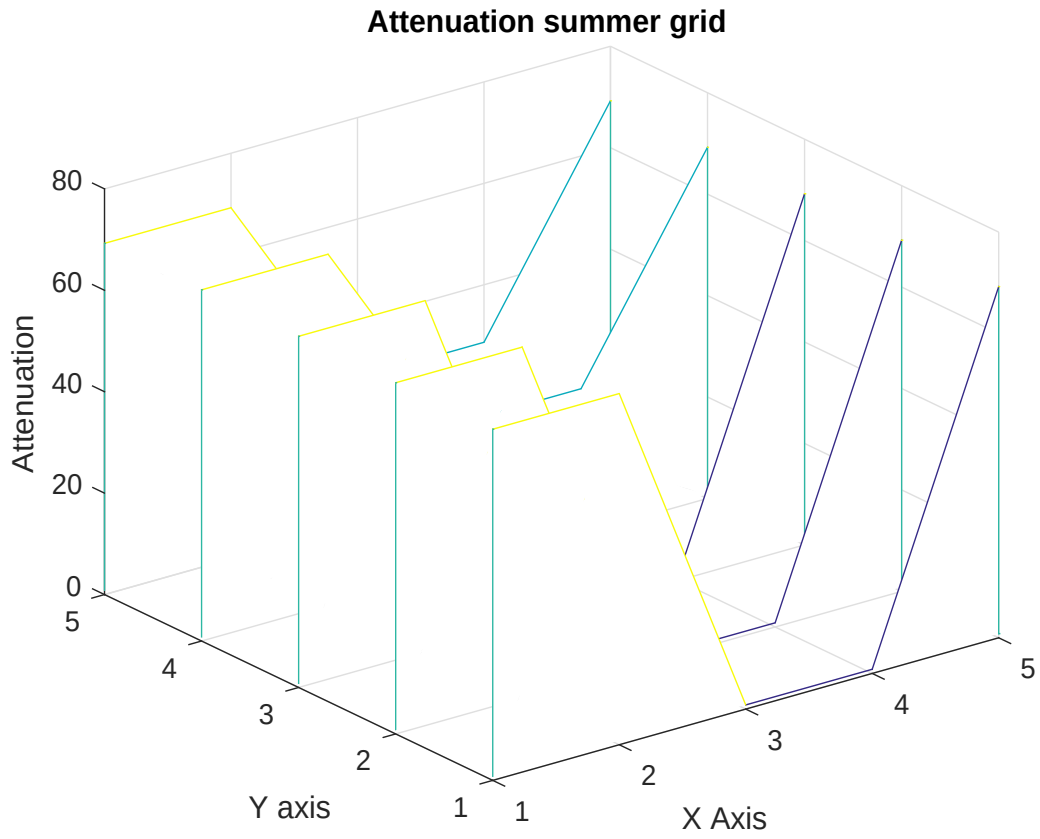

Figure 6.4: 5G mmWave grids attenuation values in a graph form for atmospheric, vegetation in-leaf and building in summer season for 28 GHz.

the vegetation attenuation and SCC with the mmWave frequencies.

Here, we have considered location DTU (New Delhi, India) as calculation experimental site for vegetation attenuation calculations. This site has big vegetation area and high vegetation density. The calculations are performed for the university campus by considering equi-probable season [16].

The vegetation density for this research study is considered constant and maximum 10 meter vegetation depth for mmWave propagation has been considered. The campus consists vegetation, buildings, soil, sand and with some areas with grass and concrete

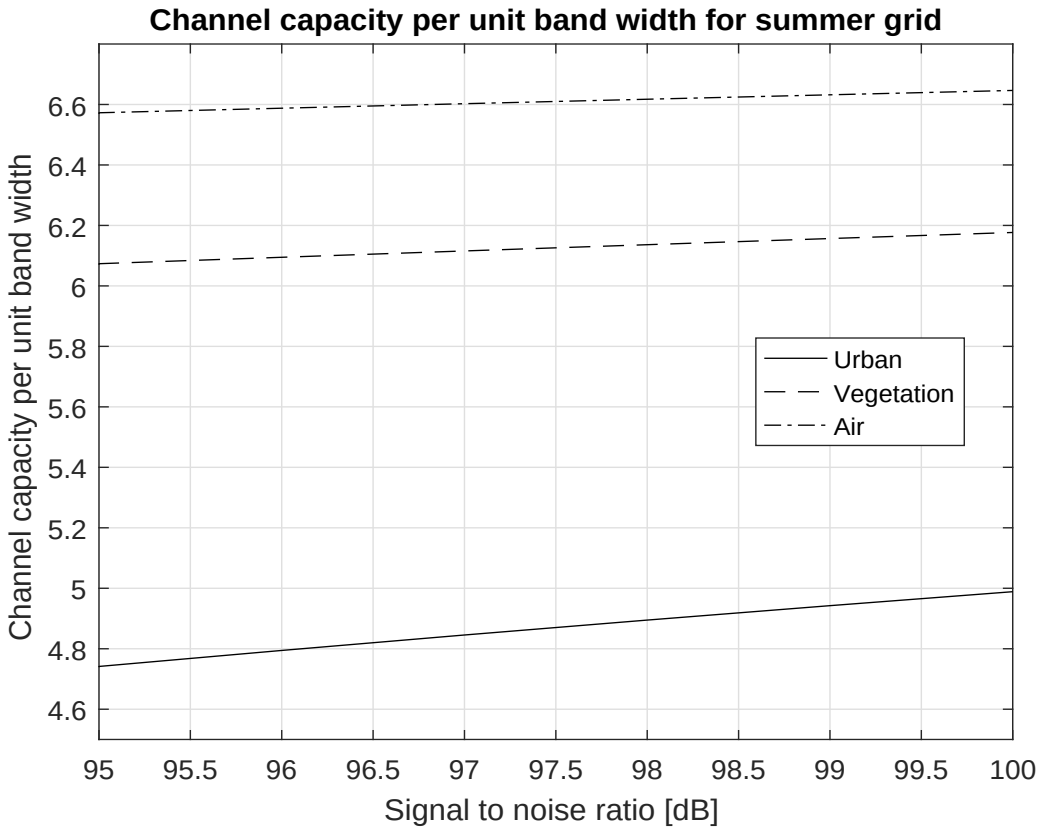

Figure 6.5: 5G mmWave channel capacity in summer season for 28 GHz.

roads. The vegetation trees average height of approximately 10 m based on equal spaced is considered here in calculations and considered that no wind.

Figure 6.4 shows vegetation attenuation for 5G mmWave channel having vegetation as obstructions. Further, Table 6.2 shows the vegetation attenuation for the proposed and simulated frequencies by using ITU-R model and ML prediction. Vegetation attenuation values for frequencies are shown for the vegetation depth 10 m for 5G mmWave Vegetation Attenuation (ITU-R Model) for frequencies having average vegetation depth 10 meters for DTU (New Delhi, India). As per figure 6.4; it is visible that for the various frequencies as dense foliage there which generates more high

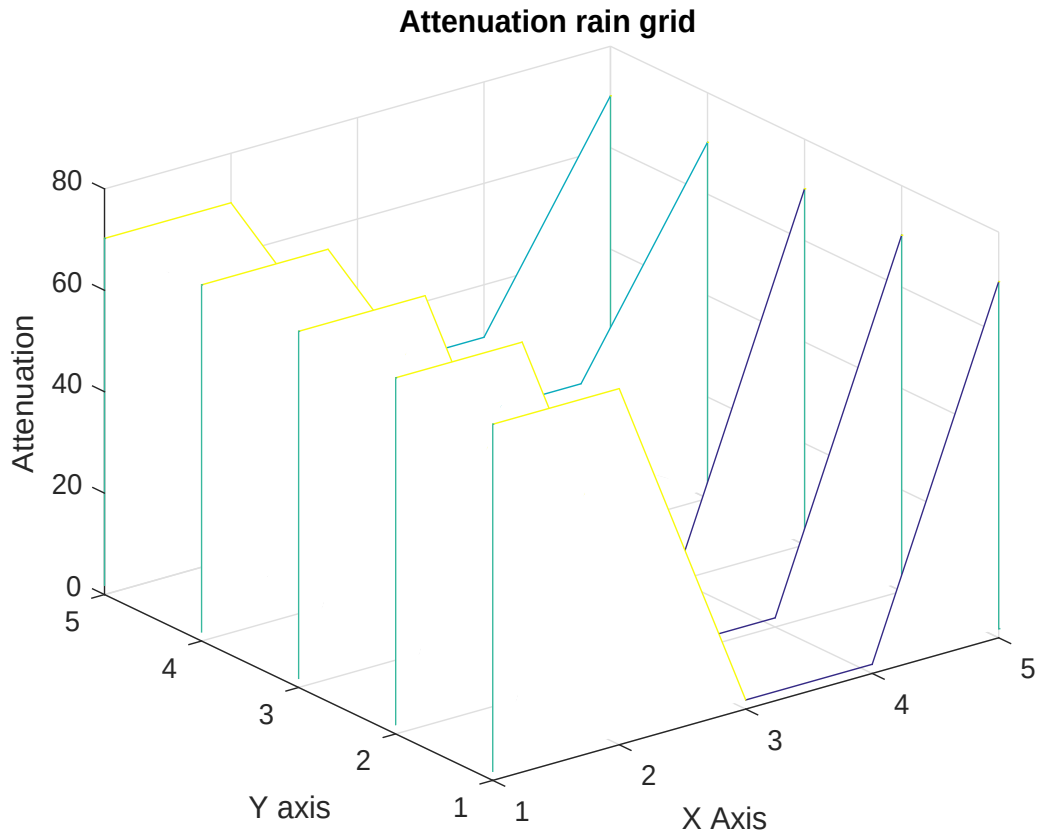

Figure 6.6: 5G mmWave grids attenuation values in a graph form for atmospheric, vegetation in-leaf and building in rain season for 28 GHz.

value vegetation attenuation and vegetation attenuation increases along with frequency increase also.

Figure 6.5 shows Shannon capacity for 5G mmWave channel having vegetation obstructions for the proposed and simulated frequencies. Shannon channel capacity values for the frequencies are shown with the S/N and vegetation depth 10m for DTU (New Delhi, India). It is clear from the Shannon channel capacity values that Shannon channel capacity keeps decreasing as vegetation depth increases. Increasing vegetation depth increases vegetation attenuation and which leads for low signal strength.

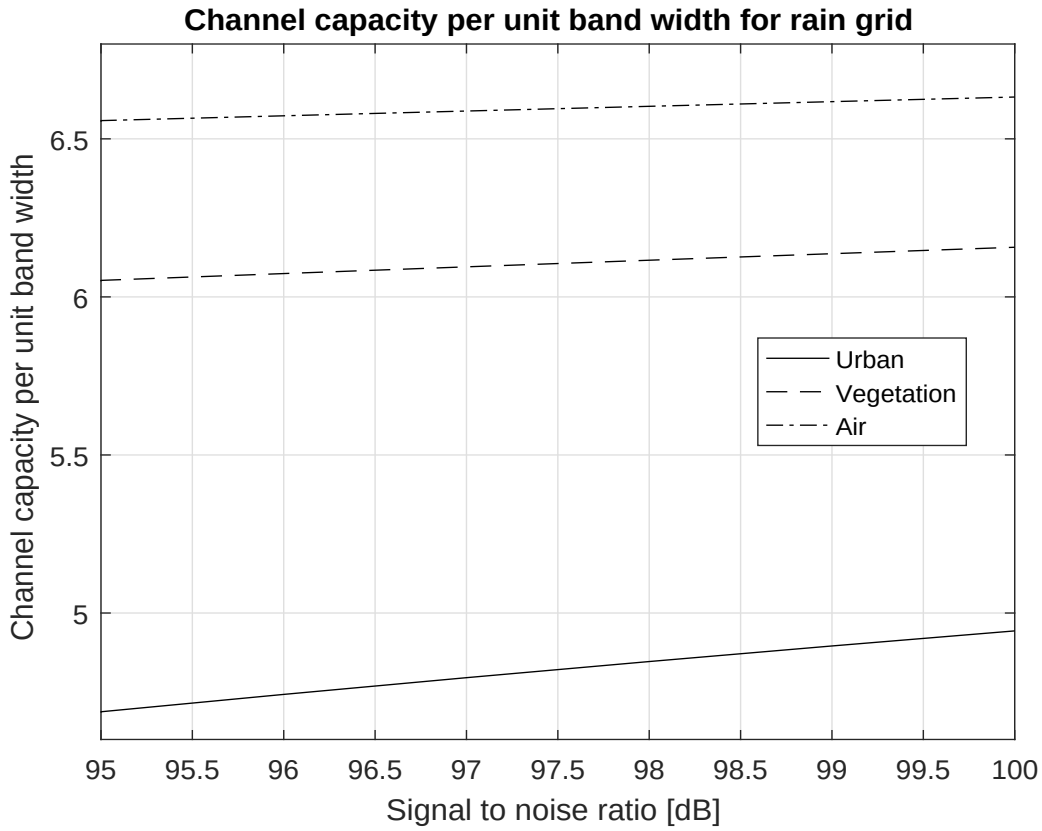

Figure 6.7: 5G mmWave channel capacity in rain season for 28 GHz.

Vegetation attenuation adds significant amount of attenuation in mmWave communication system which can be controlled through software controlling with the help of SDR. The SDR system can control the mmWave transmission as well as sense the related parameters for the efficient system performance. The SDR efficiently controls the transmission SCC by having reconfigurable automated antennas control. The software control in SDR changes the transmission results based on the received input parameters like frequency, vegetation attenuation required SCC and etc. These simulations have been performed using ML software and plot software.

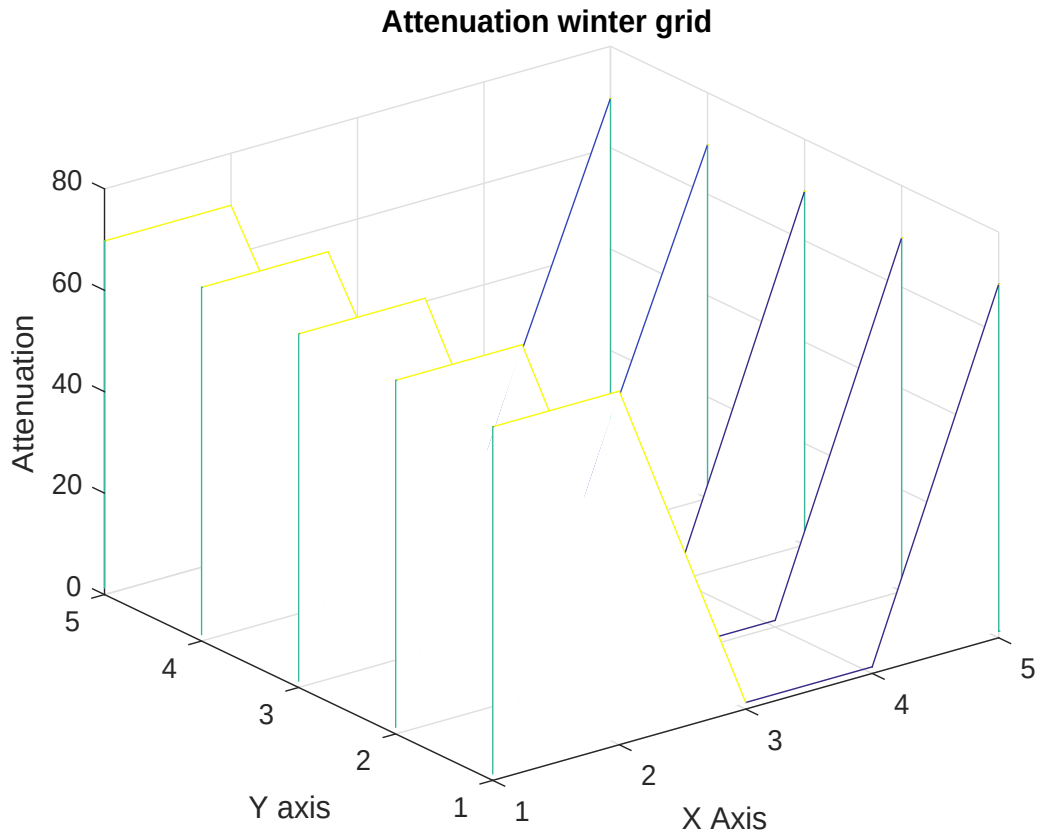

Figure 6.8: 5G mmWave grids attenuation values in a graph form for atmospheric, vegetation in-leaf and building in winter season for 28 GHz.

6.3 Atmospheric Channel Capacity Results and Discussion

Software Defined mmWave facilitates transmission power control in a real manner. 5G millimeter wave communication system transmitter and receivers can be controlled by artificial intelligent (AI) software defined (SD) mmWave communication system . AI based software defined mmWave facilitates methods to control the transceiver as per atmospheric attenuation [19-23].

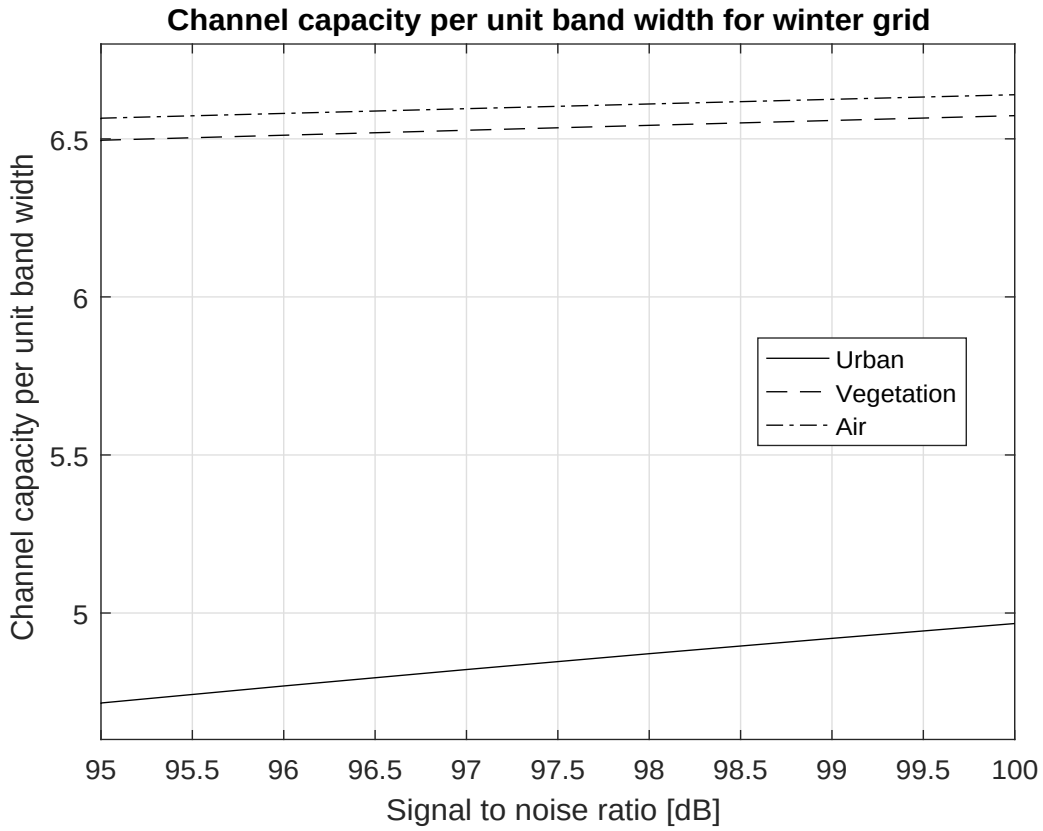

Figure 6.9: 5G mmWave channel capacity in winter season for 28 GHz.

In this research intelligent adaptive transmitter based on trend of the atmospheric conditions tunes to machine learning (ML) based derivation of channel capacity. The ML based transmitter is a supervised ML device and it has provision of self teaching learning machine based on data. Here intelligent an adaptive transmitter which is having machine learning (ML) based on previous trends of the attenuations decides the optimal channel capacity. Its intelligence is based on the various type of attenuations as per various conditions as described. The decision-directed adaptive receiver has the same structure as the gremlin receiver, but uses its own decisions . The adaptive ML based transmitter is useful to intelligently provide the required channel capacity.

$Freq.(f)$ (GHz)	$Av\ (ITU-R)$ (dB)	$Av\ \ (KNN)$ (dB)	$Av\ \ (DT)$ (dB)	$Av\ \ (RF)$ (dB)
28	17.19	15.13	15.03	14.99
37	18.68	16.83	16.78	16.69
39	18.98	16.97	16.98	16.97

Table 6.2: 5G mmWave Vegetation Attenuation Prediction Values as per ML unit for DTU (New Delhi, India)

It intelligently regulates the demand and need of channel capacity in 5G millimeter wave communication system in Delhi. Shannon channel capacity in the presence of continuous additive white Gaussian noise channel is given by equations 4.1-4.3 [19-26].

The received signal-to-noise power ratio (S/N) in dB due to water vapor, oxygen, rain and fog are classified using machine learning (ML) for various seasons. Delhi summer season includes atmospheric attenuation due to atmospheric water vapor and oxygen. For this city rainy season includes atmospheric attenuation due to atmospheric water vapor, rain and oxygen. Further, in winter season fog play one of the role for attenuation and winter season includes atmospheric attenuation due to atmospheric

$Freq.(f)$ (GHz)	$C\ (b/s)$ $50\ dB$	$C\ (b/s)$ $55\ dB$	$C\ (b/s)$ $60\ dB$	$C\ (b/s)$ $65\ dB$
28	5.08	5.28	5.45	5.61
37	5.01	5.22	5.40	5.56
39	5.00	5.21	5.39	5.55

Table 6.3: 5G mmWave SCC during Vegetation Attenuation (ITU-R Model) for Frequencies 28 GHz, 37 GHz and 39 GHz having average vegetation depth 10 meters for DTU (New Delhi, India)

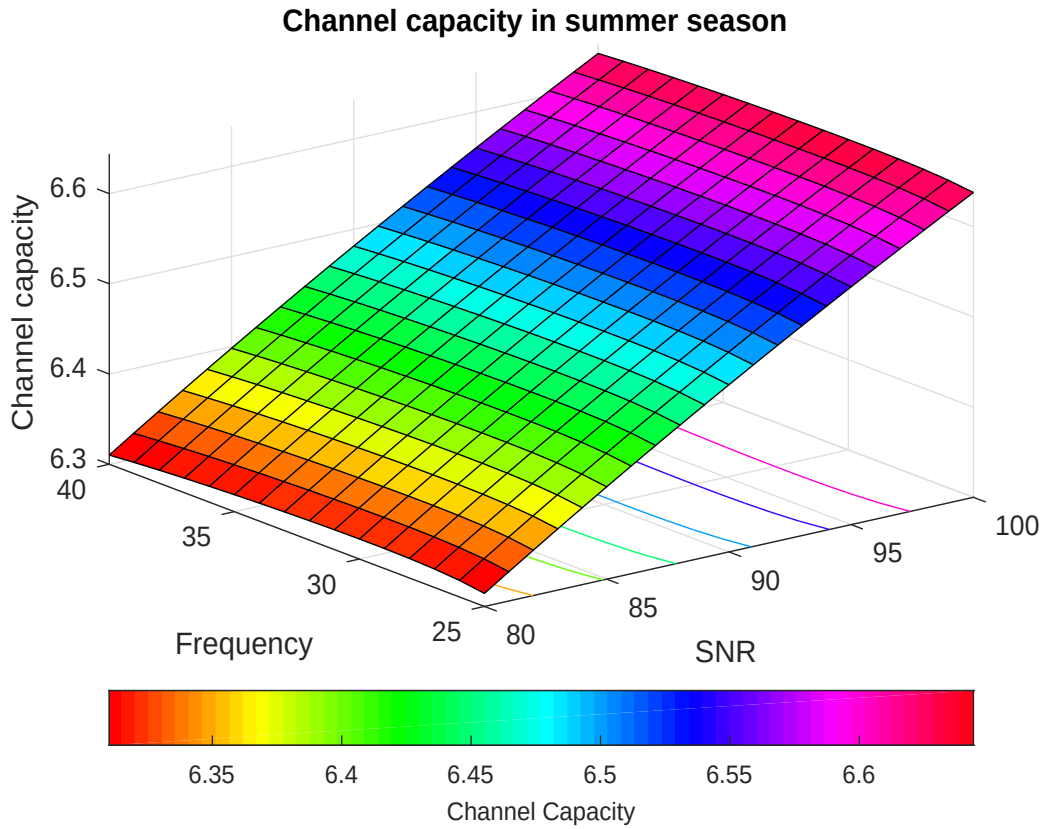

Figure 6.10: Channel Capacity in Summer Season for 5G mmWave Wireless Communication System.

water vapor, fog and oxygen. In Delhi; mmWave 5G mmWave communication system software defined channel capacity are shown for summer, rain and winter in Fig. (9), (10) and (11). These plots are shown with channel capacity as per atmosphere and shown for the frequencies 28GHz , 37 GHz and 39GHz. By using AI based software controlled transmitter and or receivers the channel capacity can be controlled intelligently. In Delhi; mmWave 5G mmWave communication system software defined channel capacity are shown for summer, rain and winter in Fig. (9), (10) and (11). These plots are shown with channel capacity as per atmosphere and shown for

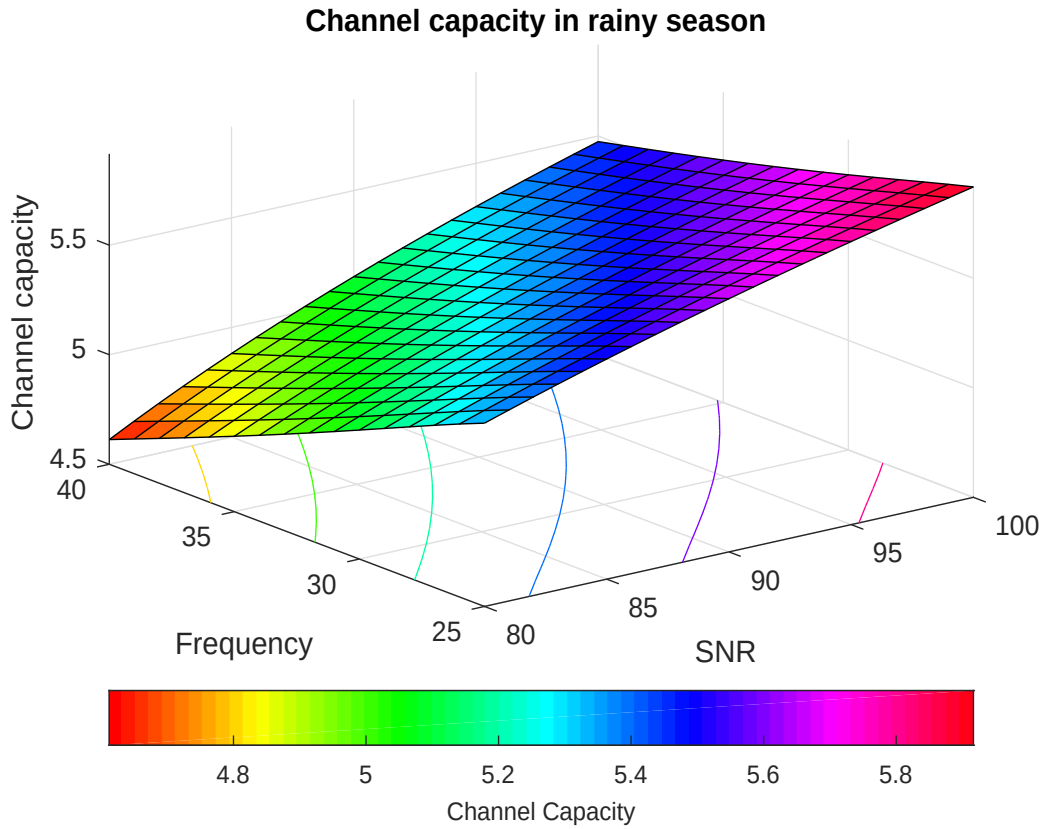

Figure 6.11: Channel Capacity in Rainy Season for 5G mmWave Wireless Communication System.

the frequencies 28GHz , 37 GHz and 39GHz. By using AI based software controlled transmitter and or receivers the channel capacity can be controlled intelligently.

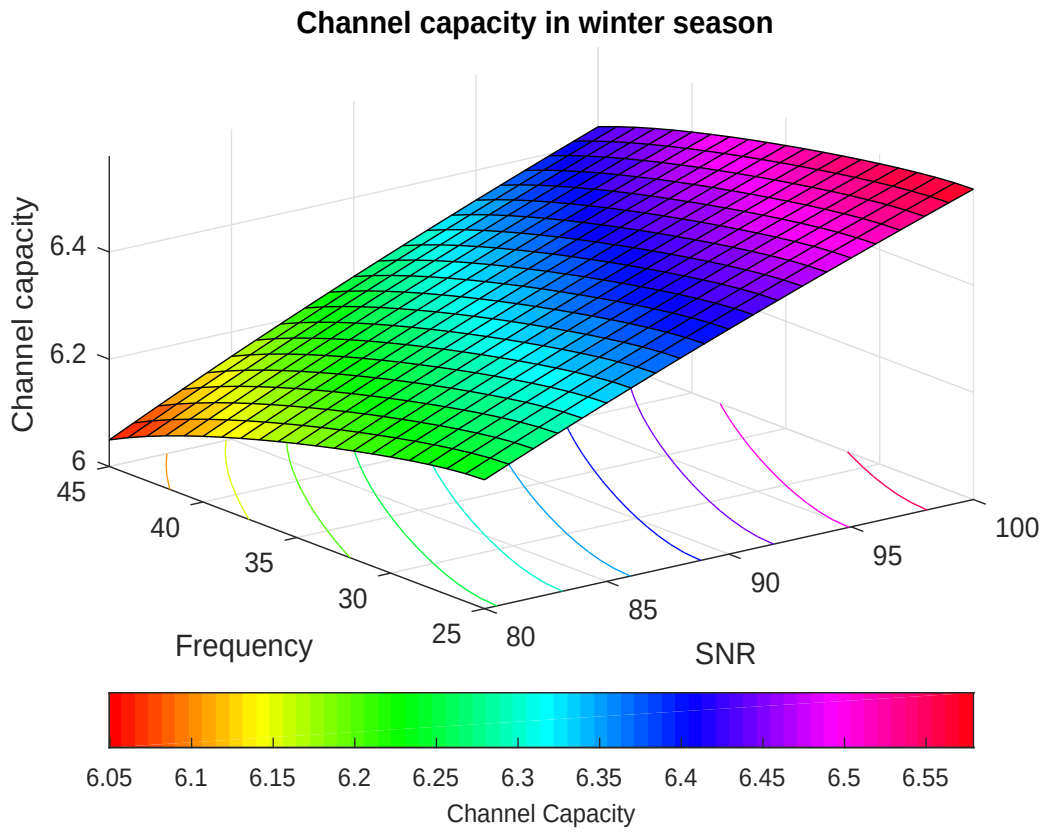

Figure 6.12: Channel Capacity in Winter Season for 5G mmWave Wireless Communication System.

Chapter 7

Conclusions and Scope for Future Work

7.1 Conclusions

In this thesis we have analyzed the performance of mmWave propagation in wireless channel. We have proposed intelligent optimum grid selection for transmission along with attenuation and capacity prediction. We have considered the simulation for the mmWave frequencies.

In chapter 3, we proposed minimal attenuation grid for 5G mmWave link in DTU campus area which is having open air, vegetation and building area. 5G mmWave antenna forms grids and calculates the minimal attenuation grids for atleast one of the purposes like; beamforming, minimal loss path, line of Sight (LoS), power planning, link budget planning and etc. The method effectively selects at least one grid from

amongst the grids as an optimum grid based on the minimal attenuation. Here we have simulated results and calculations are performed for the frequencies 28 GHz. Further, Shannon channel capacity has also been calculated for various seasons and respectively for vegetation and building. It is clear from simulation results and validation that the Shannon channel capacity in atmospheric impairments is higher as compare to other mentioned grid values. The purpose of this analysis is to review the impact of the obstacles like; atmosphere, seasons, vegetation and urban-site attenuation and choose the minimum attenuation grid as minimum attenuation path for mmWaves in 5G communication system. This method is useful in many ways for 5G mmWave communication system. This further reduces complexity of the 5G systems and optimizes performance parameters. Further, time, load and power consumption for beam forming is considerably reduced, as the beam is formed based on the selected grid rather than linear scanning. This research provides solution to have minimal attenuation path for the 5G transmitter under various type of obstructions like vegetation or urban/ buildings. However, many additional measurements/ calculations are needed to detect the type of obstructions for having quality grid attenuation values. This research provides an easy direction for low channel losses especially in dense obstruction areas.

In chapter 4 we presented our proposed attenuation prediction and channel capacity. The vegetation attenuation adds significant amount of attenuation for mmWaves during free space propagation in 5G wireless communication system. The vegetation attenuation calculation values information provides facility to control the channel capacity using SDR. The research analysis has been presented in this thesis along with

the demonstration of vegetation attenuation calculation for the mmWave as well as prediction of the values using ML (supervised regression mode with KNN, Decision Tree and Random Forest). This paper also suggests and demonstrates that SCC can be controlled using SDR and can tune the transmitter with the desired channel data rate by the virtue of SDR based control and use of the prediction values. Such type of intelligent control benefits the link budget analysis and software automatic control as per need and demand. This chapter presents the vegetation attenuation for mmWave propagation through vegetation obstruction. The vegetation attenuation calculation is performed for the frequencies 28 GHz, 37 GHz and 39 GHz by using ITU-R model. It is shown in the paper that the vegetation attenuation varies and depends on the mmWave frequencies and depth of vegetation. The vegetation attenuation can also be predicted by using ML prediction unit. Further, we described a software defined mmWave based SNR control method for improving or maintaining the Shannon Channel Capacity (SCC) for 5G mmWave communication system by considering effect of vegetation. The vegetation loss prediction unit predicts the vegetation attenuation based on ML algorithms and used to demonstrate losses for the proposed frequencies. This proposed research work is useful in power planning, network optimization and system controlling. The evaluation of this research describes that the SDR along with ML prediction unit provides solution to control the transmission with the values like power saving, data rate control, optimized power transmission and etc. Further, future work includes the machine learning based prediction for the vegetation attenuation values in the presence of air as well as rain also to deal with more complex situation in real time values

prediction.

The chapter 5 research presents atmospheric attenuation calculation for various atmosphere attenuation causes for 5G mmWave propagation attenuation at the frequencies 28 GHz, 37 GHz and 39 GHz for Delhi (India). It is shown in the research that the atmospheric attenuation due to water vapor, oxygen, rain and fog varies and depends on the mmWave frequencies. This research also signifies the reason of the selection of the frequencies 28 GHz, 37 GHz and 39 GHz for 5G mmWave Communication System with minimal attenuation. Software Defined mmWave facilitates transmission power control in a real manner. 5G mmWave communication system transmitter and receivers can be controlled by the software defined mmWave communication system. Software Defined mmWave facilitates methods to control the transceiver as per atmospheric attenuation and demand and need of channel capacity in 5G millimeter wave communication system. Here intelligent an adaptive transmitter which is having ML based on previous trends of the attenuations decides the optimal channel capacity. Its intelligence is based on the various type of attenuations as per various conditions as described. The decision-directed adaptive receiver has the same structure as the gremlin receiver, but uses its own decisions. The adaptive ML based transmitter is useful to intelligently provide the required channel capacity. This research is useful for transmission link budget for 5G mmWave Communication system for instant installation.

7.2 Future Work

There are several directions in which this work can be extended. Some important extensions for future work are given as follows:

- Real time calculations and processing in back-haul network and in cell network simultaneously.
- Simulates 2D and 3D beamfoming for mobile users by considering the impact of assorted obstructions.
- Includes the machine learning based prediction for the vegetation attenuation values to deal with more complex situation in real time values prediction.
- It involves the identifying the various other dynamic atmospheric attenuation causes for the atmospheric attenuation for 5G mmWave Communication and includes real time atmospheric data processing as per weather forecasting .

Bibliography

[1] Zhouye Pi et al., " An Introduction to Millimeter- Wave Mobile Broadband Systems," *IEEE Communications Magazine* , vol.49, no.6, pp.101- 107, Jun. 2011.

[2] Zhouye Pi et al., " An Introduction to Millimeter- Wave Mobile Broadband Systems," IEEE Communications Magazine , vol.49, no.6, pp.101- 107, Jun. 2011.

[3] Y.-W. Hong and A. Scaglione, "Energy-efficient broadcasting with cooperative transmissions in wireless sensor networks," *IEEE Transactions on Wireless Communications*, vol. 5, no. 10, pp. 2844–2855, October 2006.

[4] T. Brown, E. D. Carvalho, and P. Kyritsi, *Practical Guide to the MIMO Radio Channel*, 1st edition, West Sussex, U.K.: John Wiley and Sons Ltd, 2012.

[5] T. M. Cover and A. A. E. Gamal, "Capacity theorems for the relay channel," *IEEE Transactions on Information Theory*, vol. 25, no. 5, pp. 572–84, September 1979.

[6] A. Goldsmith, *Wireless Communications*, Cambridge University PressC, 1st edition, 2005.

[7] B. S.-Mergen and A. Scaglione, "On the power efficiency of cooperative broadcast in dense wireless networks," *IEEE Journal on Selected Areas in Communications*, vol. 25, no. 2, pp. 497–507, February 2007.

[8] Y.-R. Tsai and L.-C. Lin, "Optimal Power Allocation for Decode-and-Forward Cooperative Diversity Under an Outage Performance Constraint," *IEEE Communication Letters*, vol. 14, no. 10, pp. 945–947, October 2010.

[9] G. Zhao, C. Yang, G. Y. Li, D. Li, and A. C. K. Soong, "Power and channel allocation for cooperative relay in cognitive radio networks," *IEEE Journal of Selected Topics in Signal Processing*, vol. 5, no. 1, pp. 151–159, February 2011.

[10] R. K. Mallik, "A new statistical model of the complex nakagami-m fading gain," *IEEE Transactions on Communications*, vol. 58, no. 9, pp. 2611–2620, September 2010.

[11] A. A. Abu-Dayya and N.C. Beaulieu, "Microdiversity on Rician fading channels," *IEEE Transactions on Communications*, vol. 42, no. 6, pp. 2258–2267, June 1994.

L.-C. Wang and C.-T. Lea, "Exact analysis of co-channel interference in a shadowed-Nakagami/shadowed-Rician channel model," in proceedings of *IEEE International Conference on Communications*, Seattle, U.S.A., 18-22 June 1995.

[12] A.D. Wyner, "Shannon-theoretic approach to a Gaussian cellular multiple-access channel," *IEEE Transactions on Information Theory*, vol. 40, no. 6, pp. 1713–1727, November 1994.

[13] J. C. S. S. Filho and M. D. Yacoub, "Nakagami-m approximation to the sum of M non-identical independent Nakagami-m variates," *IET Electronics Letters*, vol. 40, no. 15, pp. 951–952, 22 July 2004.

[14] G. K. Karagiannidis, N. C. Sagias, and T. A. Tsiftsis, "Closed-form statistics for the sum of squared Nakagami-m variates and its applications," *IEEE Transactions on Communications*, vol. 54, no. 8, pp. 1353–1359, August 2006.

[15] I. Wolfram Research, *Mathematica Edition: Version 8.0*, Champaign, Illinois:Wolfram Research Inc., 2010.

[16] A. M. Salhab, F. Al-Qahtani, S.A. Zummo, and H. Alnuweiri, "Performance analysis of dual-hop AF relay systems with interference-limited destination in Nakagami-m/Rician fading channels," in proceedings of *11th International Conference on Information Science, Signal Processing and their Applications*, Quebec, Canada, 2-5 July 2012.

[17] J. Hagenauer, "Rate-compatible punctured convolutional codes (RCPC codes) and their applications," *IEEE Transactions on Wireless communications*, vol. 36, no. 4, pp. 389–400, April 1988.

[18] W. W. Bell, *Special functions for scientists and engineers*, London: Van Nostrand, 1968.

[19] S.A. Klugman, H.H. Panjer, and G.E. Wilmot, *Loss Models: From Data to Distributions*, 3rd edition, pp. 61–63, John-Wiley & Sons, 2008.

[20] A. Ribeiro, Xiaodong Cai, and G.B. Giannakis, "Symbol error probabilities for general cooperative links," *IEEE Transactions on Wireless Communications*, vol. 4, no. 3, pp. 1264–1273, May 2005.

[21] M. K. Simon and M.-S. Alouini, "Digital Communication over Fading Channels: A Unified Approach to Performance Analysis" New York, U.S.A.: *Wiley*, 2000.

[22] Zhouye Pi et al., " An Introduction to Millimeter- Wave Mobile Broadband Systems," *IEEE Communications Magazine* , vol.49, no.6, pp.101- 107, Jun. 2011.

[23] Zhouye Pi et al., " An Introduction to Millimeter- Wave Mobile Broadband Systems," IEEE Communications Magazine , vol.49, no.6, pp.101- 107, Jun. 2011.

[24] Y.-W. Hong and A. Scaglione, "Energy-efficient broadcasting with cooperative transmissions in wireless sensor networks," *IEEE Transactions on Wireless Communications*, vol. 5, no. 10, pp. 2844–2855, October 2006.

[25] T. Brown, E. D. Carvalho, and P. Kyritsi, *Practical Guide to the MIMO Radio Channel*, 1st edition, West Sussex, U.K.: John Wiley and Sons Ltd, 2012.

[26] T. M. Cover and A. A. E. Gamal, “Capacity theorems for the relay channel,” *IEEE Transactions on Information Theory*, vol. 25, no. 5, pp. 572–84, September 1979.

[27] A. Goldsmith, *Wireless Communications*, Cambridge University PressC, 1st edition, 2005.

[28] B. S.-Mergen and A. Scaglione, “On the power efficiency of cooperative broadcast in dense wireless networks,” *IEEE Journal on Selected Areas in Communications*, vol. 25, no. 2, pp. 497–507, February 2007.

[29] Y.-R. Tsai and L.-C. Lin, “Optimal Power Allocation for Decode-and-Forward Cooperative Diversity Under an Outage Performance Constraint,” *IEEE Communication Letters*, vol. 14, no. 10, pp. 945–947, October 2010.

[30] G. Zhao, C. Yang, G. Y. Li, D. Li, and A. C. K. Soong, “Power and channel allocation for cooperative relay in cognitive radio networks,” *IEEE Journal of Selected Topics in Signal Processing*, vol. 5, no. 1, pp. 151–159, February 2011.

[31] R. K. Mallik, “A new statistical model of the complex nakagami-m fading gain,” *IEEE Transactions on Communications*, vol. 58, no. 9, pp. 2611–2620, September 2010.

[32] A. A. Abu-Dayya and N.C. Beaulieu, “Microdiversity on Rician fading channels,” *IEEE Transactions on Communications*, vol. 42, no. 6, pp. 2258–2267, June 1994.

L.-C. Wang and C.-T. Lea, “Exact analysis of co-channel interference in a shadowed-Nakagami/shadowed-Rician channel model,” in proceedings of *IEEE International Conference on Communications*, Seattle, U.S.A., 18-22 June 1995.

[33] A.D. Wyner, “Shannon-theoretic approach to a Gaussian cellular multiple-access channel,” *IEEE Transactions on Information Theory*, vol. 40, no. 6, pp. 1713–1727, November 1994.

[34] J. C. S. S. Filho and M. D. Yacoub, “Nakagami-m approximation to the sum of M non-identical independent Nakagami-m variates,” *IET Electronics Letters*, vol. 40, no. 15, pp. 951–952, 22 July 2004.

[35] G. K. Karagiannidis, N. C. Sagias, and T. A. Tsiftsis, “Closed-form statistics for the sum of squared Nakagami-m variates and its applications,” *IEEE Transactions on Communications*, vol. 54, no. 8, pp. 1353–1359, August 2006.

[36] I. Wolfram Research, *Mathematica Edition: Version 8.0*, Champaign, Illinois:Wolfram Research Inc., 2010.

[37] A. M. Salhab, F. Al-Qahtani, S.A. Zummo, and H. Alnuweiri, “Performance analysis of dual-hop AF relay systems with interference-limited destination in Nakagami-m/Rician fading channels,” in proceedings of *11th International Conference on Information Science, Signal Processing and their Applications*, Quebec, Canada, 2-5 July 2012.

[38] J. Hagenauer, "Rate-compatible punctured convolutional codes (RCPC codes) and their applications," *IEEE Transactions on Wireless communications*, vol. 36, no. 4, pp. 389–400, April 1988.

[39] W. W. Bell, *Special functions for scientists and engineers*, London: Van Nostrand, 1968.

[40] S.A. Klugman, H.H. Panjer, and G.E. Wilmot, *Loss Models: From Data to Distributions*, 3rd edition, pp. 61–63, John-Wiley & Sons, 2008.

[41] A. Ribeiro, Xiaodong Cai, and G.B. Giannakis, "Symbol error probabilities for general cooperative links," *IEEE Transactions on Wireless Communications*, vol. 4, no. 3, pp. 1264–1273, May 2005.

[42] M. K. Simon and M.-S. Alouini, "Digital Communication over Fading Channels: A Unified Approach to Performance Analysis" New York, U.S.A.: *Wiley*, 2000.

[43] Zhouye Pi et al., " An Introduction to Millimeter- Wave Mobile Broadband Systems," *IEEE Communications Magazine* , vol.49, no.6, pp.101- 107, Jun. 2011.

[44] Zhouye Pi et al., " An Introduction to Millimeter- Wave Mobile Broadband Systems," IEEE Communications Magazine , vol.49, no.6, pp.101- 107, Jun. 2011.

[45] Y.-W. Hong and A. Scaglione, "Energy-efficient broadcasting with cooperative transmissions in wireless sensor networks," *IEEE Transactions on Wireless Communications*, vol. 5, no. 10, pp. 2844–2855, October 2006.

[46] T. Brown, E. D. Carvalho, and P. Kyritsi, *Practical Guide to the MIMO Radio Channel*, 1st edition, West Sussex, U.K.: John Wiley and Sons Ltd, 2012.

[47] T. M. Cover and A. A. E. Gamal, "Capacity theorems for the relay channel," *IEEE Transactions on Information Theory*, vol. 25, no. 5, pp. 572–84, September 1979.

[48] A. Goldsmith, *Wireless Communications*, Cambridge University PressC, 1st edition, 2005.

[49] B. S.-Mergen and A. Scaglione, "On the power efficiency of cooperative broadcast in dense wireless networks," *IEEE Journal on Selected Areas in Communications*, vol. 25, no. 2, pp. 497–507, February 2007.

[50] Y.-R. Tsai and L.-C. Lin, "Optimal Power Allocation for Decode-and-Forward Cooperative Diversity Under an Outage Performance Constraint," *IEEE Communication Letters*, vol. 14, no. 10, pp. 945–947, October 2010.

[51] G. Zhao, C. Yang, G. Y. Li, D. Li, and A. C. K. Soong, "Power and channel allocation for cooperative relay in cognitive radio networks," *IEEE Journal of Selected Topics in Signal Processing*, vol. 5, no. 1, pp. 151–159, February 2011.

[52] R. K. Mallik, "A new statistical model of the complex nakagami-m fading gain," *IEEE Transactions on Communications*, vol. 58, no. 9, pp. 2611–2620, September 2010.

[53] A. A. Abu-Dayya and N.C. Beaulieu, "Microdiversity on Rician fading channels," *IEEE Transactions on Communications*, vol. 42, no. 6, pp. 2258–2267, June 1994.

L.-C. Wang and C.-T. Lea, "Exact analysis of co-channel interference in a shadowed-Nakagami/shadowed-Rician channel model," in proceedings of *IEEE International Conference on Communications*, Seattle, U.S.A., 18-22 June 1995.

[54] A.D. Wyner, "Shannon-theoretic approach to a Gaussian cellular multiple-access channel," *IEEE Transactions on Information Theory*, vol. 40, no. 6, pp. 1713–1727, November 1994.

[55] J. C. S. S. Filho and M. D. Yacoub, "Nakagami-m approximation to the sum of M non-identical independent Nakagami-m variates," *IET Electronics Letters*, vol. 40, no. 15, pp. 951–952, 22 July 2004.

[56] G. K. Karagiannidis, N. C. Sagias, and T. A. Tsiftsis, "Closed-form statistics for the sum of squared Nakagami-m variates and its applications," *IEEE Transactions on Communications*, vol. 54, no. 8, pp. 1353–1359, August 2006.

[57] I. Wolfram Research, *Mathematica Edition: Version 8.0*, Champaign, Illinois:Wolfram Research Inc., 2010.

[58] A. M. Salhab, F. Al-Qahtani, S.A. Zummo, and H. Alnuweiri, "Performance analysis of dual-hop AF relay systems with interference-limited destination in Nakagami-m/Rician fading channels," in proceedings of *11th International Con-*

ference on Information Science, Signal Processing and their Applications, Quebec, Canada, 2-5 July 2012.

[59] J. Hagenauer, "Rate-compatible punctured convolutional codes (RCPC codes) and their applications," *IEEE Transactions on Wireless communications*, vol. 36, no. 4, pp. 389–400, April 1988.

[60] W. W. Bell, *Special functions for scientists and engineers*, London: Van Nostrand, 1968.

[61] S.A. Klugman, H.H. Panjer, and G.E. Wilmot, *Loss Models: From Data to Distributions*, 3rd edition, pp. 61–63, John-Wiley & Sons, 2008.

[62] A. Ribeiro, Xiaodong Cai, and G.B. Giannakis, "Symbol error probabilities for general cooperative links," *IEEE Transactions on Wireless Communications*, vol. 4, no. 3, pp. 1264–1273, May 2005.

[63] M. K. Simon and M.-S. Alouini, "Digital Communication over Fading Channels: A Unified Approach to Performance Analysis" New York, U.S.A.: *Wiley*, 2000.

[64] Zhouye Pi et al., " An Introduction to Millimeter- Wave Mobile Broadband Systems," *IEEE Communications Magazine* , vol.49, no.6, pp.101- 107, Jun. 2011.

[65] Zhouye Pi et al., " An Introduction to Millimeter- Wave Mobile Broadband Systems," IEEE Communications Magazine , vol.49, no.6, pp.101- 107, Jun. 2011.

[66] Y.-W. Hong and A. Scaglione, "Energy-efficient broadcasting with cooperative transmissions in wireless sensor networks," *IEEE Transactions on Wireless Communications*, vol. 5, no. 10, pp. 2844–2855, October 2006.

[67] T. Brown, E. D. Carvalho, and P. Kyritsi, *Practical Guide to the MIMO Radio Channel*, 1st edition, West Sussex, U.K.: John Wiley and Sons Ltd, 2012.

[68] T. M. Cover and A. A. E. Gamal, "Capacity theorems for the relay channel," *IEEE Transactions on Information Theory*, vol. 25, no. 5, pp. 572–84, September 1979.

[69] A. Goldsmith, *Wireless Communications*, Cambridge University PressC, 1st edition, 2005.

[70] B. S.-Mergen and A. Scaglione, "On the power efficiency of cooperative broadcast in dense wireless networks," *IEEE Journal on Selected Areas in Communications*, vol. 25, no. 2, pp. 497–507, February 2007.

[71] Y.-R. Tsai and L.-C. Lin, "Optimal Power Allocation for Decode-and-Forward Cooperative Diversity Under an Outage Performance Constraint," *IEEE Communication Letters*, vol. 14, no. 10, pp. 945–947, October 2010.

[72] A.D. Wyner, "Shannon-theoretic approach to a Gaussian cellular multiple-access channel," *IEEE Transactions on Information Theory*, vol. 40, no. 6, pp. 1713–1727, November 1994.

[73] J. C. S. S. Filho and M. D. Yacoub, "Nakagami-m approximation to the sum of M non-identical independent Nakagami-m variates," *IET Electronics Letters*, vol. 40, no. 15, pp. 951–952, 22 July 2004.

[74] G. K. Karagiannidis, N. C. Sagias, and T. A. Tsiftsis, "Closed-form statistics for the sum of squared Nakagami-m variates and its applications," *IEEE Transactions on Communications*, vol. 54, no. 8, pp. 1353–1359, August 2006.

[75] I. Wolfram Research, *Mathematica Edition: Version 8.0*, Champaign, Illinois:Wolfram Research Inc., 2010.

[76] A. M. Salhab, F. Al-Qahtani, S.A. Zummo, and H. Alnuweiri, "Performance analysis of dual-hop AF relay systems with interference-limited destination in Nakagami-m/Rician fading channels," in proceedings of *11th International Conference on Information Science, Signal Processing and their Applications*, Quebec, Canada, 2-5 July 2012.

[77] J. Hagenauer, "Rate-compatible punctured convolutional codes (RCPC codes) and their applications," *IEEE Transactions on Wireless communications*, vol. 36, no. 4, pp. 389–400, April 1988.

[78] W. W. Bell, *Special functions for scientists and engineers*, London: Van Nostrand, 1968.

[79] S.A. Klugman, H.H. Panjer, and G.E. Wilmot, *Loss Models: From Data to Distributions*, 3rd edition, pp. 61–63, John-Wiley & Sons, 2008.

[80] A. Ribeiro, Xiaodong Cai, and G.B. Giannakis, “Symbol error probabilities for general cooperative links,” *IEEE Transactions on Wireless Communications*, vol. 4, no. 3, pp. 1264–1273, May 2005.

[81] M. K. Simon and M.-S. Alouini, “Digital Communication over Fading Channels: A Unified Approach to Performance Analysis” New York, U.S.A.: *Wiley*, 2000.

[82] G. Zhao, C. Yang, G. Y. Li, D. Li, and A. C. K. Soong, “Power and channel allocation for cooperative relay in cognitive radio networks,” *IEEE Journal of Selected Topics in Signal Processing*, vol. 5, no. 1, pp. 151–159, February 2011.

[83] R. K. Mallik, “A new statistical model of the complex nakagami-m fading gain,” *IEEE Transactions on Communications*, vol. 58, no. 9, pp. 2611–2620, September 2010.

[84] A. A. Abu-Dayya and N.C. Beaulieu, “Microdiversity on Rician fading channels,” *IEEE Transactions on Communications*, vol. 42, no. 6, pp. 2258–2267, June 1994.

L.-C. Wang and C.-T. Lea, “Exact analysis of co-channel interference in a shadowed-Nakagami/shadowed-Rician channel model,” in proceedings of *IEEE International Conference on Communications*, Seattle, U.S.A., 18-22 June 1995.

[85] A.D. Wyner, “Shannon-theoretic approach to a Gaussian cellular multiple-access channel,” *IEEE Transactions on Information Theory*, vol. 40, no. 6, pp. 1713–1727, November 1994.

[86] J. C. S. S. Filho and M. D. Yacoub, “Nakagami-m approximation to the sum of M non-identical independent Nakagami-m variates,” *IET Electronics Letters*, vol. 40, no. 15, pp. 951–952, 22 July 2004.

[87] G. K. Karagiannidis, N. C. Sagias, and T. A. Tsiftsis, “Closed-form statistics for the sum of squared Nakagami-m variates and its applications,” *IEEE Transactions on Communications*, vol. 54, no. 8, pp. 1353–1359, August 2006.

[88] I. Wolfram Research, *Mathematica Edition: Version 8.0*, Champaign, Illinois:Wolfram Research Inc., 2010.

[89] A. M. Salhab, F. Al-Qahtani, S.A. Zummo, and H. Alnuweiri, “Performance analysis of dual-hop AF relay systems with interference-limited destination in Nakagami-m/Rician fading channels,” in proceedings of *11th International Conference on Information Science, Signal Processing and their Applications*, Quebec, Canada, 2-5 July 2012.

[90] J. Hagenauer, “Rate-compatible punctured convolutional codes (RCPC codes) and their applications,” *IEEE Transactions on Wireless communications*, vol. 36, no. 4, pp. 389–400, April 1988.

[91] W. W. Bell, *Special functions for scientists and engineers*, London: Van Nostrand, 1968.

[92] S.A. Klugman, H.H. Panjer, and G.E. Wilmot, *Loss Models: From Data to Distributions*, 3rd edition, pp. 61–63, John-Wiley & Sons, 2008.

[93] A. Ribeiro, Xiaodong Cai, and G.B. Giannakis, “Symbol error probabilities for general cooperative links,” *IEEE Transactions on Wireless Communications*, vol. 4, no. 3, pp. 1264–1273, May 2005.

[94] M. K. Simon and M.-S. Alouini, “Digital Communication over Fading Channels: A Unified Approach to Performance Analysis” New York, U.S.A.: *Wiley*, 2000.

[95] Zhouye Pi et al., “ An Introduction to Millimeter- Wave Mobile Broadband Systems,” IEEE Communications Magazine , vol.49, no.6, pp.101- 107, Jun. 2011.

[96] Y.-W. Hong and A. Scaglione, “Energy-efficient broadcasting with cooperative transmissions in wireless sensor networks,” *IEEE Transactions on Wireless Communications*, vol. 5, no. 10, pp. 2844–2855, October 2006.

[97] T. Brown, E. D. Carvalho, and P. Kyritsi, *Practical Guide to the MIMO Radio Channel*, 1st edition, West Sussex, U.K.: John Wiley and Sons Ltd, 2012.

[98] T. M. Cover and A. A. E. Gamal, “Capacity theorems for the relay channel,” *IEEE Transactions on Information Theory*, vol. 25, no. 5, pp. 572–84, September 1979.

[99] A. Goldsmith, *Wireless Communications*, Cambridge University PressC, 1st edition, 2005.

[100] B. S.-Mergen and A. Scaglione, “On the power efficiency of cooperative broadcast in dense wireless networks,” *IEEE Journal on Selected Areas in Communications*, vol. 25, no. 2, pp. 497–507, February 2007.

[101] Y.-R. Tsai and L.-C. Lin, “Optimal Power Allocation for Decode-and-Forward Cooperative Diversity Under an Outage Performance Constraint,” *IEEE Communication Letters*, vol. 14, no. 10, pp. 945–947, October 2010.

[102] G. Zhao, C. Yang, G. Y. Li, D. Li, and A. C. K. Soong, “Power and channel allocation for cooperative relay in cognitive radio networks,” *IEEE Journal of Selected Topics in Signal Processing*, vol. 5, no. 1, pp. 151–159, February 2011.

[103] R. K. Mallik, “A new statistical model of the complex nakagami-m fading gain,” *IEEE Transactions on Communications*, vol. 58, no. 9, pp. 2611–2620, September 2010.

[104] A. A. Abu-Dayya and N.C. Beaulieu, “Microdiversity on Rician fading channels,” *IEEE Transactions on Communications*, vol. 42, no. 6, pp. 2258–2267, June 1994.

L.-C. Wang and C.-T. Lea, “Exact analysis of co-channel interference in a shadowed-Nakagami/shadowed-Rician channel model,” in proceedings of *IEEE International Conference on Communications*, Seattle, U.S.A., 18-22 June 1995.

[105] A.D. Wyner, “Shannon-theoretic approach to a Gaussian cellular multiple-access channel,” *IEEE Transactions on Information Theory*, vol. 40, no. 6, pp. 1713–1727, November 1994.

[106] J. C. S. S. Filho and M. D. Yacoub, “Nakagami-m approximation to the sum of M non-identical independent Nakagami-m variates,” *IET Electronics Letters*, vol. 40, no. 15, pp. 951–952, 22 July 2004.

[107] G. K. Karagiannidis, N. C. Sagias, and T. A. Tsiftsis, “Closed-form statistics for the sum of squared Nakagami-m variates and its applications,” *IEEE Transactions on Communications*, vol. 54, no. 8, pp. 1353–1359, August 2006.

[108] I. Wolfram Research, *Mathematica Edition: Version 8.0*, Champaign, Illinois:Wolfram Research Inc., 2010.

[109] A. M. Salhab, F. Al-Qahtani, S.A. Zummo, and H. Alnuweiri, “Performance analysis of dual-hop AF relay systems with interference-limited destination in Nakagami-m/Rician fading channels,” in proceedings of *11th International Conference on Information Science, Signal Processing and their Applications*, Quebec, Canada, 2-5 July 2012.

[110] J. Hagenauer, “Rate-compatible punctured convolutional codes (RCPC codes) and their applications,” *IEEE Transactions on Wireless communications*, vol. 36, no. 4, pp. 389–400, April 1988.

[111] W. W. Bell, *Special functions for scientists and engineers*, London: Van Nostrand, 1968.

[112] S.A. Klugman, H.H. Panjer, and G.E. Wilmot, *Loss Models: From Data to Distributions*, 3rd edition, pp. 61–63, John-Wiley & Sons, 2008.

[113] A. Ribeiro, Xiaodong Cai, and G.B. Giannakis, “Symbol error probabilities for general cooperative links,” *IEEE Transactions on Wireless Communications*, vol. 4, no. 3, pp. 1264–1273, May 2005.

[114] M. K. Simon and M.-S. Alouini, “Digital Communication over Fading Channels: A Unified Approach to Performance Analysis” New York, U.S.A.: *Wiley*, 2000.

Publications based on this Thesis

Journal and Conference Publications

1. Kapil Sharma and S. K. Agrawal, "Millimeter Wave Channel Capacity for 5th Generation Software Defined Radio Communication System in Vegetation Area," *International Journal of Sensors, Wireless Communications and Control*, Scopus, Volume 8, 3 Issues, 2018.

2. S. K. Agrawal and Kapil Sharma, "5G Millimeter Wave Propagation with Intelligent Grid Selection for Obstacle Avoidance," *International Journal of Computer Information Systems and Industrial Management Applications* , Scopus, ISSN 2150-7988, Vol 10, pp. 115-124, 2018.

3. Kapil Sharma and S. K. Agrawal, "5th Generation Millimeter Wave Wireless Communication Propagation Losses Dataset for Indian Metro Cities Based on Corresponding Weather Conditions," *Science Direct, Elsevier, Data in Brief, Scopus* , DOI: 10.1016/j.dib.2018.12.003 , 2018.

4. S. K. Agrawal and Kapil Sharma, "Intelligent software defined atmospheric effect processing for 5G millimeter wave (mmWave) communication system," *International Journal of Wireless and Microwave Technologies(IJWMT)* , vol.8, no.2, pp. 15-26, DOI: 10.5815/ijwmt.2018.02.02, 2018.

5. Kapil Sharma and S. K. Agrawal, "Software defined internet of things (IoT) in 5G millimeter mave (mmWave) communication system," *4th International*

Conference at IETE Delhi on Emerging Trends in Engineering, Technology, Science and Management (ICETETSM-17), (IETE) Institution of Electronics and Telecommunication Engineers, New Delhi, India , ISBN: 978-93-86171-54-2 (Most Appropriate Paper), 2017.

6. S. K. Agrawal and Kapil Sharma, "Software defined internet of things (IoT) in 5G millimeter wave (mmWave) communication system," *International Journal of Advance Research in Science and Engineering (IJARSE)*, vol.6, no.7, 2017.

7. Kapil Sharma and S. K. Agrawal, "Software defined millimeter wave communications system," *Appl. Theory Comput. Technology* , vol.2, no.1, Invited Paper, 2017.

8. S. K. Agrawal and Kapil Sharma, "Software defined radio based channel capacity in 5G millimeter wave communication system," *1st International Virtual Conference on Computer Science, Engineering and Technology VirtualCom-16* , 2016.

9. S. K. Agrawal and Kapil Sharma, "5G millimeter wave (mmWave) communication system with software defined radio (SDR)," *International Journal for Innovative Research in Science and Engineering* , vol.2, no.9, 2016.

10. S. K. Agrawal and Kapil Sharma, "5G millimeter wave (mmWave) communication system with software defined radio (SDR)," *International Conference on Recent Trends in Engineering and Science (ICRTES-16)* , ISBN : 978-93-86171-

06-1, Best Paper Award, 2016.

11. S. K. Agrawal and Kapil Sharma, “5G millimeter wave (mmWave) communications system: vision and challenges,” *IEEE Proceedings of INDIACom-16*, 2016.

Patent

1. Kapil Sharma and S. K. Agrawal, “Beam forming method for a transmitting antenna and a device thereof,” US Patent US10326508.

2. Kapil Sharma and S. K. Agrawal, “Software defined obstruction free beam window for 5g millimeter wave communication system,” India Patent App. Number 201711007315, India Filing Date 1 March 2017, US Patent US20180254811A1.

3. Kapil Sharma and S. K. Agrawal, “Software defined optimum sub-grid based beamforming 5G millimeter wave communication system,” India Patent App. Number 201711016629, India Filing Date 11 May 2017, US Patent US20180254811A1 .

4. S. K. Agrawal and Kapil Sharma, “Coded Software defined obstruction free beam window for 5G millimeter wave communication system,” India Patent App. Number 201711029904, India Filing Date 23 August 2017, US Patent filing is in progress.

5. Kapil Sharma and S. K. Agrawal, “Proximity Based Access Control in a 5G Wireless Communication Network,” India Patent App. Number 201811021586, India Filing Date 8 June 2018, US Patent filing is in progress.

6. Kapil Sharma and S. K. Agrawal, “Optimizing Power Transfer in a Wireless Power Transmitter System,” India Patent App. Number 201811022745, India Filing Date 18 June 2018, US Patent filing is in progress.

7. S. K. Agrawal and Kapil Sharma, “Software Defined Radio Reflections from Obstructions,” India and US Patent filing is in progress.

Work in Progress

1. Kapil Sharma and S. K. Agrawal, “Millimeter Wave Channel Capacity for 5th Generation Software Defined Radio Communication System in Mixed Area,”In Progress for Springer.

2. S. K. Agrawal and Kapil Sharma, “5G Millimeter Wave Propagation with Intelligent Transmission,” In Progress for IEEE Transactions on Antennas and Propagation.

3. Kapil Sharma and S. K. Agrawal, “Intelligent software defined optimum control in 5G millimeter wave communication system,” In Progress for Patent.

4. Kapil Sharma and S. K. Agrawal, “SDR based attenuation prediction and control in 5G mmwave system,” In Progress for Patent.

Acknowledgment

The author and guide are thankful to computer engineering department (DTU), Samsung Research Institute Noida, India and Information Technology Department (DTU) India.

Technical Biography of Guide

Dr. Kapil Sharma was born in Haryana state of India. In 2011, he got Doctors Degree in Computer Science and Engineering under the Faculty of Engineering and Technology at the M. D. University, Rohtak (Haryana), India. He has obtained his B.E. and Master of Technology Degrees in Computer Science and Engineering and Information Technology from M. D. University, Rohtak and IASE, Rajasthan, India in 2000 and 2005 respectively. He is Professor and Head of Department of Information Technology Department (DTU). He has vast research and teaching experience with well known colleges and universities. His research areas are software engineering, automation and etc.

Technical Biography of Author

Sachin Kumar Agrawal received B.Tech. degree in Electronics & Communication Engineering from Uttar Pradesh Technical University, India, in 2004. He received the M.Tech. degree in Signal Processing in Signal processing (SP) from Netaji Subhas Institute of Technology (Formerly: Delhi Institute of Technology), University of Delhi, India. He is currently working towards the Ph.D. degree in Computer Engineering from DTU, New Delhi, India. His research interests include wireless communications, 5G, machine learning (ML), artificial engineering (AI) and related.